UNIVERSITEIT VAN PRETORIA
UNIVERSITY OF PRETORIA
YUNIBESITHI YA PRETORIA

Mixtures Effects of Nanoscale and Macroscale Contaminants to *Bacillus Subtilis* in Natural Water Systems

Samuel Keeng Leareng

submitted in fulfilment of requirements for the degree of

Doctor of Philosophy

Chemical Technology

In the

Department of Chemical Engineering

Faculty of Engineering, Built Environment and Information technology

University of Pretoria

April 2020

Declaration by candidate

I, **Samuel Keeng Leareng**, declare that the thesis, which I hereby submit for the degree PhD Chemical Technology at the University of Pretoria, is my own work and has not previously been submitted by me for a degree at this or any other tertiary institution.

_____ _____

Samuel Keeng Leareng Date

Mixtures effects of nanoscale and nanoscale contaminants to *Bacillus subtilis* in natural water systems

Author:	**Samuel Keeng Leareng**
Supervisor:	Prof N. Musee
Co-supervisor:	Dr E. Ubomba-Jaswa
Department:	Chemical Engineering
University:	University of Pretoria
Degree:	Doctor of Philosophy (Chemical Technology)

Synopsis

Engineered nanoparticles (ENPs) (e.g. zinc oxide (nZnO) and iron oxide ($nFeO_x$) and organic pollutants (e.g. triclosan (TCS)) are among emerging contaminants (ECs) of environmental concern. However, to date there is limited knowledge on their fate and potential deleterious effects in the ecological systems. Following simultaneous and/or sequential release of ECs in the ecological systems; they co-exist as mixtures defined by complex permutations. As such, toxicological outcomes of individual ECs may be altered as those of mixtures formed may exhibit synergistic, antagonistic or additive effects. Influenced by water physicochemical parameters, chemical interactions between multiple contaminants and the unique properties of ENPs like photoactivity, adsorption capacity and dissolution may alter the toxic outcomes to bacteria. Yet, currently, the environmental fate and toxicity ENPs as mixtures, particularly in natural water are limited.

In this work, *Bacillus subtilis* was used as a model organism to assess the toxicity of nZnO and maghemite iron oxide (γ-nFe_2O_3) as individual ENPs, binary mixtures, and ternary mixtures with TCS. Natural water from two river sources, the Elands River (ER) and the Bloubank River (BR) were used to generate environmentally relevant data; and four endpoints were used to evaluate toxicological outcomes (cell viability, cell membrane integrity, ATP production, oxidative stress from reactive oxygen species (ROS). Aggregation of the two ENPs were significantly different between the two river water matrixes with

higher aggregates observed in BR water. nZnO induced significant reduction in cell viability and membrane integrity at higher tested concentrations in ER; but none in BR under visible light. A higher decrease in ATP levels was observed in ER than in BR, and ROS production was negligible irrespective of the ENP type and exposure media under visible light. Conversely, γ-nFe_2O_3 induced no significant effects on *B. subtilis* on all tested endpoints. nZnO induced concentration-dependent effects on the cell membrane integrity of *B. subtilis* in both river water samples under solar irradiation.

For binary mixtures of ENPs under solar irradiation, nZnO toxicity was found to be concentration-dependent, with more pronounced effects in ER than BR water due to water chemistry. However, toxic effects were mitigated by γ-nFe_2O_3 in the binary mixtures, linked to heteroaggregation between the ENPs. Solar irradiation induced ROS had minimal effect on the toxicity of ENPs. For ternary mixtures, toxicity of TCS was more pronounced at the highest concentration. However, the effects were not water chemistry dependent, compared to the observed effects from nZnO. In addition, more distinctive mitigating effects were observed in ternary mixtures, where nZnO dissolution was significantly lower in the presence of TCS. These findings demonstrated that observed differences in the effects of nZnO towards *B. subtilis*, either in binary or ternary systems were influenced by the nature of interactions (TCS and γ-nFe_2O_3) as well as water chemistry of natural water in focus. Therefore, the unique physicochemical properties of natural aqueous media were established to be the key determinant attributes in enhancing or inhibiting the effects of ENPs on bacteria, and, the co-existence of ECs of different types and classes may lead to reduction of toxic effects of individual contaminants.

Acknowledgements

I would like to thank my supervisor Prof Ndeke Musee for his invaluable guidance, support and mentorship during the course of this work. I also extend my gratitude to my supervisor Dr Eunice Ubomba-Jaswa for her support and encouragement. I am grateful to the Water Research Commission (WRC) and University of Pretoria (UP) for their financial support.

I would like to thank the Centre for Microbial Ecology and Genomics (CMEG) for use of their facilities and equipment, and also thankful to the team at the laboratory for microscopy and microanalysis for their assistance with SEM and TEM. I extend my gratitude and appreciation to Razia Vizasie, Suzzette Seymore and Gymaisy Kenny for their patient support and assistance with administrative duties. I would like to thank Prof Philiswa Nomgongo, University of Johannesburg for her assistance with ICP-MS analysis.

A special thanks to my lab Colleagues Dr Ntombi Mahaye, Aston Nanja, Ernst Bekker, Ntsikelelo Yalezo, Lauren McDowell-Morris and Mpho Makofane for their support and help. My deepest gratitude to my aunt, Usinah Tshekiso for her ever-lasting support and love. My sister, Angel Tshekiso for her encouragement and unwavering love. My son Ethan Matlhogonolo Leareng, born on this PhD journey, who has kept me motivated and going to see this to the end.

Lastly, I would like to thank my family and my friends for their encouragement support and patience with my absence throughout the years of this study.

Dedication

*This thesis is dedicated to **ALL** of my family.*

List of papers and conferences

The work in this thesis has been submitted for publication in peer-reviewed journals and presented at international conferences as detailed below:

List of journal articles from this study

Leareng S. K., et al., 2020. Zinc oxide and iron oxide engineered nanoparticles toxicity on *Bacillus subtilis* in river water systems. *Environmental Science Nano*. 7:172–185, DOI: 10.1039/C9EN00585D (Chapter 4).

Leareng S. K., et al., Effects of binary mixtures of zinc oxide and iron oxide engineered nanoparticles on *Bacillus subtilis* in natural water. Chemosphere (In preparation). (Chapter 5).

Leareng S.K. et al., Interactions and toxicity of ENPs and triclosan: Ternary exposures in river water systems. (In preparation) (Chapter 6).

(book chapter) -Musee, N., **Leareng**, **S.K.**., et al., Implications of surface coatings on engineered nanoparticles for environmental systems; Status quo, challenges and perspectives. In Handbook of Functionalized Nanomaterials for Industrial Applications, 2020, https://doi.org/10.1016/B978-0-12-816787-8. 00014-4 (accepted).

List of Conferences presentations from this study

Leareng, S.K., Mechanistic insights into ecotoxicological effects of engineered nanoparticles mixtures in freshwater systems: 8th International conference on Nanoscience and Nanotechnology, NanoAfrica 2020, Enabling the Commercialization of Nanotechnological Innovation, Birchwood Hotel and OR Tambo Conference Centre, Johannesburg, South Africa, 18th–20th April 2020. (Accepted: Oral presentation).

Leareng SK., et al. Binary mixture toxicity of metal oxides nanoparticles and triclosan on *Bacillus subtilis* in freshwater systems. NanoSafe 2018 - 5-9 November 2018 – MINATEC, Grenoble, France (Oral presentation).

Table of contents

List of figures

List of Tables

List of abbreviations and acronyms

BR	Bloubank River
CA	Concentration addition
DIW	Deionised water
DOC	Dissolved organic carbon
DLS	Dynamic light scattering
EC	Effective concentration
EC(s)	Emerging contaminant (s)
EC_{50}	Concentration causing 50% toxic effect
ECx	Concentration causing x% toxic effect
EDL	Electrical double layer
ENPs	Engineered nanoparticles
ER	Elands River
HA	Humic acid
HCl	Hydrochloric acid
HDD	Hydrodynamic diameter
IA	Independent action
IONPs	Iron oxide nanoparticles
IS	Ionic strength
kDa	Kilo Daltons
MECs	Measured environmental concentrations
MgL^{-1}	Milligrams per litre
mM	Millimolar
mV	millivolts
NaOH	Sodium hydroxide

nm	Nanometre
NOM	Natural organic matter
OD	Optical density
OECD	Organization for Economic Co-operation and Development
PCPs	personal care products
PECs	Predicted environmental concentrations
XRD	X-ray diffractometer
PZC	Point of zero charge
ROS	Reactive oxygen species
rpm	Revolutions per minute
SEM	Scanning electron microscope
sp-ICP-MS	Single Particle Inductively Coupled Plasma Mass spectrometry
TEM	Transmission electron microscope
TU	Toxic unit
USEPA	United States Environmental Protection Agency
USGS	United States Geological Survey
XRD	X-ray diffraction
ZP (ζ)	Zeta potential

Chapter 1: Introduction

1.1 Background

Engineered nanoparticles (ENPs) are materials synthesized and manipulated to nanoscale dimensions (< 100 nm) in at least one dimension (European Commission, 2011; Rauscher et al., 2014). The interest in ENPs arises from their small size which confers enhanced physical and chemical properties compared to their , making them applicable in diverse applications, compared to their bulk forms (El-Sayed, 2001; Nel et al., 2006; Klaine et al., 2008; Nagarajan, 2008; Schwartzberg & Zhang, 2008; Fan & Alexeeff, 2010). As such, ENPs have increasingly been incorporated in consumer products (nano-enabled products) (Vance et al., 2015; Moeta et al., 2019; Lehutso et al., 2020), and used in applications such as medicine and bioremediation (Penn, He & Natan, 2003; Kohli & Alpar, 2004; Yezhelyev et al., 2006; Cao, 2008; Onyekonwu & Ogolo, 2010; Dickinson, 2012; Hansen et al., 2016).

As production volumes of ENPs continue to increase to meet their market demand, their risk to the environment have also been highlighted. Following usage, ENPs presence in both technical and natural aquatic systems, i.e., wastewater treatment plants (WWTPs) effluent and surface water wastewater have been reported (Bäuerlein et al., 2017; Choi et al., 2018; Peters et al., 2018; Cervantes-Avilés, Huang & Keller, 2019). From these sources, freshwater systems are recognized as the final sinks for ENPs. Environmental contamination by ENPs and the growth of nano-enabled products has led to their classification as a threat to biodiversity (Sutherland et al., 2008; Dumont et al., 2015), and are categorised with numerous other contaminants with unknown ecological effects, recognised as emerging contaminants (ECs) (Klaine et al., 2008; Farré et al., 2009; Boxall, 2012; Sauvé & Desrosiers, 2014; Dumont et al., 2015; Richardson & Kimura, 2016).

The threats of ENPs have given rise to the study of their potential environmental hazard termed nanoecotoxicology (Behra & Krug, 2008; Scheringer, 2008; Kahru & Ivask, 2012). Progress has been made since the advent of nanoecotoxicology to understand the transformation and potential effects of environmental presence of ENPs, however, these concerns are mostly limited to single ENPs. Realistic environmental scenarios show that ECs effects will be from co-exposure of chemical mixtures (Heys et al., 2016; Deng et al., 2017;

Naasz, Altenburger & Kühnel, 2018; Besha et al., 2019; Bopp et al., 2019), for instance, whether ENP-ENP or ENPs with other contaminants.

1.2 Study motivation

Numerous studies have pointed to strong evidence for ENPs antimicrobial properties on microorganisms and other toxicological effects to other organisms at different trophic levels in aquatic systems as reviewed by (Suresh, Pelletier & Doktycz, 2013; Skjolding et al., 2016; Vale et al., 2016; Hou et al., 2018). However, there remains a paucity of information on the toxicity of ENPs in natural water systems (Juganson et al., 2015; Amde et al., 2017). The effects of ENPs on aquatic organisms are closely linked to their transformations, including aggregation, dissolution, surface charge through adsorption or interactions with naturally occurring organics (Lowry et al., 2012; Hartmann et al., 2014; Vale et al., 2016).

Whereas our understanding of transformations of ENPs has improved over the past decade, there is still inadequate data for consensus on the effects of ENPs to aquatic organisms such as bacteria in aquatic systems. This is due to; (i) most studies are conducted in simplistic media that is not representative of the actual environmental matrices (ii) use of varying endpoints across studies that cannot be compared to draw conclusions, (iii) the ENPs concentrations considered in toxicity are incomparable with predicted or measured amounts in the natural environment, and lastly, (iv) the limited studies that consider ENPs effects from their mixtures (co-existing ENPs) or their mixtures with other contaminants (tertiary mixtures), as they exist in the environment .

Therefore, to aid our ability to draw definite conclusions on ENPs effects to aquatic organisms, mixture toxicity data on the co-existence of ENPs as well as their co-existence with other pollutants to the risk assessment for ENPs is key to the systematic management of their human and environmental health. Overall, this study aims to generate data and knowledge that offers insights on the interactions of multiple ENPs simultaneously to the microbes, and their underlying mechanisms. There is a need to develop a holistic understanding on the interactions of combined effects of multiple ENPs as influenced by the aquatic matrix as this has implications on their transformations, and hence, the final form of

ENPs likely to alter ecosystem functioning of aquatic organisms in the environment. Bacteria were chosen for their ease of use in rapid and routine assessment of toxicity risks (Holden, Schimel & Godwin, 2014). Any observed effects on bacteria would likely impact organisms in other trophic levels, making bacteria a suitable for evaluating overall environmental health (Buchman et al., 2018). The bacteria *Bacillus subtilis* is a model organisms that has been used in ENPs toxicity testing (Gambino et al., 2015; Baek et al., 2017; Ranmadugala et al., 2017; Yi & Cheng, 2017), and is an environmentally ubiquitous organism found in both aquatic and terrestrial environments (Earl, Losick & Kolter, 2008).

1.3 Research aim

The aim of the study is to assess the toxicological effects of individual and mixtures of ENPs on *Bacillus subtilis* in freshwater systems. Insights on the influence of water parameters on ENPs transformation, and interactions of mixtures pollutants and toxicity under exposure conditions were assessed.

1.3.1 Objectives

The specific objectives of the project were to;

i. Investigate toxicological effects of zinc oxide and iron oxide ENPs on *Bacillus subtilis* in river water systems
ii. Determine the joint toxicity of zinc oxide and iron oxide ENPs on *Bacillus subtilis* in river water systems
iii. Assess the effects of zinc oxide, iron oxide and triclosan binary and ternary mixtures on *Bacillus subtilis* in river water systems

1.4 Thesis organization

This thesis is divided into six chapters, presented as detailed below.

Chapter 1provides a background to the study, the rationale for the project, research aim and objectives, and thesis layout.

Chapter 2 examines the effects of ENPs in aqueous media with specific reference to zinc oxide and iron oxide nanoparticles to microorganisms. This includes proposed mechanisms of toxicity under environmentally relevant conditions. Moreover, currently reported findings on joint effects of (i) ENPs-ENPs mixtures, (ii) ENPs-Organic pollutant, and (iii) ENPs- ENPs-Organic pollutants are discussed.

Chapter 3 provides detailed information on the materials, experimental setup, and analytical methods employed in this work.

Chapter 4 presents findings and discussions on the toxicity of nZnO and nFe_2O_3 on *Bacillus subtilis* in natural water samples. The role of water chemistry on the behaviour of ENPs, and the mechanisms associated with toxicological outcomes are discussed.

Chapter 5 summarises results and discussions on the interactions and toxicity of nZnO and nFe_2O_3 as binary mixtures. The interactions of ENPs in the natural water systems, and toxicity under solar irradiation are presented.

Chapter 6 provides findings on the ternary mixtures of nZnO, nFe_2O_3 and triclosan. The influence of TCS on the fate of ENPs and the resulting toxicity are discussed.

Chapter 7 highlights the key findings herein, conclusions, recommendations, and future perspectives from the study regarding the toxicity of mixtures.

Chapter 2: Literature review

2.1 Introduction

Occurrence of different classes of chemicals in the environment from anthropogenic activities and sources – have added to newly recognised potential hazards to the ecological and human health. As a result, these chemicals have attracted attention from environmental scientists, regulatory bodies and policy makers in the past decades (Noguera-Oviedo & Aga, 2016; Gogoi et al., 2018; Hartmann et al., 2018). Collectively recognised as emerging contaminants (ECs), these chemicals are either natural or synthesized, not routinely monitored , with limited knowledge on their behaviour and fate in the environment, and largely unknown ecological effects (Petrovic, 2003; Naidu & Wong, 2013; Sauvé & Desrosiers, 2014; Rimayi et al., 2018). These include historical conventional chemicals present in the environment for a long time, but only detected recently due to improvements in detection techniques, or new chemicals, or have begun to be studied (effect on the environment) (Daughton, 2004; Richardson & Ternes, 2005).

With more than 80 000 chemicals released into the environment annually (Naidu et al., 2016), the list of ECs is rapidly increasing annually, with regulatory bodies, e.g. USEPA continually working to increase its drinking water contaminants list for priority chemicals (USEPA, 2016). Critical to this monitoring is a need for prioritization of chemicals of concern, where screening methods typically consider the persistence, potential bioaccumulation, toxicity and risks of chemicals (Arnot & Mackay, 2008; Diamond et al., 2011; Caldwell et al., 2014; Mansour et al., 2016; Musee, 2017; Burns et al., 2018)(Arnot & Mackay, 2008; Diamond et al., 2011; Caldwell et al., 2014; Mansour et al., 2016; Burns et al., 2018). Furthermore, evaluation of impacts in different environmental matrices (e.g. soil, surface waters and sediment), assessments of the available data, methods and technologies (and limitations) are urgently required for regulatory purposes (Naidu et al., 2016). Given the large number of different types and classes of ECs; hence, it is not practical and cost prohibitive to study and gather toxicity information for each chemical.

ECs can be separated into two groups. First, natural compounds which are released or excreted from vertebrates and some invertebrates. And secondly, synthetic compounds

manufactured for many uses as raw materials, or incorporated in everyday products (Daughton, 2004). Synthetic ECs include compounds used in pharmaceuticals, pesticides, personal care products, endocrine disrupters, flame retardants, antimicrobials, nanomaterials, just to mention a few (Richardson & Ternes, 2005; Murray, Thomas & Bodour, 2010; Boxall, 2012; Besha et al., 2019). Recently, definition of ECs has also been expanded to include not only the chemicals and but also daughter chemicals produced as transformation products (TPs), and most importantly, mixtures of chemicals (Naidu et al., 2016). These developments are important because chemicals: (i) once into the environment can either be transformed into more toxic products, (ii) from different sources co-exist in the environment (unlikely to exist as individuals) with their combinations exerting higher degrading imprints to the environment compared single chemicals. In this context, to monitor and manage ECs risks effectively based on scientifically defensible decisions; current critical knowledge gaps must be addressed as a priority including mixtures of various ECs classes.

2.2 Risk assessment of chemical mixtures

Environmental risk assessment of chemicals, including ECs largely focuses on single chemicals with emphasis on the link between chemical exposure and observed effects. In reality, however, consideration of multiple chemicals as mixtures, multiple stress factors, and their combined effects are needed owing to co-existence of cocktails of contaminants in the environment (Backhaus & Faust, 2012; Heys et al., 2016; Bopp et al., 2019). As such, calls to evaluate the effects of contaminants as mixtures and their concomitant threat to water systems have increased over the last decade (Backhaus & Faust, 2012; European Commission, 2012; Brack et al., 2017; Altenburger et al., 2019).

Since the environment is exposed to a huge number of chemicals combined with limited information on their toxicity, and their infinite possible number of combinations render risk assessment of mixtures high challenging. Chief among these challenges include identification and prioritisation of chemical mixtures of great concern (Brack et al., 2017). To aid in selection and prioritization of mixtures of concern, criteria used includes prioritising contaminants likely to be present at concentration where effects can be observed, have no

threshold, and likely to be persistent in the environment (Bopp et al., 2019). Notwithstanding, the choice of contaminants for assessment is also based on environmental monitoring and toxicological data. However, often is not the case for ECs due to inadequacy of analytical methods and instruments and lack of toxicological data, or consensus on toxicity thereof.

Among contaminants falling within this category are engineered nanoparticles (ENPs). ENPs are difficult to identify and quantify in the environment, albeit progress have been made over the last few years (Mitrano et al., 2014; Bitragunta et al., 2017; Reed et al., 2017; Peters et al., 2018). This makes it difficult to assess the extent of ENPs distribution, concentrations, and likely environmental impacts. ENPs once in the environment will co-exist with other contaminants from different classes such as Triclosan (TCS). TCS is an antimicrobial widely used in personal care products (PCPs), household, and medical products (Nishi, Kawakami & Onodera, 2008; Dann & Hontela, 2011; Ramaswamy et al., 2011; Lyndall et al., 2017). With concentrations in surface water and terrestrial environment ranging from ng/L to low µg/L levels worldwide, regulatory bodies e.g. European Union (EU) has disapproved TCS in January 2016 (European Commission, 2016) whereas the US followed by banning over-the-counter (OTC) consumer antiseptic wash products containing TCS effective from September 2016 (Food and Drug Administration, 2016; Halden et al., 2017). However, in developing countries, including South Africa, this is not been the case. Therefore, an assessment of both contaminants, especially their mixtures toxicological outcomes can aid to better understand, and better manage them towards their responsible use including to enhance ecological health.

2.3 Engineered nanoparticles

Engineered nanoparticles are materials synthesised and manipulated to nanoscale dimensions with at least one dimension in the size range of 1 nm and 100 nm (European Commission, 2011; Boverhof et al., 2015; Boholm & Arvidsson, 2016). The external dimensions or size of nanoparticles, across all definitions by governments, standard organisations and industries, is the more common element, even though there are variations in the upper size limits (Boverhof et al., 2015). ENPs, particularly at below 30 nm, have about

40 % of their atoms localized at the surface increasing their surface/volume (S/V) ratio (Auffan et al., 2009; Fan & Alexeeff, 2010). As a result, ENPs exhibit size dependent unique physico-chemical, opto-electronic properties compared to their bulk materials (El-Sayed, 2001; Nel et al., 2006; Klaine et al., 2008; Nagarajan, 2008; Schwartzberg & Zhang, 2008; Fan & Alexeeff, 2010). These size-dependent properties also form the basis for high diversity of ENPs elemental and structural composition, and in turn, enabling a wide range of possible applications (Auffan et al., 2009; Bundschuh et al., 2018).

ENPs are used in products such as household products, textiles, paints, transport, electronics, communication, agriculture, energy and environment (Wiechers & Musee, 2010; Amenta et al., 2015; Grillo, Rosa & Fraceto, 2015; Schirmer & Auffan, 2015). Reported data on nano-enabled products have shown significant increases in the market globally, with more than 2000 products spanning a variety of product categories ("Project on Emerging Nanotechnologies (PEN).", n.d.; Vance et al., 2015) with exponential growth expected due to ever-increasing demands (Ricardo Energy and Environment, 2016). The Nanotechnology Consumer Product Inventory (Vance et al., 2015) which started in 2005, The Nanodatabase (2016) and PEN 2016 (n.d.) continues to highlight constantly increasing products that have incorporated ENPs, going into thousands. In addition, expected global average production of ENPs is expected to reach about 500 000 tons by 2020 with the global market value expected to rise from 125 million USD in 2000, and reach estimates of 1-3 trillion USD between 2015 and 2020 (Roco, Mirkin & Hersam, 2011).

ENPs fall into five broad classes, viz.: metal oxides, metals, semiconductor nanocrystals known as quantum dots, carbon-based nanoparticles and dendrimers (Klaine et al., 2008; Bhatt & Tripathi, 2011; Suresh, Pelletier & Doktycz, 2013). Among these, metals (Ag, Cu, Au, etc.); carbon-based ENPs (e.g. fullerenes and carbon nanotubes); quantum dots (which are metal-containing ENPs (CdS, ZnS, CdSe); and metal-oxides (e.g. ZnO, CuO, Fe_2O_3, etc.)are broadly categorized as metallic ENPs, are produced in large quantities and highly utilized (Piccinno et al., 2012; Wang & Nowack, 2018a). The diversity of elemental and structural composition that give ENPs their unique general properties have also posed a challenge to environmental scientists concerning their possible adverse effects (Moore, 2006; Klaine et

al., 2008; Bundschuh et al., 2018). Therefore, the growth in ENP utilisation is bound to increase their environmental presence, raising concerns about their short- and long-implications as singles and mixtures with other pollutants to biological life-forms in the ecological systems.

These concerns are driven by emerging data on their negative impacts to biota; hence are classified among rapidly increasing ECs into the environment (Sutherland et al., 2008; Boxall, 2012). Secondly, production and utilisation of ENPs has advanced much faster in comparison to knowledge required to adequately assess their ecological consequences (Colman et al., 2014). And thirdly, ENPs have warranted thorough investigations due to their size and others inherent physicochemical properties, that render them markedly distinctive from other pollutants. To address these challenges, a comprehensive assessment of the risk associated with ENPs, specifically related to release and presence in the environment as well as toxicological implications are necessary.

Among the most produced ENPs with increasing growth and widely used in nano-enabled products are zinc oxide (nZnO) and iron oxide (IONPs) due to their wide-ranging applications (Schmid & Riediker, 2008; Bystrzejewska-Piotrowska, Golimowski & Urban, 2009; Piccinno et al., 2012; Lei et al., 2018). These ENPs have been noted highlighted for prioritization in research for regulatory purposes based on production volumes and usage in (Lai et al., 2018).

2.3.1 Zinc oxide nanoparticles

nZnO is the third highest ENP in annual global production volume by mass, after $nTiO_2$ and $nSiO_2$ (Piccinno et al., 2012; Ivask et al., 2014; Vance et al., 2015). nZnO is a class II – IV semiconductor with two main forms, being wurtzite (hexagonal) and zinc blende (cubic). Wurtzite is more common and stable crystal structure at room temperature, with ionic bonding structures that give it its piezoelectric properties, wide direct band gap of 3.37eV, and a large excitation binding energy at about 60 meV (Ma, Williams & Diamond, 2013; Sirelkhatim et al., 2015; Haq et al., 2017). These properties confer unique optical, and piezo- and conductive- electric properties. nZnO optical absorption at 315–400 nm and 280–315

nm regions for UVA and UVB regions, respectively, makes it beneficial for use in personal care products, paints, semiconductor, catalyst in environmental remediation and antimicrobial agent in products such as food handling packages (Cheng et al., 2004; Lee et al., 2005; Huang et al., 2006; Piccinno et al., 2012; Ma, Williams & Diamond, 2013; Sun, Gottschalk, et al., 2014; Baek et al., 2017).

Thus, large-scale use of nZnO in numerous consumer and industrial applications has resulted to their wide dispersion into technical systems such as wastewater treatment plants (WWTPs). In addition, due to incomplete removal of nZnO in the effluent, finally they enter into freshwater systems as well as from run-offs as the final sink To date, nZnO have been reported in natural water and wastewater as summarized in Table 2.1.

2.3.2 Iron oxide nanoparticles

Iron oxide nanoparticles (IONPs) include zero valent iron (nZVI), magnetite (Fe_3O_4), hematite (α-Fe_2O_3), maghemite (γ-Fe_2O_3), e-Fe_2O_3 and b-Fe_2O_3. nZVI, Fe_3O_4 and maghemite γ -Fe_2O_3 are the main representative of magnetic ENPs and most studied (Tang & Lo, 2013; Ranmadugala et al., 2017). Both the large surface area (due to small size), magnetic properties, and high adsorption capacity of nFe_2O_3 render them suitable for remediation applications (Xu et al., 2012; Tang & Lo, 2013; Kumar & Chawla, 2014; Lei et al., 2018), and as fertilizer (Ali et al., 2016; Ruttkay-Nedecky et al., 2017).

The magnetic, catalytic and reactivity properties of γ-Fe_2O_3 and Fe_3O_4 makes them suitable for use in biomedical applications, such as magnetic resonance imaging, drug delivery, and cell labelling, catalysis, magnetic storage devices, solar energy conversion (Patil et al., 2015; Valdiglesias et al., 2016; Dinali et al., 2017; Lei et al., 2018; Parveen et al., 2018). Fe_2O_3 is also being incorporated into paints (Tiede et al., 2016; Musee, 2017), and also directly applied in water for removal of both inorganic and organic pollutants (Lei et al., 2018). Currently, the predicted environmental concentrations for IONPs are estimated at about 36 ng/L (Wang & Nowack, 2018a). As uses of IONPs increase in the future along with global nanotechnology projections, their environmental concentrations in water will inadvertently increase.

Table 2.1: Examples of commonly used ENPs, their uses and production volumes

ENP	Applications and nanoproducts	Global Production (Tonnes/ year) *	Detected environmental concentration (µg/L)	Predicted environmental concentrations (µg/L)
nFe_xO	Environmental remediation, paint, pigments, drug delivery, cell labelling, magnetic resonance imaging, concrete additive, cements	5.5 – 5500 [1]	-	0.00047 – 0.1 [2] 0.000271 – 0.171 [8]
nZnO	Sunscreen, skin protectant, UV filters, photocatalysis, batteries, food packaging, cements	55 – 10 000 [1] >1 400, 000 [4]	0.09 – 0.61 [3] 20 – 212 [7]	1.5 – 360]5] 0.22 – 1.42 [6] 12.8 – 44.2 [8]

[1] (Piccinno et al., 2012); [2], (Wang & Nowack, 2018b); [3] (Sun, Gottschalk, et al., 2014); [4], (Kunhikrishnan et al., 2015), [5], (Dumont et al., 2015), [6], (Gottschalk et al., 2009);]7], (Choi et al., 2018); [8], (Wang & Nowack, 2018a)

ENPs will also interact with other pollutants that are present in the environment, either conventional or emerging. Their interactions which possibly could exert mixture effects in aquatic organisms either by adsorption and mitigation of toxicity as ENPs do act as carriers for various organic chemicals and heavy metals (Naasz, Altenburger & Kühnel, 2018) or increased effects of the other. One such emerging contaminant that is used in household consumer goods and medical products with high concentrations in aquatic systems is triclosan (Brausch & Rand, 2011; Blair et al., 2013; Sun, Lv, et al., 2014; Lehutso, Daso & Okonkwo, 2017).

2.3.3 Triclosan

Triclosan is broad spectrum antimicrobial agent used in consumer products such as toothpaste, cosmetics, shampoo, household and hospital soap, and is mostly released into drains from these personal care products following use (Lindström et al., 2002; Reiss, Lewis & Griffin, 2009; Clarke & Smith, 2011; Montaseri & Forbes, 2016; Jagini et al., 2019). The halogenated aromatic hydrocarbon has phenolic, diphenyl ether and polychlorinated

biphenyl substructures, and the structural halogenated biphenyl ether chemical properties are similar to other organic ECs such as PCBs, polybrominated diphenyl ethers, bisphenol A and dioxins (Dhillon et al., 2015; Montaseri & Forbes, 2016).

Triclosan has low solubility and a high sorption coefficient (12 mg L^{-1} at 25, 18408 K_{OC}). Hence, it is mostly removed through WWTPs by adsorption to solids (Bock et al 2010). However, the complete removal of TCS in WWTPs is often not achieved, with removal rates varying from about 10 – 100 % due to factors associated with plants design as well as input load and operational conditions (Lehutso, Daso & Okonkwo, 2017). It is one of the widely detected micropollutants at high concentrations ranging from 0 to 5160 ng/L in surface water and wastewater effluent in South Korea, USA, Europe, China, Japan, India and South Africa (Nishi, Kawakami & Onodera, 2008; Ramaswamy et al., 2011; Blair et al., 2013; Ebele, Abou-Elwafa Abdallah & Harrad, 2017; Lehutso, Daso & Okonkwo, 2017; Lyndall et al., 2017). Hence, likely to interact with increasing ENMs concentrations in the environment where synergistic interactions can result to deleterious effects to the aquatic systems.

Although TCS is used for target organisms, the ecological effects for non-targeted biological lifeforms in the environment remain largely unknown (Clarke & Smith, 2011; Dann & Hontela, 2011). For example, TCS ecotoxicological data has demonstrated can induce antibiotics resistance in microbial communities (Drury et al., 2013; Oggioni et al., 2013), cause shifts and altercations in microbial communities (Stasinakis et al., 2008; Carey & McNamara, 2015), and induce high toxicity on aquatic microorganisms compared to other disinfectants (Brausch & Rand, 2011). Toxicity to microorganisms occurs through inhibition of fatty acid synthesis (Ricart et al., 2010; Grandgirard et al., 2015). To date, however, there is little information on the chemical interactions and toxicity of ENPs and TCS on microorganisms, where both classes of ECs are known to be antibacterial.

Modelling results have demonstrated high environmental risk of TCS in aquatic systems (Guo & Iwata, 2017; Musee, 2018a) based on commutated risk quotient of about or above 1. Similar to ENPs, studies on the fate and effects of these ECs in aquatic systems are needed

for effective monitoring and risk assessment purposes. Further, there is a need to consider the toxicological outcomes of their mixture effects with ENPs arising from their co-existence.

2.4 Risk assessment of ENPs in the environment

Uncertainties impedes understanding risks of ENPs in the environment, including their routes into the environment, specific parameters that influence their behaviour and toxicity. This has led to the emergence of ENPs-tailored risk assessment research area termed nanoecotoxicology. Nanoecotoxicology aims to establish the relationship between the presence of ENPs (exposure) and adverse effects on living organisms by the use of specific endpoints in a given environment (Kahru & Ivask, 2012; Peijnenburg et al., 2015; Vale et al., 2016). Considerable efforts have been expended to elucidate the ecotoxicological effects of single ENPs at different position of the taxa in the food chain such as bacteria, aquatic higher plants, crustaceans, among others. Excellent reviews on the effects of ENPs to different organisms (Heinlaan et al., 2008; Baek & An, 2011; Hou et al., 2018), algae (Aruoja et al., 2015), plants (Thwala, Klaine & Musee, 2016), invertebrates and vertebrates (Zhu et al., 2014; Hou et al., 2018).

A myriad of ecotoxicological studies have employed standardised test media following traditional test guidelines for conventional chemicals (Park et al., 2014; Petersen et al., 2015). Although these studies have provided an understanding on species-specific toxicity, however, they fail to take into account the complex environmental parameters essential in fully elucidating the actual effects of ENPs in the ecosystems (Bour et al., 2015; Peijnenburg et al., 2015). Risks of ENPs in environmental systems still require more studies for comprehensive understanding of influences of physicochemical properties of relevant media (e.g. freshwater, groundwater, etc.,) and their contribution to ENPs observed toxicity. For instance, a review by Juganson *et al.* (2015) showed that the most studies were conducted in artificial media (75%, n=224) compared to natural water systems (n=33, 15%). It is therefore important for nanoecotoxicological results be carried out in realistic environmental matrixes to enhance their value in understanding the potential risks of ENPs in the environment. This would provide more information on the three-way relationship

between freshwater chemistry, ENPs attributes, and species responses at different trophic levels.

2.5 ENPs in aquatic systems

Freshwater systems are among the key final sinks of ENPs (Selck et al., 2016; Vale et al., 2016). Wastewater treatment plant effluents are commonly the leading sources of chemical contaminants in surface water due to incomplete/inefficient removal, including ENPs (Kiser et al., 2009; Schriks et al., 2010). ENPs presence in the aquatic environment also occurs from direct use, leachate wash off from agricultural application of sludge, manufacturing and industrial discharges of nanowaste streams (Musee, 2010). As shown in Table 2.1, quantities of released ENPs have largely been determined using modelling approaches by calculating the predicted environmental concentrations (PECs) due to lack of suitable analytical techniques. These models are largely based on global production volumes, production volume in product categories, product release of ENPs and flow coefficients of ENPs between different environmental compartments as input parameters (Keller & Lazareva, 2013; Musee, 2017; Wang & Nowack, 2018a). Upon entry into the dynamic aquatic environment, with varying physicochemical properties, ENPs invariably undergo transformations that alter their fate, reactivity, bioavailability, and ultimately toxicity to aquatic organisms (Peng, Zhang, et al., 2017).

2.6 Fate and behaviour of ENPS in aquatic systems

The fate and behaviour of ENPs is impacted by environmental processes including chemical transformations (e.g. adsorption, dissolution, etc.) and physical transformations (aggregation and disaggregation)) (Lowry et al., 2012; Wang, Zhang, et al., 2016). These transformations are dependent on the variable factors such ENP properties and water chemistry. These are discussed below, with focus on how the ENP properties and water chemistry influence two major transformations: aggregation and dissolution. Processes such as adsorption and surface transformation have a direct influence on the aggregation and dissolution of ENPs, which in turn, are key to elucidating the toxicity of ENPs in aquatic systems.

Environmental fate of ENPs is dependent on their inherent properties such as size, material type and surface modification, and charge (Caballero-Diaz & Cases, 2016; Lead et al., 2018). Physical and chemical transformations of ENPs such aggregation and dissolution are also influenced by water chemistry parameters (see Figure 2.1). The influence of water chemistry components such as pH, natural organic matter (NOM) and ionic strength (IS) have been reviewed elsewhere (Lowry et al., 2012; Garner & Keller, 2014; Vale et al., 2016; Wang, Zhang, et al., 2016; Lead et al., 2018). To date, there has been limited reporting on the transformations of ENPs in most previous nanotoxicity studies, thereby impeding the interpretation of toxicity in relation to the chemical and physical nature of ENPs (Vale et al., 2016). Herein, we examine aggregation and dissolution to create a clear link between the potential transformation and consequent effects ENPs may pose to aquatic organisms.

2.6.1 Aggregation and disaggregation

ENPs tend to form clusters by coming together or combining with other particles, forming larger sizes than the primary particle size. Collision frequency and attachment efficiency of the particles drive the extent of aggregation (Quik et al., 2011). ENPs properties, including their net charge in aqueous media also determine particle interactions (Westerhoff et al., 2008). ENPs either have a positive or negative charge based on the localization of ions towards the outer surface as a result of chemical interactions. ENPs charge is also influenced by pH range in natural water which typically has a pH range from acidic (5.5) to alkaline (8.5) (Westerhoff et al., 2008). This charge determines how the ENPs will interact with macromolecules and/or biological systems (Caballero-Diaz & Cases, 2016).

Depending on the charge on the particles, repulsive or attractive forces can lead to formation of aggregates or disaggregation. In aqueous media, pH influences the stability of ENPs. Surface charge on ENPs either stabilises them if it is strong enough to prevent attractive forces due to Brownian diffusion forces, otherwise, particles will aggregate at their point of zero charge (pH_{PZC}) (Collin et al., 2014; Fatehah, Aziz & Stoll, 2014a). Functional groups present on metal based ENPs generally associate with H^+ and OH^- in aqueous media. In turn,

these interactions determine ENPs stability through surface charge and charge density changes (Peijnenburg et al., 2015; Peng, Zhang, et al., 2017).

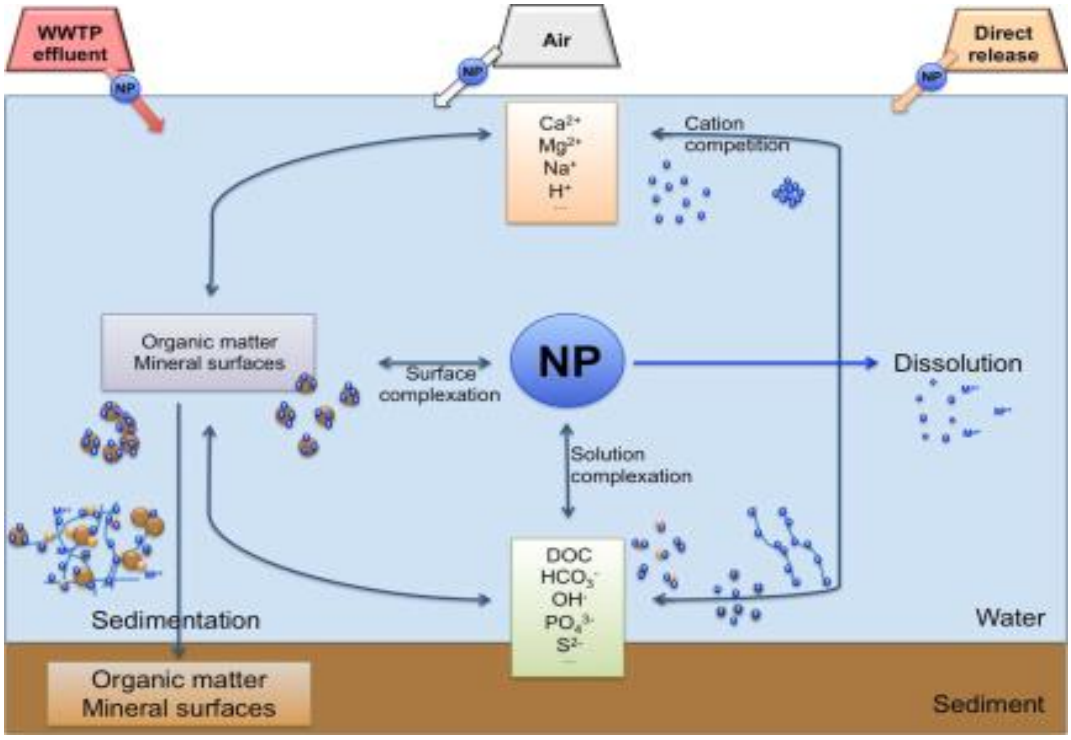

Figure 2.1: Illustration of transformation processes ENPs undergo upon entering aquatic systems. (Figure sourced from Vale et al. (2016) who adapted it from (2015).

Aggregation can also be influenced by water chemistry parameters such NOM and ionic strength in natural water (Baalousha, 2009; Leopold et al., 2016). NOM adsorption occurs mostly via electrostatic interactions and ligand exchange between carboxyl and hydroxyl groups of NOM and hydroxyl groups on ENPs for metal and metal oxide nanoparticles, among other interactions (e.g. hydrophobic interactions and non-covalent bonding), depending on the charge of the ENPs (Wang, Lin, et al., 2016; Yu et al., 2018). Through adsorption of NOM onto ENPs, two aspects can arise. Aggregation may occur through bridging effects (Figure 2.2) of NOM molecules (Philippe & Schaumann, 2014; Wang, Zhang, et al., 2016). Conversely, particles dispersion may take place by stabilization through electrostatic repulsion, increasing their bioavailability and mobility in the aqueous environment (Lowry et al., 2012;

Vale et al., 2016). Although NOM readily coats ENP surfaces in aqueous media, its conformation shifts due to surface charge changes; hence influencing NOM- ENP particle dispersion. Therefore, high pH values would lead to lesser aggregation due to increased electrostatic repulsions whereas increased aggregation would be observed at lower pH for metal-based ENPs.

The ionic strength (IS) of the exposure media plays an important role in the stability of ENPs by altering the electrical double layer (EDL) and surface charge on particles (Keller et al., 2010; Ren, Hu & Zhou, 2016). In high IS media, aggregation is enhanced due to a decrease in the electrostatic repulsive forces between particles. These effects are further affected by ion valency, with higher valence cations such as divalent ions enhancing aggregation (Peng, Tsai, et al., 2017). However, cations can also aid in the formation of NOM enhanced aggregation through cation bridging of NOM molecules between particles (Philippe & Schaumann, 2014; Wang, Zhang, et al., 2016).

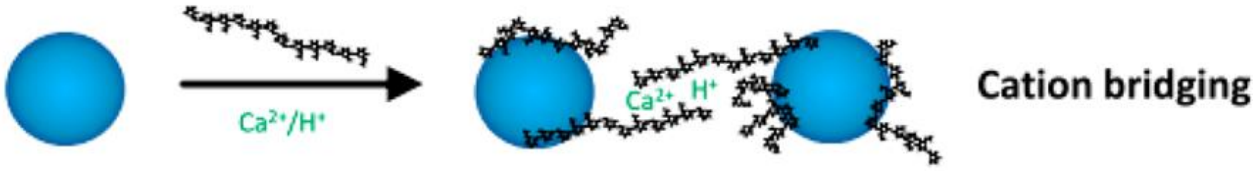

Figure 2.2: Illustration showing the role of cations in formation of ENP aggregates by cation bridging. (This figure is from (Philippe & Schaumann, 2014).

Two types of aggregation, namely; homoaggregation, and heteroaggregation can occur in an aqueous media (Peijnenburg et al., 2015; Goswami et al., 2017). Homoaggregation is the form mainly discussed in the preceding paragraphs, where particles of the same material form aggregates. In the natural environment, however, heteroaggregation is favoured as ENPs will aggregate with natural colloids and any other particles in solution (Quik et al., 2012; Philippe & Schaumann, 2014) as the later prominently outnumbers the former in actual environmental systems. This is especially true in mixture studies where heteroaggregation has been shown to play a role in the behaviour and toxicity of ENPs. These may include ENPs

heteroaggregation with natural colloids such as clay minerals (Wang et al., 2015; Fréchette-Viens, Hadioui & Wilkinson, 2019) or other ENPs (Huynh, McCaffery & Chen, 2014; Tong et al., 2014; Iswarya et al., 2016). For instance, Huyhn et al (2014) showed lessened toxicity of silver ENPs (nAg) through heteroaggregation with α-Fe_2O_3. Aggregation can therefore influence mobility, reactivity, and potential toxicity of ENPs in the environment, whether as individuals or as mixtures as highlighted above

2.6.2 Dissolution

The release of dissolved ions from ENPs is a surface-dependent process that is specific to soluble ENPs e.g. Ag, ZnO, CuO, or Al_2O_3. The release of ions by ENPs typically occurs by oxidation of their surface area where the ENPs physicochemical properties and water chemistry play a significant role (Stabryla et al., 2018). For instance, adsorption of NOM onto ENP surfaces may either accelerate dissolution through complexation, or alternatively inhibit overall dissolution (Klaessig, 2018). Resultant ions from ENPs such as Ag, ZnO, Cu and CuO can also be toxic to aquatic life, changing the route of exposure, dose and nature of ENP toxicity (Misra et al., 2012; Tong et al., 2015; Wilke et al., 2019; Leareng, Ubomba-Jaswa & Musee, 2020).

The role played by released ionic species is an important aspect on nanotoxicity in order to fully understand the risks posed by ENPs in the aquatic systems. For example, the toxicity of nZnO has been associated with dissolved Zn^{2+}, whereas other studies have reported that the mechanism of toxicity may be different from dissolved metal concentrations (Kadiyala et al., 2018). The released metal ions can also interact with the components of the surrounding media, leading to changes in the speciation of the metals through formation of water-soluble complexes as well as precipitates (Baun et al., 2017). Interestingly, both the particulate and dissolved Zn^{2+} have been shown to play a role in the toxicity to bacteria as influenced by the particulate and released ion ratio (Song et al., 2020). Hence, the role of dissolution and resultant released ions needs to be evaluated to understand the toxicity of ENPs, and the mechanisms arising from exposure, including for ENP mixtures as well as other mixtures. For instance, Tong et al. (2014) demonstrated the behaviour of ENPs may be altered when they co-exist where the nZnO dissolution and bioavailable ions were controlled by the presence of titanium dioxide ($nTiO_2$).

Overall, understanding, the transformation of ENPs, especially in complex matrices such as natural water is essential to fully elucidate their risks to aquatic organisms. Numerous studies evaluating the toxicity of ENPs have largely taken no account of physicochemical transformations in the exposure media and conditions in their reporting, limiting the usefulness of important interpretation of exposure, transformation and effects outcomes (Vale et al., 2016; Lead et al., 2018). Secondly, the use of simplistic media that is not representative of the environment, coupled with ENPs concentrations much higher than expected in the environment hampers full understanding of ENPs behaviour and toxicity outcomes (Holden et al., 2016; Lead et al., 2018). The influence of exposure conditions, for example, is important on the relationship between transformations and toxicity of ENPs.

Illumination play a significant role in the toxicity of ENPs with semi conductive and photocatalytic properties such as $nTiO_2$ and nZnO (Barnes et al., 2013; Vale et al., 2016). ENPs such as $nTiO_2$ and nZnO are known to generate photo- induced ROS species due to their ultra-bandgap excitation in solar or UV light (Fatehah, Aziz & Stoll, 2014b). Therefore, physical and chemical changes of ENPs discussed above need to be carefully evaluated to establish the causative effects of ENPs under different conditions, and likely mechanisms of toxicity imparted on organisms to understand the risk and implications of ENPs in aquatic systems.

Recently, studies have reported the fate and behaviour of ENPs in natural water systems under varying exposure conditions (Odzak et al., 2014; Conway et al., 2015; Son, Vavra & Forbes, 2015; Odzak, Kistler & Sigg, 2017; Peng, Tsai, et al., 2017; Adeleye et al., 2018; Xiao, Vijver & Peijnenburg, 2018). For instance, certain findings have demonstrated that the dissolution of ENPs e.g. nAg and nZnO to be highly variant under exposure conditions (e.g. darkness, visible light or UV irradiation) as influenced by different water chemistry parameters as a function of sources (Odzak, Kistler & Sigg, 2017). Thus, to aid realistic risk assessment of ENPs in the environment, toxicity studies under the same conditions as well as relevant exposure media and realistic concentrations are required to elucidate the causative link between ENPs physicochemical properties, transformations, and toxicological outcomes. This is essential for both individual and mixtures of ENPs including with other environmental contaminant classes.

2.7 Nanotoxicity assessment

In nanotoxicity studies, bacteria are good models for toxicological analysis in the ecosystems as they are an important ecological target that offers convenient, rapid and routine way to get meaningful information on likely impacts at the cellular level (Heinlaan et al., 2008; Navarro et al., 2008; Baek & An, 2011; Holden, Schimel & Godwin, 2014). This is important as it aids to understand the relationship between exposure, affected biochemical processes, underpinning mechanisms, and final biological outcomes (Qiu, Clement & Haynes, 2018).

Moreover, bacteria are a primary feed for organisms in water (Holden, Schimel & Godwin, 2014; Hou et al., 2018). In addition, they play an important role in the ecosystem due to their function in natural life cycles such as carbon cycling, decomposition of organic matter, nitrogen ammonia fixation – all important in maintaining ecological integrity (Holden, Schimel & Godwin, 2014). To date, microorganisms such as *Bacillus subtilis*, *Escherichia coli, Shiwanella Oneidensis MR-1, Vibrio fischeri*, *Nitrosomonas europaea* and *Pseudomonas aeruginosa* have been used to assess ENP toxicity (Niazi & Gu, 2009; Fang et al., 2010; Baek & An, 2011; Aal et al., 2015; Tong et al., 2015; Hou et al., 2018). Notably, investigations evaluated for individual ENPs, mixtures of ENPs as well as ENPs and other pollutants, whether assessing cell death or bacterial function as ammonia removal (Yu et al., 2016).

Bacillus subtilis a gram-positive bacterium and an environmentally ubiquitous microorganism has been demonstrated to be highly susceptible to ENPs toxicity compared to other bacteria types e.g. *Escherichia coli*, *Pseudomonas aeruginosa*, and *Staphylococcus areus* (Jiang, Mashayekhi & Xing, 2009; Baek & An, 2011; Emami-Karvani & Chehrazi, 2011; Orou et al., 2018). The bacterium has been used in other toxicity studies in both synthetic (Baek & An, 2011; Rago et al., 2014; Gambino et al., 2015; Luche et al., 2016; Ranmadugala et al., 2017; De Leersnyder et al., 2018; Pramanik et al., 2018) and natural water (Lin et al., 2017; Yi & Cheng, 2017) exposure media. As such, its choice in this work will aid to draw comparisons with studies as referenced above and draw conclusions on possible ENPs and TCS implications to aquatic systems. For example, likely deleterious effects of ENPs and other pollutants on *B. subtilis* may impair their resilience and aquatic environments and important role in ecological systems such association its association with plants (Kunst et al., 1997; Earl, Losick & Kolter, 2008).

2.7.1 Toxicity of ENPs on bacteria

ENPs ability to trigger cell death has traditionally been used to determine the exposure–response (or dose–response) curves and lowest concentrations at which ENPs may not cause death to specific species (Landis & Chapman, in press; Musee, 2018b). However, no observable effect concentrations (NOECs) used in such investigations do not fully account for the biological processes, mechanisms and sub-lethal effects before mortality is observable (Landis & Chapman, in press; Musee, 2018b).

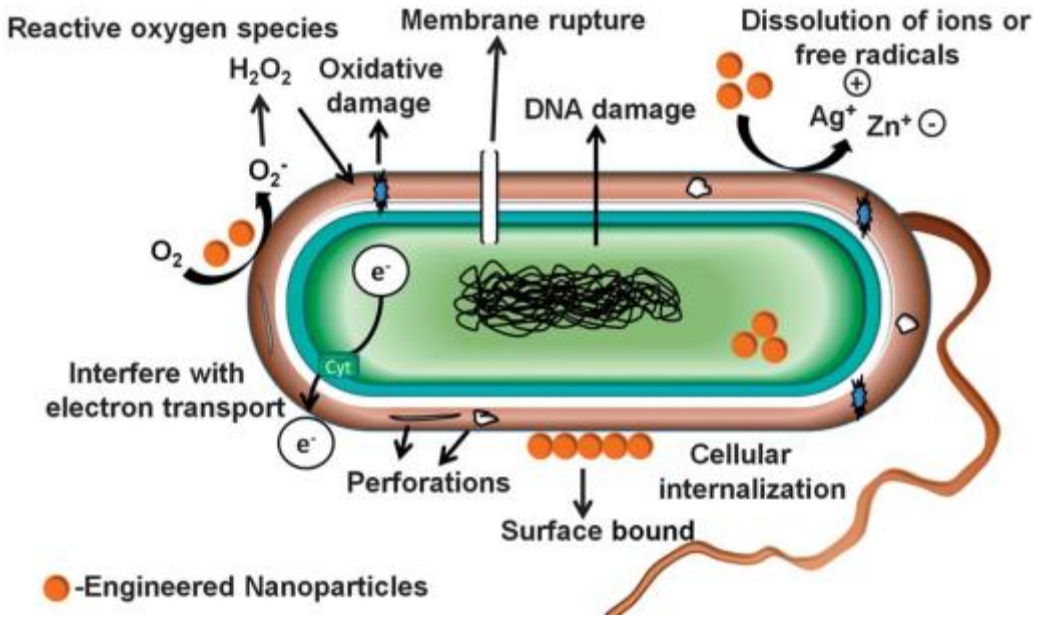

Figure 2.3: Illustration on the potential interactions and modes of toxicity following ENPs interaction with bacterial cells. Various ENP forms may render bactericidal toxicity through one or a combination of these mechanisms. DNA: deoxyribonucleic acid; Cty: cytochromes. (from Suresh et al 2012).

Studies are now beginning to link adverse effects in aquatic organisms to ENPs and their transformation (Qiu, Clement & Haynes, 2018). Moreover, traditional endpoints like viability are gradually being used together with more sensitive receptors to measure other endpoints and elucidate the mechanisms of toxicity (Maurer-Jones et al., 2013; Caballero-Diaz & Cases, 2016; Qiu, Clement & Haynes, 2018). Several endpoints and mechanisms have been

reported, linked to the properties of ENPs, and include cell membrane disruption, release of toxic ions and oxidative stress from ROS production (Hegde et al., 2016; Buchman et al., 2019).

2.7.1.1 Cell membrane disruption

ENPs can impart toxicity by direct contact between their particulates and exterior bacterial cell surfaces (Kang et al., 2007, 2008; Tu et al., 2013; Ivask et al., 2014; Rago et al., 2014; Lai et al., 2017; Mensch et al., 2017). Cell-ENPs interactions at the surface can occur through strong electrostatic attractions between the negatively charged cell membrane and positively charged ENPs. This gives positively charged ENPs more association with bacteria compared to negatively charged ones – and the interaction leads to structural damage of the membrane. However, similar ENPs–bacteria interactions, including for negatively charged particles occur through mechanisms such as hydrogen bonding, van der Waals forces, and receptor–ligand interactions through bacterial cell moieties under weak electrostatic repulsion settings (Jiang, Mashayekhi & Xing, 2009; Wang et al., 2014; Leung et al., 2016; Kadiyala et al., 2018).

Cell membrane bound ENPs can: cause pits and gaps, damage the lipid membrane, disturb vital cell functions and respiratory chain enzymes, and in turn, induce internal signalling pathways, cellular metabolic disturbances, and homeostatic imbalances that may lead to cell death (Jiang, Mashayekhi & Xing, 2009; Tu et al., 2013; Buchman et al., 2019; Farnoud & Nazemidashtarjandi, 2019). nZnO toxicity, for example, has been reported via close contact with bacteria through causation of perforations on the bacterial outer membrane (Rago et al., 2014). Ligand exchange and formation of hydrogen bonds between nZnO have been suggested (Jiang, Mashayekhi & Xing, 2009; Leung et al., 2016; Kadiyala et al., 2018), where the membrane protein structure is modified, electron transport and energy transduction processes interrupted, and ultimately, cell membrane integrity disrupted (Jiang, Mashayekhi & Xing, 2009; Kadiyala et al., 2018).

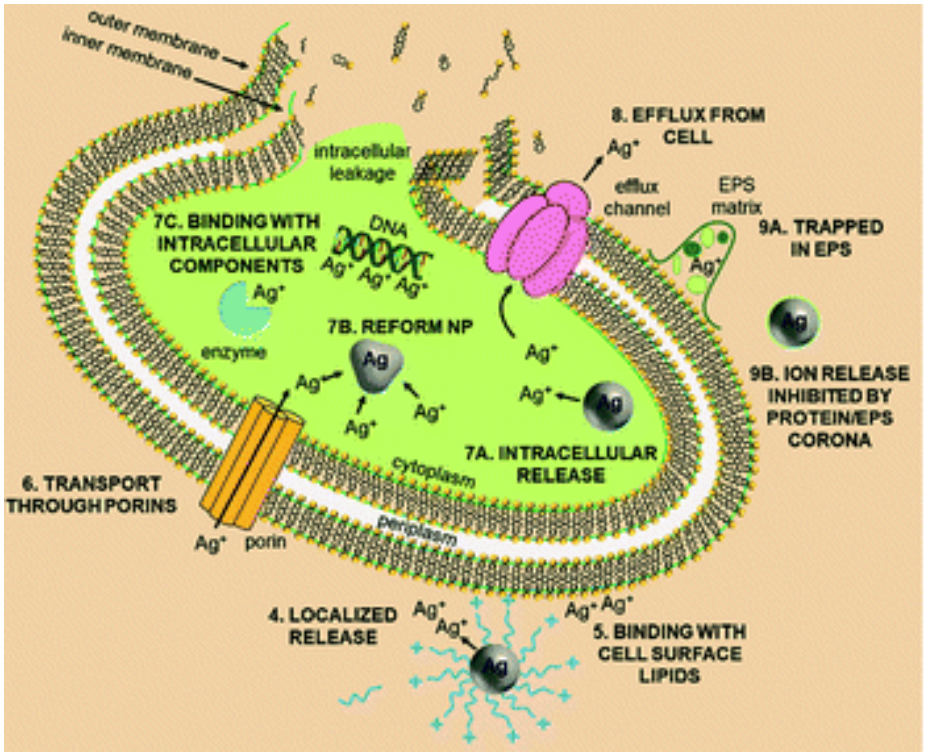

Figure 2.4: Interactions of soluble ENPs (in this case, nAg) with bacterial cells. Cell membrane damage may occur through ENP binding to cell membrane, released ions binding to cell surface lipids, ROS from internalized particulates, all eventually leading to cell rupture and cell death (This figure is published by Stabryla et al. 2018).

Following close contact of ENPs with bacteria, uptake leading to membrane permeability has been reported (Kumar et al., 2011). For example, Kumar et al. (2011) reported uptake and internal distribution of nZnO by *salmonella typhimurium*, linking the toxicity the ENPs to their small size and potential to cross the bacterial cell membrane. However, to our knowledge based on the published literature, no other study has corroborated uptake of nZnO by bacteria.

Metal ions have been shown and linked to damage of the cell membrane through direct interactions with cellular phospholipid membrane, or genetic material (Dupont, Grass & Rensing, 2011; Matuła et al., 2016; Buchman et al., 2019; Leareng, Ubomba-Jaswa & Musee,

2020). Lipid peroxidation from ROS production has also been linked to cell membrane damage (Leung et al., 2016).

Although the role of particulates, released ions and ROS in cell membrane damage are highlighted above, there is no consensus on the ENPs physicochemical properties that predominantly contributes to the disruption of the membrane and the mechanisms through which ENPs alter the structure or disrupt the integrity of the plasma membrane (Farnoud & Nazemidashtarjandi, 2019). However, evaluation of membrane damage to ENPs remain important in assessing the toxicity of ENPs and mixtures of ENPs, and/or with other classes of environmental contaminants. For example, in evaluations of ENPs and their mixtures in all combinations possible for testing, cell membrane integrity assays remain useful as can be rapidly tested as well as the ease to compare results across different studies. For instance, studies by Tong et al. (Tong et al., 2015) and Wilke et al. (2016; 2017; 2018, 2019) investigated individual ENPs and ENPs mixtures under different exposure conditions. The researchers inferred the bacterial effects caused by nAg, nZnO, silver sulphide (nAg_2S), gold (nAu) and platinum nPt) nanoparticles in mixtures with $nTiO_2$ under both dark and simulated irradiation conditions.

2.7.1.2 Toxicity from release of ions

The release of toxic elements by ENPs have been reported to lead to antibacterial effects. Pt-, Au-, Pd-, AgS- and Ti- and FeO_x- based ENPs are regarded to have low toxicity or non-toxic due to their poor solubility and negligible release of ions in aqueous media (Suresh, Pelletier & Doktycz, 2013; Bundschuh et al., 2016). Conversely, ENPs such as nCuO, nAg and nZnO have been reported to be toxic largely due to their dissolved ion species (Du et al., 2018). Although microorganisms and other living organisms require trace metals like Zn, Cu and cobalt for metabolic pathways and enzymatic activities, their ions can be induce toxic effects when present in elevated concentrations beyond required doses (Scherer, Lippert & Wolff, 1983; Jarrell, Saulnier & Ley, 1987; Oleszkiewicz & Sharma, 1990; Florencio, Field & Lettinga, 1994). For ENPs, ions released in the surrounding environment or cell surface-bound particulates are taken up via ion transport proteins responsible for transportation of

essential cations such as sodium (Fabrega et al., 2011). Once in the cells, metal ions may cause denaturation of protein components of the cell wall, bind to enzymes, and genetic material, affect cellular metabolic pathways, and induce oxidative stress (Tong et al., 2015; Buchman et al., 2019).

Dissolved zinc ions from nZnO have been highlighted as one of the main toxicity mechanisms (Heinlaan et al., 2008; Li, Zhu & Lin, 2011; Li, Lin & Zhu, 2013; Aruoja et al., 2015; Tong et al., 2015). Zn^{2+}, a micronutrient for most living organisms, can cause mitochondrial damage, disruption of cellular homeostasis – and ultimately cell damage and death in elevated concentrations (Li, Zhu & Lin, 2011; Li, Lin & Zhu, 2013; Aruoja et al., 2015; Tong et al., 2015). However, one key limitation of these studies on the toxicity of nZnO is that were largely conducted in synthetic media. This is attested by a recent review by Hou et al (2018) which had no study on effects from nZnO in freshwater systems at the time the time of the review.

As discussed in Section 2.6, the concentration of released ions for the ENPs and their resultant toxicity is dependent on the media chemistry. For example, Li et al (2013) illustrated the toxicity of Zn^{2+} to *E. coli* was mitigated by higher concentrations of divalent cations in synthetic water, while complexation of metal ions with NOM and phosphates was also postulated to account for the reduced dissolution of nZnO (Lv et al., 2012; Li, Lin & Zhu, 2013). These outlined transformations thus have direct or indirect influence on the bioavailability and toxicity of nZnO.

Similar outcomes where toxicity was altered due to complexations have also been reported for mixtures results for ENPs as well. For instance, Tong and colleagues (Tong et al., 2015) reported reduced toxicity of $nTiO_2$ by adsorption of ions from nZnO when they co-exist. Huyhn et al. (Huynh, McCaffery & Chen, 2014) demonstrated that co-existence of hematitie (nHe-NPs) and AgNPs mitigated the toxicity of nAg to *E. coli* by limiting the extent of dissolution by the later ENPs. Therefore, from the illustrated examples presented herein, the need to establish the role of released ions in nanotoxicity studies is clear, and especially in mixtures where co-existence of contaminants leads to different set of outcome scenarios.

2.7.1.3 Oxidative stress from ROS

The devastating effects of oxygen-containing molecules in living organisms are typically mediated by superoxide and hydrogen peroxide, which are continuously produced from autoxidation of redox enzymes in living cells. The balance between the presence of oxidants and their counterparts, antioxidant scavenging enzymes and non-enzymes, is maintained below the toxicity-inducing threshold during normal metabolism of oxygen (Manke, Wang & Rojanasakul, 2013; Suresh, Pelletier & Doktycz, 2013; Imlay, 2015).

ENPs can catalyse production of ROS where at elevated concentrations can lead to oxidative stress (Manke, Wang & Rojanasakul, 2013). ROS production can be due to ENPs contact with cells; whereas intracellular can arise from released ions, and, in some instances uptake of ENPs (von Moos & Slaveykova, 2014; Vale et al., 2016) (Figure 2.5).

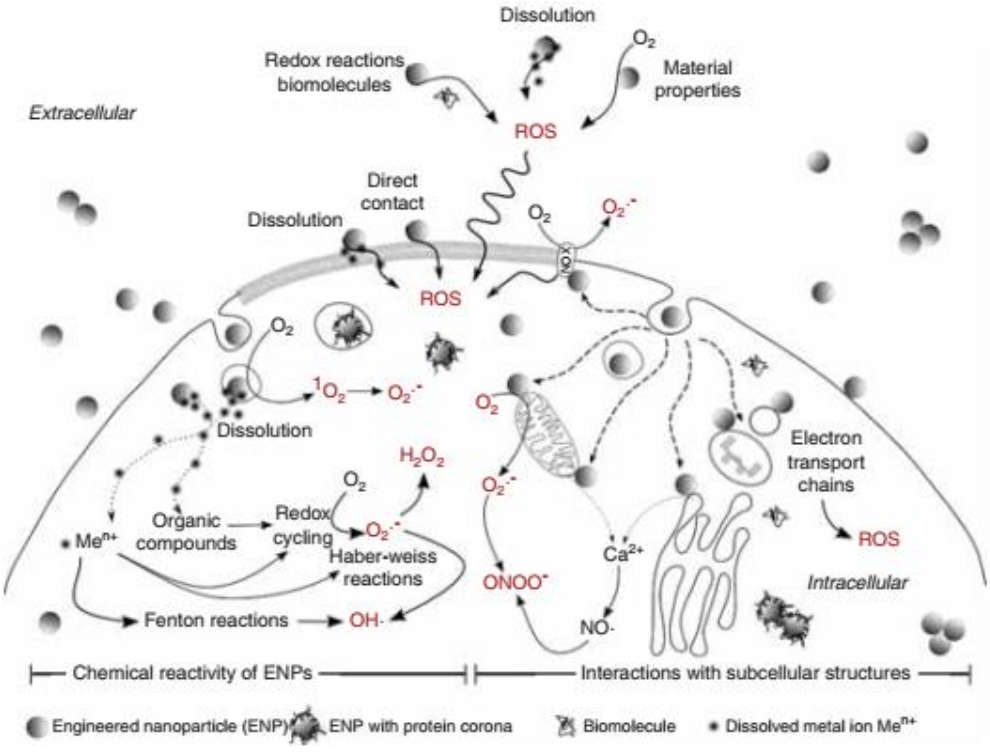

Figure 2.5: Illustration of cellular mechanisms of ROS generation by ENPs. (Image from von Moos et al (2013).

During cell contact with ENPs, electron transfer occurs leading to generation of radicals such as superoxide (O^{2-}), hydroxyl radicals (-OH), singlet oxygen ($O_2\bullet-$), and hydrogen peroxide (H_2O_2) on the ENPs surfaces. These radicals can, in turn, interact with the cell wall membrane leading to damage and subsequent peroxidation of the polyunsaturated phospholipid component of the membrane. Similarly, the same can occur internally if ENPs permeate and enter the cells (Figure 2.5) (Maness et al., 1999; Barnes et al., 2013; von Moos & Slaveykova, 2014; Wang, Lin, et al., 2016)

Due to challenges linked to measurements of ROS generation; raises the need for adaptable and specific tests(Gunsolus & Haynes, 2015; Caballero-Diaz & Cases, 2016; Qiu, Clement & Haynes, 2018). For example, using assays that measure lipid peroxidation, colorimetric and fluorescence of ROS species O^{2-}, -OH, $^1O_2$ and H_2O_2, and general detection of reactive oxygen species (Qiu, Clement & Haynes, 2018). These offer fast, reliable and efficient screening for the variable environmental factors and ever increasing ENPs. Oxidative stress from both nZnO and released Zn^{2+} have been reported to be the cause of observed toxicity in other studies (Leung et al., 2016), where damage to lipids, carbohydrates and membrane integrity loss have been linked to the increased oxidative stress. Although the effects from oxidative stress have been reported under light conditions, other studies have suggested that these effects occur even under dark conditions (Barnes et al., 2013).

Investigations on the toxicity and the mechanisms of ENPs is important to fully understand their risks in the environment. Although the above discussed aspects associated with toxicity such as dissolution and ROS and mechanisms of ENPs on bacteria are well documented as per cited literature, additional data is needed to fully understand their toxicity in environmentally relevant media (e.g. in natural water such as river water), conditions (e.g. NOM, pH, IS, etc.), , dam water, etc.) and concentrations. Assessment of toxicity in environmentally relevant media is limited (Juganson et al., 2015; Holden et al., 2016; Sharma et al., 2019), and in turn, impedes our understanding on key regulating factors on the transformation and toxicity of ENPs under such conditions. For example, ROS production may vary according to shape of ENPs or NOM content in a given exposure media (Lekamge et al., 2020).

Conversely, the dissolution of nZnO may be enhanced or mitigated by the variant media physicochemical properties, with resultant mitigation of toxicity due to certain cations and anions present in aqueous media (Li, Lin & Zhu, 2013). Understanding the toxicity of ENPs requires use of natural media (Gunsolus & Haynes, 2015) since; (i) in synthetic media, varying one ENPs property makes it difficult to fully elucidate other traits since physicochemical properties are integrated, and (ii) the interlinked changes rendered by co-existing variable factors may lead to inaccurate conclusions from singular outcomes (Qiu, Clement & Haynes, 2018). Natural waters from a variety of systems have been studied (Odzak et al., 2014; Odzak, Kistler & Sigg, 2017), fate processes like dissolution have been shown to be affected highly variably by these complex systems (Lead et al., 2018). For example, the toxicity of nZnO was mitigated in synthetic freshwater due to complexations with divalent cations such as Mg^{2+} and Ca^{2+} (Li, Zhu & Lin, 2011). Different fractions of NOM were also shown to mitigate the toxicity of nZnO (Li, Zhu & Lin, 2011; Dasari & Hwang, 2013).

Overall, with almost absence of environmentally relevant studies invariably limits the understanding on the adverse outcomes and ecological consequences. In turn, this impedes the advancement on risk assessment of ENPs in ecological systems. And, evaluation of the same endpoints in the determination of ENPs toxicological outcomes as mixtures (ENPs-ENPs), and with other contaminants is also needed to fully understand the full extent of ENPs risks to the aquatic systems.

2.7.2 Mixture toxicity of ENPs and other pollutants

The concerns of ENPs implications in the environment are also linked to their co-existence with other pollutants as mixtures. These could be mixtures of ENPs or co-existence with other classes of pollutants, where exposed organisms induced effects could significantly exceed the summed effects of the individual mixture components (Deng et al., 2017; Naasz, Altenburger & Kühnel, 2018; Besha et al., 2019). Several studies have evaluated the behaviour, and toxicity of ENPs as mixtures on organisms in aqueous media at different trophic levels (Miranda et al., 2016; Ko, Koh & Kong, 2017; Liu et al., 2017; Pagano et al., 2017; Liu, Nie, et al., 2018), including bacteria, and review will only focus on bacteria (Table 2.2). Interactions of ENPs and bacteria generally may lead to alterations on the transformations of the later. For example, such transformations may include physical (e.g.

aggregation) and chemical changes (e.g. dissolution), which in turn, significantly play a role on their bioavailability and toxicity to organisms. For soluble ENPs e.g. nZnO and nAg, under mixture exposure scenario with non-soluble ENPs different toxicity outcomes compared to their individual effects was observed. For example, Hyunh et al (2014) demonstrated the toxic effects of nAg due to their ionic species were mitigated due to heteroaggregation of positively charged HemNPs and negatively charged nAg. In another study, toxicity of $nTiO_2$ was reported to be mitigated by adsorption of Zn^{2+} form co-exposure with nZnO, preventing surface contact and heteroaggregation of TiO_2 with *E. coli* cells (Tong et al., 2015). A similar effect was observed where adsorption and heteroaggration of $nTiO_2$ with nZnO mitigated the effects of dissolved zinc on *Nitrosomonas europea* (Yu et al., 2016).

Under variant exposure conditions, however, the toxicity outcomes of mixtures have been reported to be different. For example, Tong et al (2015) showed that synergistic effects were observed under UV light exposure conditions; whereas in darkness $nTiO_2$ effects were mitigated by nZnO released ions. Similarly, Wilke et al (2016) showed that the effects of $nTiO_2$ were attenuated when co-existing with nAg under darkness, compared to UV light exposure conditions where synergistic effects were reported (Wilke, Gaillard & Gray, 2017). Further, the complications of joint mixtures were highlighted where formation of nAg from dissolved Ag^+ due to oxidation by $nTiO_2$ occurred (Wilke, Gaillard & Gray, 2017). Similarly, Wilke et al. (2017) reported synergistic effects on cell membrane integrity and ATP levels under simulated solar irradiation but these effects were not observed under dark conditions.

Taken together, these studies show that ENPs toxicity can be altered in joint mixtures. For example, evaluation on the toxicity of IONPs and other ENPs was reported for bacteria (Huynh, McCaffery & Chen, 2014). In their study, the pH was adjusted to 5.5 where the Hem-NPs and nAg were negatively and positively charged, so that heteroaggregation was possible. In another mixture study, heteroaggregation between Hem-NPs and nAg was not observed, however, adsorption of released ions onto the IONPs was reported as the mitigative effect on nAg toxicity on freshwater algae (Huang et al., 2019). Both these studies used bacterial growth media. Therefore, under environmentally relevant media and conditions and concentrations, for Iron based ENPs and other nanoparticles may be different.

In aquatic systems, the presence of organic pollutants may alter ENPs stability. The large surface area of ENPs, e.g. nFe_2O_3 render them suitable for adsorption of organics and metals, and known to adsorb with diverse chemical species in aqueous environments (Srivastava, Gusain & Sharma, 2015; Wilke et al., 2016; Deng et al., 2017; Lei et al., 2018). Due to adsorption of ENPs for other ENPs and micropollutants, formation of aggregates may be enhanced or reduced, altering the reactivity of ENPs (Turan et al., 2019). Triclosan, as discussed in section 2.3.3, due to its presence in aquatic systems, will interact with ENPs. Chen et al. (2018), for example, showed that TCS could be adsorbed by nCu. However, the effects of the mixtures were similar to those of TCS at lower concentrations while at higher nCu concentrations, synergistic effects were observed due to the enhanced dissolution form the TCS stabilised nCu. To date, for bacteria, there are no reported effects for either binary effects of TCS and ENPs, or any ternary system including ENP-ENP- TCS (organic pollutant). Hence, such systems form part of this thesis objective to examine what likely effects may arise or absent thereof in such mixture systems.

Table 2.2: toxicity of ENP binary mixtures to bacteria in aqueous media

Bacteria	ENP properties	Exposure media	Exposure concentrations and conditions	Endpoints and reported effects	Reference
Escherichia coli	nAg; 64.6 nm, spherical, -ve charged HemNPs; 64.6 nm, spherical, +ve charge	phosphate-reduced Davis minimal	2.2 mg/L nAg 1, 5 and 30 mg/L Hem-NPs	nAg inhibited cell growth, whereas cells growth was uninhibited in the mixture.	Huyhn et al. 2014
E. coli, Aeromonas Hydrophila	$nTiO_2$ (P25): P25-TiO_2: 20 ±3 nm, spherical, -17 mV nZnO: spheres, 63.6 nm; rods: 156.6 nm (l),47.1 nm (d), -ve charged	LMW (1 h), pH = 8.2, DOC: 1.77 mg/L, IS : 4.77 mM	Dark and UV light exposure, 1 h 1-25 mg/ L nZnO, 10 mg/ L TiO_2	Bacterial cell membrane damage under UV irradiation for individual ENPs, Non-additive phototoxicity for binary mixture. Reduced $nTiO_2$ -bacterial contact by adsorbed nZnO, Zn^{2+}, and Shown by ATP inhibition rather than ROS.	Tong et al. 2015
E. coli	nAg Size: 7.9 ± 2.4 nm, citrate coated P25-TiO_2: 20 ±3 nm, spherical, -17 mV	LMW, pH 8.2, (Dark conditions)	Dar k conditions, 1 h 5-40 µg/ L nAg, 1-10 mg/ L TiO_2	nAg Concentration -dependent decrease of ATP and minimal effects from TiO_2. As mixtures, higher concentrations of TiO_2 (10 mg/L) significantly reduced minimised effects of nAg through adsorption of ag^{+}.	Wilke et al 2016
E. coli	nAg: Size: 7.9 ± 2.4 nm, citrate coated nAu: 8±1 nm, nPt: 31±2 nm	LMW, pH = 8.2, DOC: 2.41 mg/L, IS : 5.4 mM	I h Dar k conditions, 15 min simulated solar irradiation 0 – 30 u/L nAg, nAu and nPt	No observed effects on ATP level and membrane integrity were observed for tested ENPs under dark conditions. Synergistic effects on cell membrane damage and ATP levels observed for nAng, nAg, and nPt mixtures with $nTiO_2$ due to enhanced Ros production.	Wilke et al 2018a

	P25-TiO_2: 20 ±3 nm, spherical, -17 mV		0, 1 and 2 mg/L		
E. coli	nAg Size: 7.9 ± 2.4 nm, citrate coated P25-TiO_2: 20 ±3 nm, spherical, -17 mV	LMW, pH = 8.2, DOC: 1.77 mg/L, IS : 4.68 mM	Simulated Solar irradiation, 30 min nAg: 0 – 30 ug/L TiO_2: 0, 1, 10 mg/L	No observed effect on ATP levels and cell membrane (TiO_2 lower than 2 mg/L) by nAg while TiO_2 reduces bacterial ATP levels. Cell membrane integrity and ATP levels synergistically reduced by mixtures.	Wilke et al 2018b
E. coli	Ag_2S: 38±18 nm, spherical, -27 mV P25-TiO_2: 20 ±3 nm, spherical, -17 mV	LMW, pH = 8.1, DOC: 2.41 mg/L, IS: 5.4 mM	UV light conditions, 1 h	Depletion of ATP production due to increased ROS production from TIO2 under UV light conditions	Wilke et al 2019
Nitrosomonas europaea	$nTiO_2$, nZnO, $nCeO_2$	Steric cultivation media, pH 7.4-7.5, temperature 28 ^{0}C, DO= 2.0 mg/L	Time: 72 h nZnO: 10 mg/L TiO_2: 0, 1, 10 mg/L	Antagonistic effects observed for $nTiO_2/nCeO_2$ whereas Synergistic effects observed for $nZnO/nCeO_2$ mixtures. NP toxicity caused cell membrane disruption and NPs internalization for each individual NPs. Ternary mixture was not considered.	Yu et al 2016a
Nitrosomonas europaea	$nTiO_2$, nZnO	Steric cultivation media, pH 7.4-7.5, temperature 28 ^{0}C, DO= 2.0 mg/L	Time: 96 h, 1-50 mg/ L TiO_2, 10 mg/L nZnO	More differentially expressed genes noted for nZnO and $nTiO_2/nZnO$ mixture had more differentially expression of genes compared to $nTiO_2$. More stress response genes were down- regulated in $nTiO_2/nZnO$ mixture and $nTiO_2$ compared to nZnO. Thus, $nTiO_2/nZnO$ mixture exhibited antagonistic cytotoxicity.	Yu et al 2016b

Considering that the mixture scenarios highlighted are more likely to occur in the environment, heightens the need to explore the likely interactions of such systems –to fully understand the ecological consequences of ENPs presence and interactions with organic pollutants like TCS in aquatic systems. The role of water physicochemical parameters on the interactions of ENPs and their organic counterparts should also be examined to get a better understanding of their fate and behaviour and toxicity mechanisms and outcomes. Such data and knowledge can inform the necessary steps towards scientific-evidenced based regulation of ENPs. To conclude, given the number of emerging studies on the toxicity of ENPs mixtures, ENPs environmental risk assessment needs a continuous update to contribute to risk assessment needs with different interactions for ENPs. There is also a need to carry out toxicity studies of ENPs with concentrations closer to the those likely to be found in the environment, under relevant exposure conditions (e.g. natural environmental matrixes), and with bioassays that can be easily compared across studies. This will make it possible to fully correlate ENPs behaviour, contribution of water chemistry components and the toxicity outcomes observed across various studies.

Chapter 3: Materials and methods

3.1 Chemicals and reagents

Zinc oxide nanoparticles (nZnO , < 100 nm, 20% dispersion in H_2O, CAS 1314-13-2), iron oxide nanoparticles(γ-nFe_2O_3, < 50 nm, nano powder, CAS 1309-37-1), humic acid (HA), 2′,7′-Dichlorofluorescin diacetate (DCF-DA), Dimethyl sulfoxide (DMSO), Lysogeny broth (Miller) agar and Lysogeny broth (LB) were purchased from Sigma-Aldrich, South Africa. According to the manufacturer, the particle sizes were < 100 nm and < 50 nm for nZnO and nFe_2O_3, respectively. Ultrapure water (18 MΩ cm resistivity, Elga PureLab option system, United Kingdom) was used in all experiments. All other chemicals used were of analytical grade reagents and used as received without further purification.

3.2 Characterization of ENPs

3.2.1 Transmission electron microscopy (TEM) characterization of ENPs

The ENPs size and morphology were characterised by transmission electron microscope (TEM). Samples of both ENPs were dispersed in ultrapure water by sonication for 30 min and a small volume of the ENPs solution was drop cast onto a TEM copper grid, allowed to dry overnight in a desiccator, and imaged using a JEM 2010F TEM (JEOL Ltd., Japan). The TEM images were then analysed using the ImageJ software (National Institutes of Health, USA) to determine diameter measured using imageJ software, based on particle size analysis from several micrographs using at least 100 nanoparticles.

3.2.2 Powder X-ray diffraction (PXRD) analysis

Phase composition was determined using Bruker D8 Advance powder X-ray diffractometer (XRD) with monochromatized Cu Kα radiation (1.54 Å). with Cu Kα radiation at 40 kV and 50 mA. Samples were scanned from a 2θ of 2–80° at a scanning rate of 0.5° min−1 and a

scanning step of 0.02°. All experimental data were analysed with the aid of MDI jade 6.0 software.

3.2.3 Aggregation and zeta potential of ENPs

The hydrodynamic diameter (HDD) of size distributions and zeta potential (ζ-potential) for ENPs suspensions in river water was measured using dynamic light scattering (DLS) on a Zetasizer Nano-ZS instrument (Malvern Instruments, UK) using suspensions of 20 mg L^{-1} nZnO and 5 mg L^{-1} nFe_2O_3. These were measured at post sonication (0 hrs) and after 2 h for different exposure scenarios, respectively. Surface charges are indirectly measured as average zeta potential (ZP) of the particles in suspension via electrophoretic mobility using a Zetasizer. Three measurement replicates for each sample were performed.

3.2.4 Measurement of aggregation kinetics for binary and ternary mixtures

Hydrodynamic diameter (HDD) was measure using dynamic light scattering (DLS) on a Zetasizer Nano-ZS instrument (Malvern Instruments, UK) to determine the size trends of ENPs as a function of time. HDD measurements were carried out every 2 min of 2 h each of the binary and tertiary mixture samples. A maximum of 1 mg L^{-1} for nFe_2O_3 was used to keep aggregate sizes within 1 μm, while 1 and 2 mg L^{-1} nZnO was chosen as the closest environmentally relevant concentration to avoid analytical interference due to dissolution.

3.2.5 Dissolved elemental analysis using ICP-MS

Concentrations of the dissolved ionic species from nZnO and nFe_2O_3 throughout this study were measured by Inductively Coupled Plasma Mass Spectroscopy (ICP-MS). For the preparation, suspensions of ENPs were prepared similar to the experimental conditions, without the bacteria. Nanoparticle suspensions were filtered through regenerated cellulose centrifugal filters with a 3 kDa molecular weight cut-off (Merck Millipore, Darmstadt, Germany) by centrifuging for 15 min at 4000 xg (Eppendorf 5810 R, Eppendorf, Germany), to remove any undissolved ENPs but allow dissolved ions in the aqueous phase to pass. The filtrate from the ENP suspensions were then acidified with 5 μL of concentrated HNO_3. Quantitative analysis on the concentration of dissolved ions in the supernatant was analysed

by inductively coupled plasma mass spectrometer (ICP-MS) (ICP-MS, ICPE-9820, Shimadzu, Japan or 7900 ICP-MS, Agilent Technologies, South Africa).

Visual MINTEQ (Version 3.1, https://vminteq.lwr.kth.se) was used to predict speciation of zinc in ER and BR water based on parameters listed in Table 4.1. The Stockholm Humic Model (SHM) was used with default parameters as model inputs, and solid mineral zincite was selected to mimic solid nZnO.

3.3 Freshwater sampling and analysis

The freshwater samples used for the experiments were collected from two river systems; the Elands River (25°32'58.4"S 28°33'53.4"E, Gauteng Province, South Africa), and Bloubank River (26°01'20.3"S 27°26'31.6"E, North West Province, South Africa). These water samples were chosen to represent different complex environmental surface freshwater systems. The collected river water was filtered using Whatman No. 1 filter paper (pore size: 11 µm) followed by filtration through 0.2 µm pore sized membrane filters to remove microorganisms and larger particles. All water samples were stored at 4°C until analysis.

The chemical analysis of freshwater samples (Table 1) was performed in a certified laboratory (based on the South African National Accreditation System, SANAS) using the following standard analytical methods. The anions of Cl^-, NO_3^-, SO_4^{2-}, PO_4^{3-} and cations of Na^+, K^+, NH_4^+, Ca^{2+}, Mg^{2+} in the water samples were determined using the colorimetric methods and inductively coupled plasma- optical emission spectroscopy analysis, respectively. pH and electrical conductivity were measured by potentiometric determination (pH meter) whilst the DOC was determined by high temperature combustion using a Shimadzu – Total Organic Carbon analyser. The water was only kept for 90 days from every sampling date, and the physicochemical properties of both river water systems were analysed, and results are listed in Table 4.1 and Table 5.1.

3.4 Bacterial maintenance and preparation

The *Bacillus subtilis* (ATCC 11774) strain was purchased from Anatech (Johannesburg, South Africa). The culture was maintained on sterilized lysogeny broth (LB) agar plates and stored at 4°C until use. For exposure studies, a single colony was incubated in 100 mL of LB broth in a 500 mL Erlenmeyer flask, at 30°C with shaking at 150 rpm overnight until cells reached mid-exponential phase (0.4 – 0.5 at OD_{600nm}). 25 mL of the bacteria culture were transferred then transferred to 50 mL centrifuge tubes, and the cells were harvested by centrifugation at 7 500 g for 5 min, and subsequently washed them once with physiological saline (0.85 % NaCl) followed by filtered river water. Following washing, the bacterial cells were re-suspended in filtered river water, adjusted to an optical density of ~1 at 600 nm, ready to be used for exposure studies.

3.5 Bacterial exposure conditions for single and mixtures

3.5.1 Single ENPs exposures

For exposure studies, a single colony was incubated in a LB broth at 30°C with shaking at 150 rpm overnight until cells attained mid-exponential phase (0.4 – 0.5 at OD_{600nm}). The cultured cells were harvested by centrifugation at 7 500 g for 5 min, and subsequently washed them once with physiological saline (0.85 % NaCl) followed by filtered river water. Following washing, the bacterial cells were re-suspended in filtered river water, adjusted to an optical density of ~1 at 600 nm, ready to be used for exposure studies.

Stock solutions of ENPs at a concentration of 200 mg L^{-1} were prepared using ultrapure water and sonicated for 20 min in an ultrasonic bath prior to exposure experiments. Exposure experiments were conducted in 250 ml flasks at a final volume of 25 mL. The ENP nominal concentrations used were 10, 100 and 1000 1000 µg L^{-1} nZnO, and 10, 100 and 10 000 µg L^{-1} for nFe_2O_3, and contained bacteria at OD600 of ~0.3 at 600 nm, which corresponds to 10^8 cells mL^{-1} as measured by plate counting. The control samples contained the bacteria

without the ENPs. All exposure tests were carried out at room temperature (20 –23°C) on a rotating shaker at low 75 rpm for 2 h under visible light (338 lux).

3.5.2 Binary mixtures exposures

Exposure cultures were prepared by inoculating a single colony from overnight solid agar plates into LB broth and shaken for 4 h at 30 °C until mid-exponential phase (0.4 – 0.5 at OD_{600nm}). Following centrifugation at 4500 xg for 10 min, cells were subsequently washed twice and lastly resuspended in the filtered river water. The cells were finally diluted to a final concentration of 2 x 10^8 cells/mℓ as measured by plate counting. Nominal concentrations of 0, 500, 1 000, 2 000 and 5 000 µg L^{-1} for nZnO; and 1 000 µg L^{-1} nFe_2O_3 were used to assess toxicity in a final volume of 20 mL in 250 mL flasks from Stock solutions of 200 mg L^{-1} nZnO and nFe_2O_3 were prepared in ultrapure water (18 MΩ cm resistivity, Elga PureLab Option System, United Kingdom) and sonicated for 10 min in an ultrasonic bath prior to exposure experiments. The combined toxicity of both ENPs were assessed by using 500, 1000, 2000 and 5 000 µg L^{-1} nZnO with 1 000 µg L^{-1} of nFe_2O_3. All exposure studies were done under natural sunlight at noon at the university of Pretoria, South Africa by placing them in a tub with water to maintain incubation temperature for all samples (Dasari, Pathakoti & Hwang, 2013), and incubated for 30 min.

3.5.3 Ternary mixtures exposures

TCS stock solution was prepared in analytical grade acetone (> 99%) to a concentration of 1 g L^{-1}. Exposure experiments in both river water samples were conducted in 250 mL flasks, with 20 mL different nominal concentrations of 0 – 200 mg/L for nZnO, 0 – 250 mg L^{-1} for nFe_2O_3 and 0 – 100 µg L^{-1} for TCS. The concentrations of ENPs were fixed to 1 000 µg L^{-1} nZnO, and 1 000 µg L^{-1} nFe_2O_3, which were tested with varying concentrations of 1, 10, and 100 µg L^{-1} TCS. Bacteria were diluted to and contained bacteria at OD600 of ~0.3 at 600 nm, which corresponds to 10^8 cells mL^{-1} as measured by plate counting. The control samples contained the bacteria without the ENPs. All exposure tests were carried out at room temperature (20 –23°C) on a rotating shaker at low 75 rpm for 2 h under visible light (338

lux). These conditions were selected to avoid or minimise any transformation of TCS by ENPs solar and UV irradiation.

3.6 Bacterial cell viability

Both exposed and non-exposed (control) bacteria exposure samples were serially diluted in 0.85% NaCl, and then viable bacteria were determined on LB agar plate following the drop count method (Miles e t al. 1938). For the drop count method, nine drops of each 20 µL each, were transferred onto solid LB agar medium. The plates were incubated overnight at 37°C. The viability of the bacteria in the ENPs suspensions was measured by counting the number of colony forming units (CFU) from the appropriate dilution on nutrient agar plates. Hence, the percentage of viable cells was determined by comparing CFU per mL of the culture as a ratio of the number of CFU from ENPs exposed samples to non-exposed (control) samples following 2 h exposure. The viability experiments were repeated twice with three replicates.

3.7 Membrane cell integrity assays

The Live/Dead BacLight kit (Molecular Probes, US) was used to test the cell membrane integrity of bacteria following exposure to ENPs. Hundred-µL of ENPs exposed and non-exposed (control) samples were transferred to individual wells in a 96-well microplate (Greiner Bio-One, Austria), combined with 100 µL of SYT09/PI mixture (10/60 µM), and mixed thoroughly. The PI and SYTO9 stain nucleic acids were used to differentiate between cells that were intact (live organisms–stained in green) and damaged cells (dead organisms – stained in red), respectively. The microplate was then incubated with assay reagents for 15 min at room temperature (20–23°C) in dark. Fluorescence was measured with excitation and emission wavelengths for SYTO9 and PI of 485/538 nm (green) and 485/635 (red), respectively, using a Flouroscan Ascent FL microplate reader (ThermoFisher, USA). A calibration curve was obtained using cells with known percentages of intact cells, where each set of experiment was done in triplicates in two microplates.

3.8 Bacterial ATP levels

Bactiter-Glo assay (Promega, Germany) was used to measure the bacterial ATP levels as described elsewhere (Tong et al., 2015; Wilke et al., 2016). The luminescence-based assay measures luminescence signal intensity from reaction of luciferin and ATP signifying the extent of ATPs. Hundred-µL of ENPs exposed and non- exposed (control) samples were transferred to individual wells in a 96-well microplate (Greiner Bio-One, Austria), combined with 100 µL, and mixed thoroughly. The microplate was then incubated for 5 min at room temperature (20–23°C) in the dark (wrapped with aluminium foil). The luminescence signal was measured using the Flouroskan Ascent FL microplate reader. Three replicates of each experimental condition were included in two microplates. The potential interference of the ENPs with this assay were analysed and corrected from the results.

3.9 Analysis of oxidative stress in bacteria

3.9.1 Intracellular ROS

Intracellular ROS following exposure to the ENPs in the river water systems was determined as measure of oxidative stress, using the membrane permeable non-fluorescent dye 2′, 7′-dichlorofluorescin diacetate (DCF-DA, Sigma Aldrich). DCF-DA is converted into the fluorescent 2′, 7′-Dichlorofluorescin (DCF) after reacting with ROS, thus making the cell to fluoresce.

3.9.1.1 Preparation of DCF-DA and storage

30 mM DCFH-DA stock solution was prepared by dissolving 50 mg (97 %, Sigma Aldrich) in 3.4 mL DMSO. The stock was maintained at -20°C and wrapped with aluminium. For working concentration (100µM), 33. 33 µl of 30 mM solution added to 1966.67 µL of DMSO.

3.9.1.2 ROS assay using DCF-DA

Following the 2 h exposure, 150 µL of the exposure samples and the control were incubated with DCF-DA (100 µM final concentration) for 30 mins at 37°C. DCF fluorescence intensity was then measured using a Flouroscan Ascent FL microplate reader (ThermoFisher, USA) at an excitation and emission wavelengths of 485 and 538 nm, respectively, to quantify ROS activity both in the treated and control groups. ROS production was expressed as percentage fluorescence of the control over the exposed samples. Three replicates of each experimental condition were done two microplates.

3.10 Detection of nanoparticle- induced reactive oxygen species (ROS) in exposure media

Colorimetric and luminescent molecular probes were used for quantification of ROS species. For the preparation, suspensions of ENPs were prepared similar to the experimental conditions, without the bacteria. All tests were performed in 96-well microtiter plates, with three replicates were performed for each measurement.

3.10.1 Quantification of $O_2^{\bullet-}$

Hundred and eighty-µL of ENPs were made by diluting stock solutions to 500, 1 000, 2 000, and 5 000 µg L^{-1} of nZnO, alone or with 1 000 µg L^{-1} nFe_2O_3, and 20 µL of 100 mM XTT were added to wells of a 96 well plate. The plates were placed under solar irradiation for 30 min. Following exposure, absorbance of the orange-coloured XTT formazan formed by reaction of $O_2^{\bullet-}$ was measured at wavelength 470 nm using a UV-Vis spectrophotometer (xMark microplate absorbance spectrophotometer, Bio-Rad).

3.10.2 Quantification of $^{\bullet}OH$

Hundred and eighty-µL of ENPs were made by diluting stock solutions to 500, 1 000, 2 000, and 5 000 µg L^{-1} of nZnO, alone or with 1 000 µg L^{-1} nFe_2O_3, and 20 µL of 100 µM HPF were added to wells of a 96 well plate. The plates were placed under solar irradiation for 30 min.

Following exposure, fluorescence was measured on a Flouroskan Ascent FL microplate reader (Thermo Fisher), with excitation and emission wavelengths of 485 and 538 nm, respectively.

3.10.3 Quantification of H_2O_2

Hundred and eighty-µL of ENPs were made by diluting stock solutions to 500, 1 000, 2 000, and 5 000 µg L^{-1} of nZnO, alone or with 1 000 µg L^{-1} nFe_2O_3, were added to 96 well plates and combined with 180 µL of Milli-Q (MQ) H_2O. The plates were placed under solar irradiation for 30 min. After exposure under the sun, 10 µL each of 1 g/L phenol red (Sigma-Aldrich), 0.5 mg/mL horseradish peroxidase (type II, salt-free powder, Sigma-Aldrich in DMSO), and 0.77 M NaOH were each added to every well and mixed thoroughly. reagents were added to the plate after SSI exposure to prevent phenol red damage by the light. The absorbance at 610 nm was measured to detect the oxidation product of phenol red and hydrogen peroxide. The absorbance of the purple coloured product from the reaction of the phenol red and hydrogen peroxide was measured at wavelength of 610 nm.

3.11 Microscopic observations of bacterial cells

3.11.1 Whole cells

TEM was used to observe the direct contact between the NPs and the bacterial cells. A drop of the bacteria exposed to the NPs and the NP-free control was placed onto a copper grid, air-dried for 24 h and was then imaged by the TEM.

3.11.2 Cross-sections of bacterial cells

To observe the internalization and localization of the NPs in the cells and the changes in cellular structure as affected by the NPs, NPs exposed, and non-exposed bacteria were fixed in 2.5% glutaraldehyde, dehydrated in graded concentrations of ethanol (50%, 70%, 80%, 90%, 95% and 100%) for 15 minutes at each step and transferred to absolute ethanol for 20 minutes. The samples were immersed in 1:1 and subsequent 1:3 mixtures of ethanol and

epoxy resin for 1 h and 4 h, respectively, and then let to polymerize for 36 h. Ultrathin sections were cut, stained with uranyl acetate and lead citrate and observed with TEM (Huang & Yeung, 2015).

3.12 Statistical analysis

Data herein are expressed as mean with corresponding standard deviation (SD). Two-way analysis of variance (ANOVA) was used to evaluate statistical differences followed by *post hoc* Tukey's multiple comparisons tests. Differences between samples were considered statistically significant when $p < 0.05$ in all cases. All analyses were done with GraphPad Prism V7.04 (GraphPad Prism software Inc., San Diego, CA, USA) unless otherwise stated.

Chapter 4: Zinc oxide and iron oxide engineered nanoparticles toxicity on *Bacillus subtilis* in river water systems

This chapter investigates the toxicological effects of nZnO and nFe_2O_3 as influenced by natural water chemistry characteristics. The cell viability, membrane integrity, ATP production and oxidative stress responses of *B. subtilis* were assessed. This was done to better understand the risk of these ENPs in microorganisms in natural water matrices.

4.1 Natural water characteristics

Composition of the river water samples is presented in Table 4.1. Both river water samples had pH around 8. Bloubank River (BR) water had higher concentration of major elements and thus a higher ionic strength compared to Elands River (ER) water. Dissolved organic matter (DOC) content was significantly higher in in BR water than in ER water (Table 4.1).

Table 4.1**:** Physicochemical parameters of freshwater samples from Bloubank and Elands River (July 2018)

Parameter	Unit	Bloubank River (BR) water	Elands River (ER) water
pH		7.9	8.1
DOC[a]	mg C L^{-1}	8.25	5.51
Electrical conductivity	ms/m 25°C	39.8	19.6
COD[b]	mg L^{-1}	21.3	6.67
Alkalinity	mg L^{-1}	217	75.6
NH_4	mg L^{-1}	3.4	4.27
NO_3	mg L^{-1}	0.2	0.33
Cl^-	mgL^{-1}	12.9	17.1
SO_4	mg L^{-1}	6.77	9.03
PO_4	mg L^{-1}	1.23	0.57
Fe^{3+}	mg L^{-1}	<0.004	<0.004

Zn^{2+}	mg L^{-1}	0.01	0.008
Ca^{2+}	mg L^{-1}	36	14
Mg^{2+}	mg L^{-1}	31	9.82
Na^{+}	mg L^{-1}	22.4	15.6
K^{+}	mg L^{-1}	3.13	4.24
IS[c]	mM	4.94	2.45

[a]Dissolved organic matter; [b] Chemical oxygen demand; [c] Ionic strength, calculated by Visual MINTEQ, ver. 3.1.

4.2 Nanoparticles characterization

The γ-nFe_2O_3 had a hexagonal shape and an average particle size of 41 ± 25 nm. nZnO exhibited non-uniform shapes consisting of hepta-, penta-, hexa-gonal, and rod shapes, with diameter ranging from 15 to 57 nm due to asymmetry of the morphology. The representative TEM images of the ENPs are shown in Figure 4.1 a, b, e and f. Results from XRD revealed the crystalline phase of nZnO was zincite (Figure 4.1 1 c) whereas that of nFe_2O_3 was maghemite (γ-nFe_2O_3) (Figure 4.1 d). The ζ-potential for both ENPs were negative in all river water samples (Table 4.2), and at narrow range between -12.3 ± 0.6 and -15.1 ± 1.3 mV. Zetasizer results indicated immediate aggregation of nZnO and nFe_2O_3 in both river water samples post-sonication (Table 4.2). nZnO had average sizes of 512 ± 22 and 1 069 ± 187 nm in ER and BR, respectively, whereas nFe_2O_3 had HDD of 958 ± 188 nm and 1 056 ± 120 nm in ER and BR, respectively (Table 4.2). High aggregation of ENPs observed in both river water samples was associated with low ζ-potential of between -12.3 ± 0.6 and -15.1 ±1.3 mV; considered to be too low as ζ-potential of above ± 30 mV is required to maintain ENPs dispersed by charge stabilization (Hitchman et al., 2013), or against aggregation, or

dispersion (Riddick, 1968; O'Brien & White, 1978; Lowry et al., 2016). For both ENPs, increased aggregation was more significant in BR compared to ER after 2h (Table 4.2).

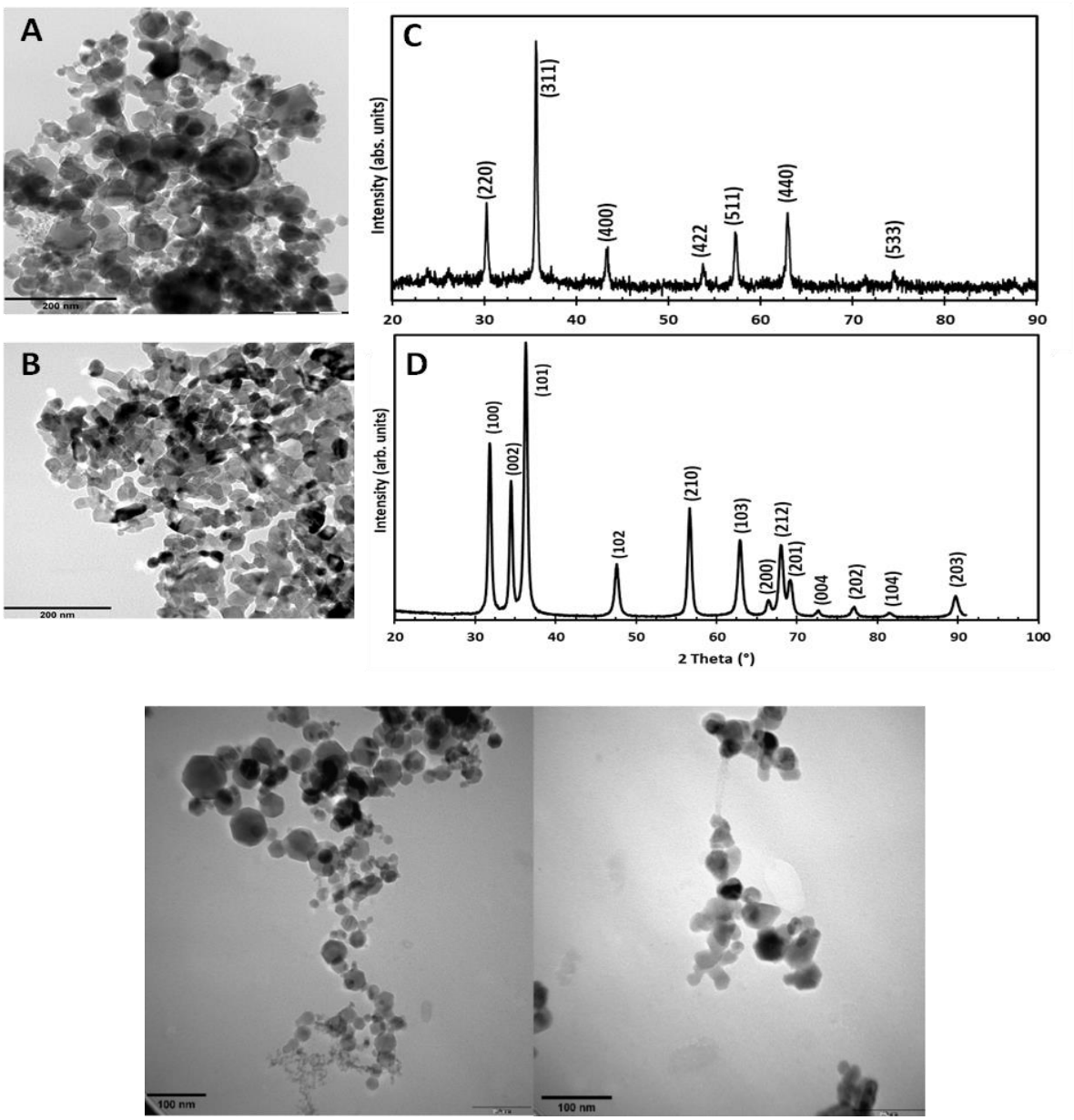

Figure 4.1: TEM images of (a and e) nFe_2O_3 and (b and f) nZnO. XRD patterns of (c) nFe_2O_3 (d) nZnO.

Table 4.2: Hydrodynamic diameter and zeta potential of ENPS in river water samples

Parameter	nZnO (20 mg L^{-1})		γ-nFe_2O_3 (5 mg L^{-1})	
	Bloubank River	Elands river	Bloubank river	Elands river
ζ^a (mV)	-13.4 ± 0.4	-15.1 ± 0.6	-12.3 ± 1.3	-15.1 ± 1.3
$D_h{}^b$ (nm), 0 h	1069 ± 187	512 ± 22	1056 ± 120	958 ± 188
D_h (nm), 2 h	1372 ± 257	557 ± 29	1627 ± 194	1098 ± 287

Figure 4.2 summarizes dissolution results of nZnO in both river water samples. Fe ions could not be detected as their concentration were below analytical detection limit. Indeed, nFe_2O_3 are known to exhibit very low or no dissolution in aqueous matrices (Lei et al., 2016; Wang, Lin, et al., 2016).

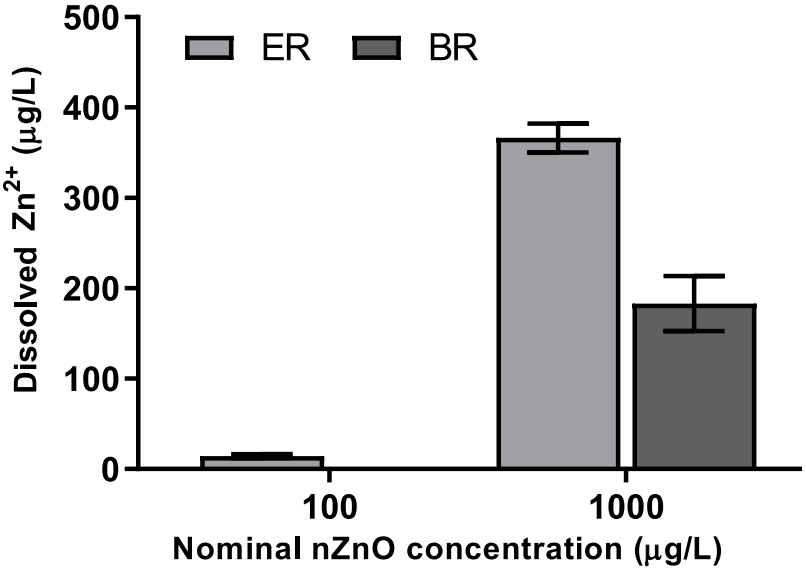

Figure 4.2: Dissolved zinc concentrations in the river water samples following 2h incubation under visible light. Errors bars denote standard deviation (n = 3). Concentration of 100 µg L^{-1} ZnO in BR below detection limit (10 µg L^{-1}, not shown). Nominal nZnO exposure concentrations used were 100 and 1000 µg L^{-1}.

Dissolution of nZnO was observed to be concentration-dependent in similar fashion to earlier studies (Li et al., 2010; Li, Lin & Zhu, 2013; Musee et al., 2014; Rago et al., 2014). At

nominal exposure concentration of 100 µg L^{-1}, 14 µg L^{-1} of Zn^{2+} ions were measured in ER compared to less than 2 µg L^{-1} in BR. At higher nominal exposure concentration of 1000 µg L^{-1}, higher dissolution of nZnO was observed in ER and BR water at values of 366 and 183 µg L- Zn^{2+}, respectively.

The observed differences in aggregation and dissolution in ER and BR were attributed to differences in water physicochemical properties (Table 4.1); which are known to influence the transformation processes of ENPs in aqueous matrices (Wang, Zhang, et al., 2016; Odzak, Kistler & Sigg, 2017; Peng, Tsai, et al., 2017). Natural organic matter (NOM) coating on ENPs in aquatic systems can either enhance or inhibit their aggregation and stability through mechanisms like electrostatic interaction and ligand exchange, among others (Baalousha et al., 2008; Philippe & Schaumann, 2014; Khan et al., 2018; Yu et al., 2018). Moreover, it has been reported that under high IS conditions and in the presence of NOM, likely cation binding enhances the aggregation of ENPs (Collin et al., 2014; Wang, Zhang, et al., 2016; Khan et al., 2018).

In this study, aggregation of both ENPs was observed, with larger aggregate sizes in BR. This may be due to higher NOM content in BR (Table 4.1) that could have resulted in adsorption onto ENPs surfaces, likely through ligand exchange since both ENPs were negatively charged in both water samples. This is because NOM is known to strongly adsorb due to ligand exchange between carboxyl and hydroxyl groups of NOM, and the hydroxyl groups on ENPs (Wang, Zhang, et al., 2016). Both river water samples had high NOM content (> 5 mg L^{-1}) which is within reported range of 0.1 to 30 mg L^{-1} in surface water (Nebbioso & Piccolo, 2013; Philippe & Schaumann, 2014; Louie, Tilton & Lowry, 2016), and therefore, rendered NOM dependent aggregation highly likely (Philippe & Schaumann, 2014; Wang, Zhang, et al., 2016).

Secondly, differences in IS with both monovalent and divalent ions being higher in BR compared to ER (Table 4.1), could also explain the enhanced aggregation in the former, as such conditions are known to increase NOM and ENP complexes (Miao et al., 2010; Bian et al., 2011; Philippe & Schaumann, 2014; He et al., 2015). Increased aggregation in BR were also linked to higher concentration of electrolytes (mainly divalent ions e.g. Ca^{2+}, Mg^{2+}, etc.)

via compression of the electric double layer (EDL) through the reduction of electrostatic repulsion between particles and/or formation of aggregates by cation bridging (Miao et al., 2010; Zhou & Keller, 2010; Musee et al., 2014; Wang, Zhang, et al., 2016) . Consequently, nZnO dissolution in BR was significantly lower due to reduced surface area as larger aggregates were formed compared to those in ER water samples. Released Zn^{2+} from nZnO could have also been reduced due to complexation with NOM and PO_4, resulting to lesser concentration of ions measured in BR water. Li et al. (2013) and Lv et al. (2012) showed that release of Zn^{2+} decreased with increasing concentrations of PO_4 due to strong metal-complexation between the phosphates and metal ions. In this study, BR water had higher concentration of PO_4 than ER water, pointing to reduced bioavailability of the ions in the former.

The observed differences in the dissolution of nZnO were therefore linked to differences in aggregation and water chemistry component differences observed between ER and BR water samples. Similarly, results of Odzak et al. (2017) indicated enhanced aggregation and low dissolution of nZnO in freshwaters sourced from river and lake waters with high IS ranging between 3.4 and 6.4 mM compared with those characterized by low IS. These researchers' results are consistent with findings reported herein where in BR water samples with high IS of 4.95 mM had higher aggregation and low dissolution of nZnO when compared to low aggregation and high dissolution observed in ER with low IS of 2.45 mM.

Overall, results therefore point to NOM coating-controlled release of ions from ENPs in freshwater due to the blockage of active sites – which in turn – inhibits the diffusion of ions from ENPs surfaces; thus accounting for high aggregation and low dissolution observed in BR water samples characterised by both high NOM, and IS. In addition, complexation of metal ions with NOM and phosphates could also account for reduced dissolution of nZnO. These outlined transformations have direct or indirect influence on the bioavailability and toxicity of nZnO and γ-nFe_2O_3 in the two freshwater systems as discussed in the following sections.

4.3 Cell viability and membrane integrity

Results of *B. subtilis* exposure to nZnO and γ-nFe_2O_3 in ER and BR revealed distinctive cytotoxic effects (Figure 4.3 a and b). At higher concentrations of 100 and 1000 μg L^{-1}, nZnO

reduced *B. subtilis* viability in ER with markedly significant effects observed at 1000 µg L^{-1} ($p \leq 0.001$); whereas at 10 µg L^{-1} nZnO no viability inhibition was apparent. Conversely, exposure to nZnO in BR had no effect on cell viability at all tested concentrations (Figure 4.3 a) which was linked to larger aggregates formed in BR water samples as discussed in nanoparticles characterization section. This is because larger aggregates could not compromise cell integrity due to limited or lack of contact with cells. For the γ-nFe_2O_3, irrespective of the exposure concentration (10 – 10 000 µg L^{-1}) no effect on cell viability were observed in both water samples (Figure 4.3 b).

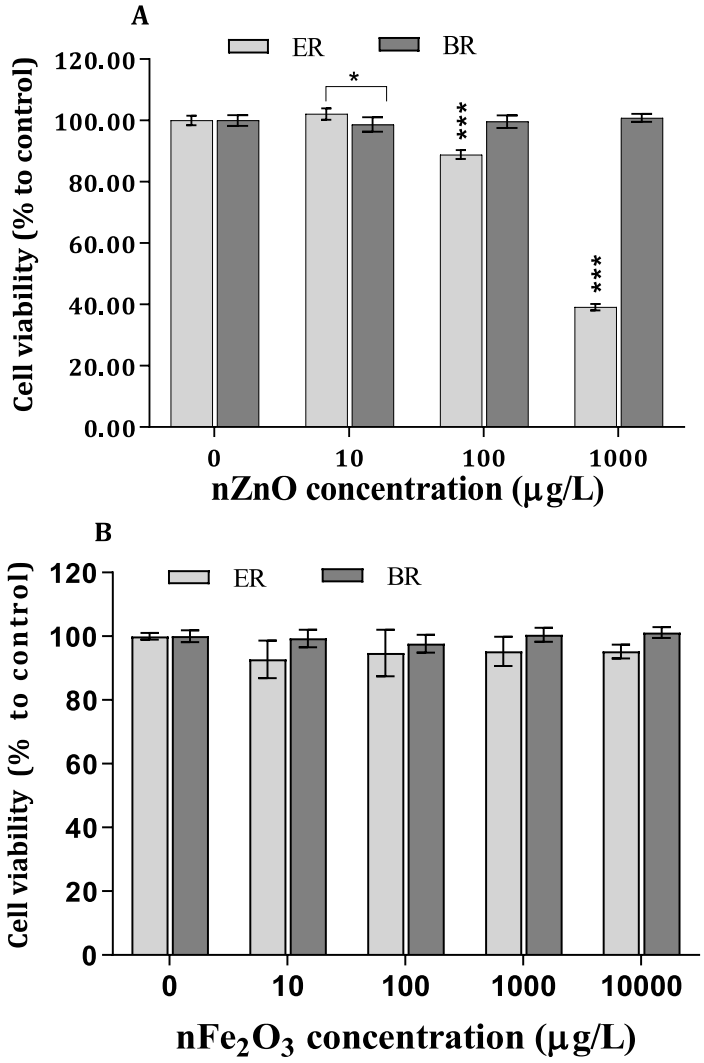

Figure 4.3: Effects of (a) nZnO and (b) γ-nFe_2O_3 on B. subtilis viability in river water. Data represents the average ± SD (n=3). Asterisks (*) represent significance levels from Tukey's post hoc tests in two-way ANOVA (*$p < 0.05$, **$p \leq 0.01$, ***$p \leq 0.001$).

Bacterial cell membrane integrity was also evaluated for both ENPs, and the results are summarized in Figure 4.4. Effects of nZnO on cell membrane integrity were found to be concentration dependent in both river waters. For instance, results indicated that nZnO induced significantly higher effects on cell membrane integrity disruption at all concentrations in ER with maximum reduction of 46% (Figure 4.4a), and the trend was similar to reduction in cell viability (61%) observed at the same concentration (Figure 4.4a). A 26% cell membrane integrity disruption was observed in BR at 1 000 μg L^{-1}, but insignificant minimal effects at lower concentrations (Figure 4.4a). Moreover, the cell membrane integrity significantly decreased ($p \leq 0.01$) in BR (1 000 μg L^{-1}) for nZnO, and the results were similar to those of 100 μg L^{-1} in ER (Figure 4.4a). The observed differences on cell membrane integrity were attributed to two factors: (i) water physicochemical properties (Table 4.1) where in ER a marked reduction was observed, likely due to low aggregation and high dissolution of ENPs (specifically nZnO), and (ii) the type of ENPs with nZnO inducing a higher disruption compared to that of γ-nFe_2O_3 (Figure 4.4).

To date, the toxic effects of nZnO on bacteria have been widely reported, with effects linked to mechanisms such as nanoparticles surface contact and uptake, release of ions (Zn^{2+}), and ROS production (Heinlaan et al., 2008; Aruoja et al., 2009; Baek & An, 2011; Kumar et al., 2011; Jain, Bhargava & Poddar, 2013; Li, Lin & Zhu, 2013; Huang et al., 2014; Leung et al., 2016). In this study, the three mechanisms were evaluated in an effort to account for the observed cytotoxic effects of both ENPs on *B. subtilis*, and the results are discussed in the following paragraphs and sections. Concentration-dependent effects on cell membrane integrity were observed in both water samples (Figure 4.4a) but cell viability effects were only observed in ER water samples (Figure 4.3a). Our findings are consistent with other studies (Li et al., 2010; Kumar et al., 2011) where bacterial viability was found to be dependent on nZnO exposure dosage (2 ug L^{-1} to 5000 mg L^{-1}). Herein, the observed effects were linked to the increasing Zn^{2+} concentrations as the exposure concentration increased (Figure 4.2), and the release of Zn^{2+} was dependent on the river water chemistry (Table 4.1). This is consistent with earlier findings where Zn^{2+} from nZnO was established to be responsible for the observed toxicity to bacteria as influenced by exposure media chemistry (Li et al., 2010; Li, Lin & Zhu, 2013). Herein, the effects of nZnO in ER may be linked to

measured Zn^{2+} of 366 ug L^{-1} compared to 183 ug L^{-1} in BR at nominal exposure concentration of 1 mg L^{-1}.

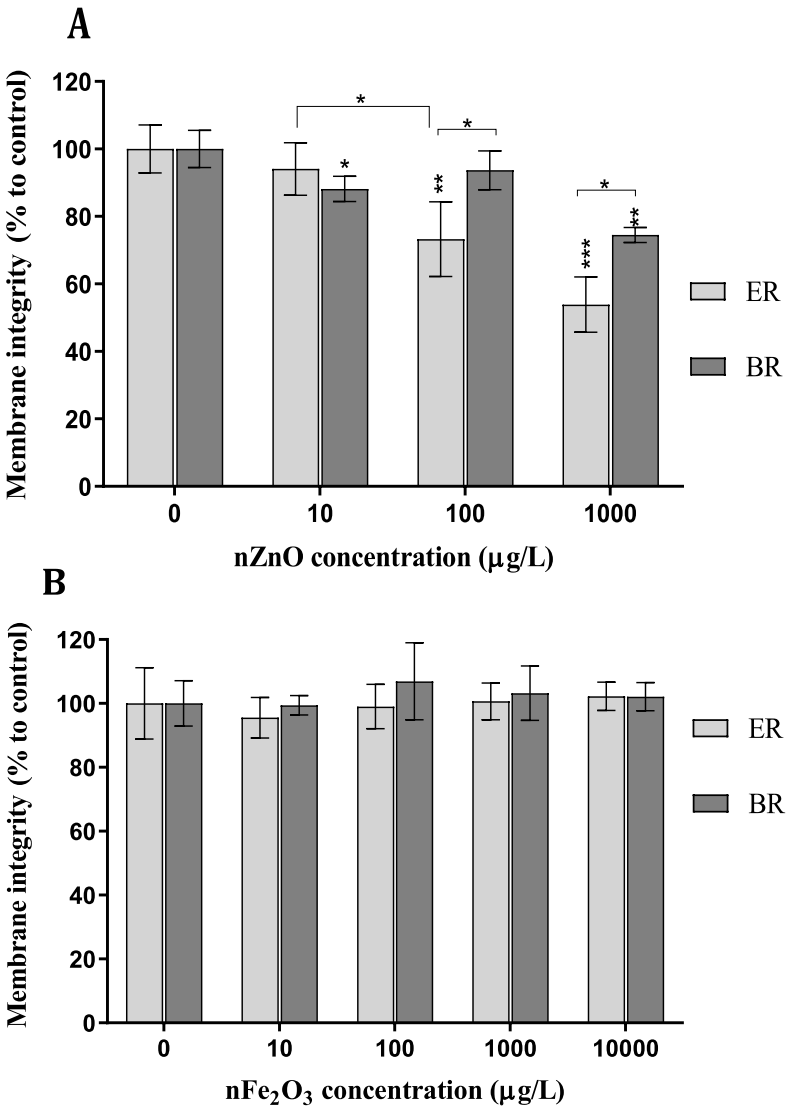

Figure 4.4 Effects of (a) nZnO and (b) γ-nFe_2O_3 against B. subtilis cell membrane integrity in natural water. Data represents the average ± SD (n=3). Asterisks (*) represent significance levels from Tukey's post hoc tests in two-way ANOVA (*$p < 0.05$, **$p \leq 0.01$, *** ≤ 0.001).

Modelled speciation results of nZnO in both river water systems using Visual MINTEQ showed complete dissolution of 1 mg L^{-1} with 61 and 53 % of the dissolved zinc as free Zn^{2+} in BR and ER (Table 4.3), respectively. These values were higher than experimentally measured value of Zn^{2+}. The marked differences between measured and modelled results

may be due to model being based on equilibrium solubility of bulk materials, and hence, different from the kinetics of nZnO (Leung et al., 2019). Speciation calculations of the dissolved Zn showed about 50% of the Zn^{2+} formed complexes with DOM in BR water compared to about 39% in ER water (Table 4.3); whereas the rest formed labile complexes that could also account for the observed toxicity as similarly reported elsewhere (Li, Zhu & Lin, 2011).

Table 4.3**:** Zn distribution calculated by VMINTEQ from dissolved Zn concentrations measured by ICP-MS in BR and ER water.

	0.183 mgL^{-1}	**0.366 mgL^{-1}**
Species	BR water (% of total concentration)	ER water (% of total concentration)
Zn^{2+}	42.956	45.901
/FA-Zn+2G(aq)	0.171	0.385
$ZnOH^{+}$	2.711	4.89
$Zn(OH)_2$ (aq)	2.52	7.36
$ZnCl^{+}$	0.033	0.051
$ZnSO_4$ (aq)	0.857	1.62
$ZnNH_3^{2+}$	0.068	0.145
$ZnHPO_4$ (aq)	1.017	0.786
/FAZn+(aq)	11.071	14.089
/FA2Zn(aq)	38.592	24.765

The γ-nFe_2O_3 showed no cell membrane integrity effects to *B. subtilis* irrespective of water samples source across all exposure concentrations (Figure 4.4b), and the results are in agreement with literature where no effects were observed on bacteria at concentrations of < 70 mg L^{-1} (< 70 000 μg L^{-1}) (Auffan et al., 2008; Azam et al., 2012; Wang, Lin, et al., 2016).

In this study, no cytotoxic effects of γ-nFe_2O_3 were observed due to high aggregation (Table 4.2) that, in turn, reduced bacterial cell-nanoparticle contact. High aggregation was evident at higher exposure concentrations where γ-nFe_2O_3 sedimented to the bottom of the exposure vessels. And, due to γ-nFe_2O_3 low solubility, implied very low or, non-release of ions especially in the short 2 h exposure period used in this study; further accounts why no cytotoxic effects were evident.

Herein, TEM was used to observe bacteria-ENPs interactions and the likely resultant effects on the bacterial cells, and the micrographs are shown in Figure 4.5. For the γ-nFe_2O_3, intact bacteria cells at all nominal exposure concentrations (10–10 000 μg L^{-1}) were observed with only limited contact between the ENPs and cells as the exposure concentration increased (Figure 4.5 a-d). Raptured cells were observed at higher concentrations of 100 and 1 000 μg L^{-1} for nZnO (Figure 4.5 f and g), but the cells remained apparently intact at the lower concentration of 10 μg L^{-1}. The cross-sections of *B. subtilis* following exposure to ENPs (Figure 4.6) depicts a qualitative assessment on the integrity of membrane structures. At lower concentrations of 10 and 100 μg L^{-1}, γ-nFe_2O_3 intact cells were evident (Figure 4.6 a and b), however, at higher ones (1 000 and 10 000 μg L^{-1}) as shown in Figure 4.6 c and d, impairment of cell walls and membrane were observed likely due to close proximity of ENPs to the cells enhanced by increased aggregation as concentration increased as well as likely entrapment of cells in the formed aggregates. For nZnO, raptured cells were observed at 1 000 μg L^{-1} (Figure 4.6 g), but at 10 and 100 μg L^{-1} qualitatively higher proportions of unimpaired cells were observed (Figure 4.6 e and f).

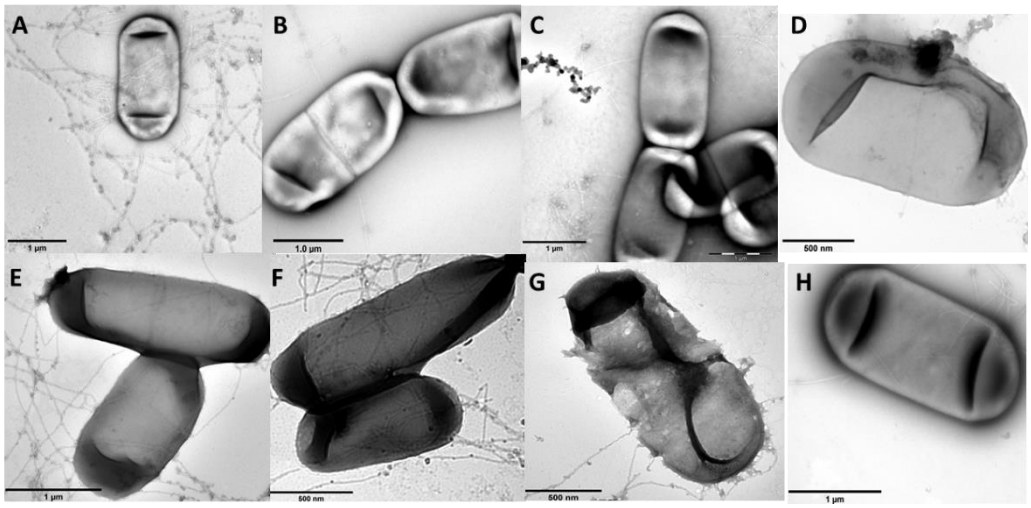

Figure 4.5 Transmission electron micrographs of B. subtilis following exposure in (a) 10, (b) 100, (c) 1000, (d) 10000 μg L^{-1} γ-nFe_2O_3; (e) 10, (f) 100, (g) 1000 μg L^{-1} nZnO; and (h) control in ER.

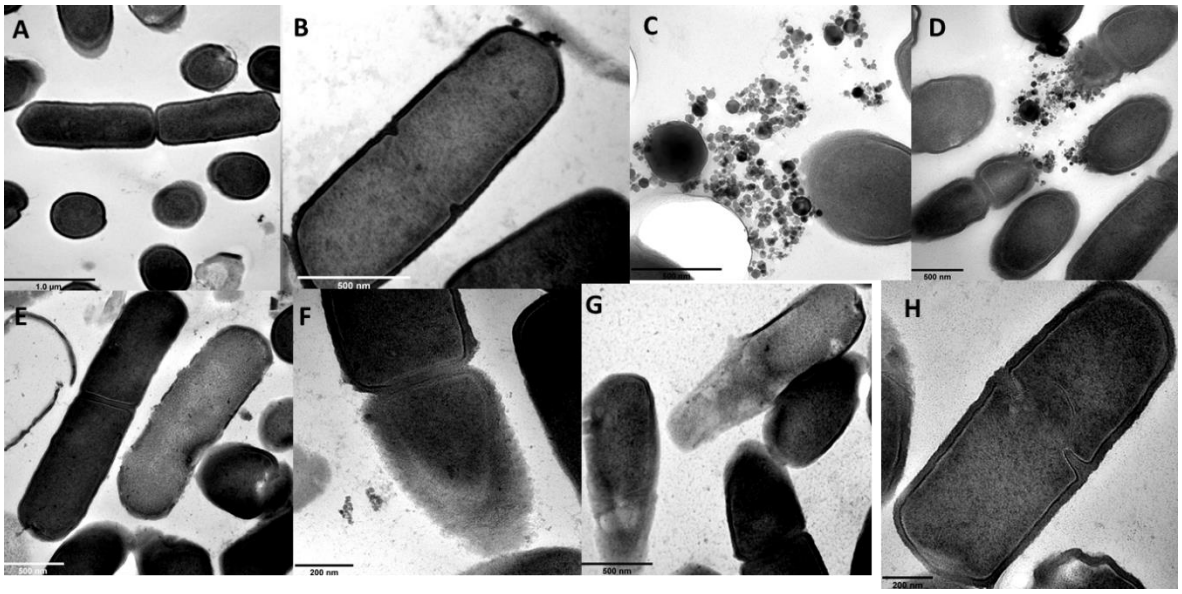

Figure 4.6 Cross-sections of transmission electron micrographs of B. subtilis following exposure to (a) 10, (b) 100, (c) 1 000, (d) 10 000 μg L^{-1} γ-nFe_2O_3; (e) 10, (f) 100, (g) 1 000 μg L^{-1} nZnO; and (h) control in ER.

Bacterial cell wall serves as a barrier that controls and/or prevents the entry of certain compounds from the surrounding environment into the cell interior (Dowhan & Bogdanov, 2002; Murínová & Dercová, 2014). Engineered nanoparticles have been reported to show anti-microbial activity through ENPs-induced disruption of the membrane (Kumar et al., 2011; Sirelkhatim et al., 2015; Hou et al., 2018). Contact between the ENPs and bacteria, for example, where nZnO have been observed to cause cell wall permeability on *B. subtilis* was reported by Rago (2014) and on other organisms (Kumar et al., 2011; Bandyopadhyay et al., 2015). Herein, TEM results point to restricted contact between ENPs (nZnO and γ-nFe_2O_3) and bacteria cells with no evidence of uptake; yet cell membrane damage was observed in the case of nZnO. From our findings, negatively charged ENPs (as reported herein for both river water samples, Table 4.2) suggest minimal ENP-cell interactions (if any) due to repulsion, however, ENP-cell surface contact could not be ruled-out especially at higher concentrations where membrane damage occurred for nZnO. For instance, nZnO with HDD of 558 ± 28 nm as measured by DLS represents the average size of larger-sized particles; however, smaller-sized particles can still interact with the bacteria cells due to the concentration effect as suggested by other researchers (Wang et al., 2014). Such nZnO - bacteria interactions could also occur aided by mechanisms such as hydrogen bonding, Van der Waals forces, and receptor-ligand interactions through bacterial cell moieties where there's weak electrostatic repulsion (Jiang, Mashayekhi & Xing, 2009; Leung et al., 2016; Kadiyala et al., 2018). However, no such similar effects were observed for γ-nFe_2O_3 due to formation of larger aggregates (μm sized) that tended to sediment and settle at the bottom of the vessels; thus leading to no plausible ENPs-cell interactions. Zn^{2+} have also been suggested to attach to the cell membrane and rupture the cell wall leading to membrane integrity loss (Yu-sen et al., 1998; Lemire, Harrison & Turner, 2013). In addition , in circumstances where disruption of zinc homeostasis occurs due to internalised Zn^{2+} cell death may occur through the denaturation of protein (Yu-sen et al., 1998; Matuła et al., 2016; Anders et al., 2018). Tong et al. (2015) for example, reported marked inhibition of between 10 and 20% on *Aeromonas hydrophila* and *E. coli* by nZnO (1 000 μg L^{-1}) under dark and light conditions without increased ROS production and with minimal contact between nZnO and bacterial cells. Therefore, results herein show Zn^{2+} effects may be via reduction of cellular functioning due to pure chemical effect in the bacterial cells.

4.4 ATP production

In this study, the ability of ENPs to disrupt ATP production was also evaluated. Results of measured ATP abundance following exposure to nZnO and γ-nFe_2O_3 on *B. subtilis* in both water samples for 1 h are summarised in Figure 4.7. ATP levels were observed to decline as a function of time, nominal exposure concentration, and water chemistry (Figure 4.7).

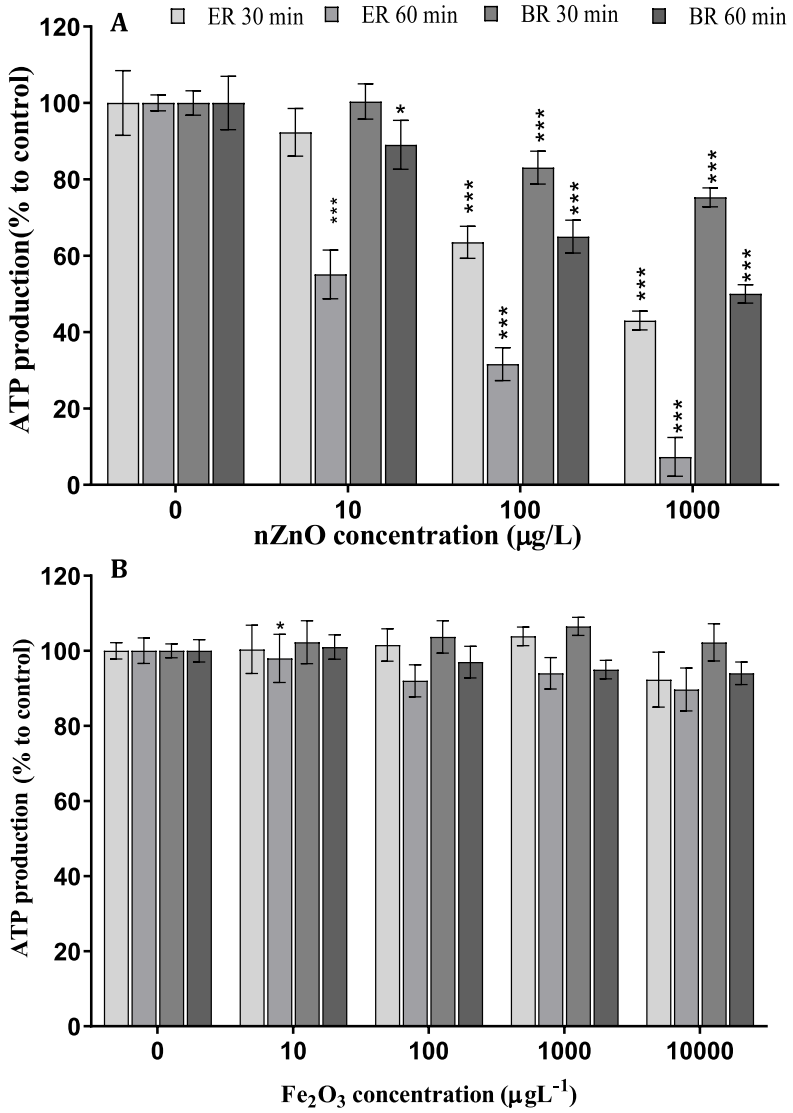

Figure 4.7 Effects of (a) nZnO and (b) γ-nFe_2O_3 on B. subtilis ATP levels in ER and BR water samples. Percentage of bacterial ATP was normalized to that of the control (no exposure to ENPs). Asterisks (*) represent significance levels from Tukey's post hoc tests in two-way ANOVA (*$p < 0.05$, **$p \leq 0.01$, ***$p \leq 0.001$).

For example, nZnO exhibited significant concentration-dependent effects on ATP levels which were more pronounced in ER compared to BR water samples (Figure 4.7a). To date, only limited studies have investigated the likely effects of ENPs on bacterial ATP levels (Tong et al., 2015; Wilke et al., 2016; Wilke, Gaillard & Gray, 2017). Tong et al. (2015) for example, reported significant concentration-dependent reduction in ATP levels exerted on *E.coli* and *A. hydrophila* by nZnO in lake water at concentrations of 250 and 1 000 μg L^{-1} following 1 h incubation under dark conditions.

Herein, our results revealed significant reduction on ATP levels even at lower concentration of 10 μg L^{-1} nZnO ($p < 0.05$) following 1 h incubation in river water under visible light. To account for these findings, we propose two plausible mechanisms. First, the depletion of cellular ATP may have been due to the disruption of cellular membrane leading to the loss of homeostasis in cells (Rago et al., 2014; Matuła et al., 2016). Secondly, release of ions following the dissolution of ENPs (in this case nZnO into Zn^{2+}) may have deactivated energy-dependent reactions in the cells as previously observed in toxicity studies of silver and zinc (Lapresta-Fernández, Fernández & Blasco, 2012; Alhasawi et al., 2014). In most organisms, Zn is an essential micronutrient required for biochemical processes, however; when present at elevated quantities may also interfere with biological pathways (Alhasawi et al., 2014). Therefore, the released Zn^{2+} from nZnO may have been taken up via the transport chains without causing damage to the cell membrane – but rather induced denaturation of ribosome and suppression of enzymes and proteins involved in ATP production – leading to the disruption of the cell functionality(Yamanaka, Hara & Kudo, 2005; Krishnaraj et al., 2010). This is consistent with the findings of nZnO toxicity in this study as evidenced by reduction in cell viability (Figure 4.3a), and cell membrane integrity (Figure 4.4a). This correlation is highly plausible due to two reasons. First, because minimal ENPs-cell contact was established, thus indicated unlikely cell membrane perforations (Figure 4.5 e - g). And secondly, results herein indicate that the observed reduction in ATP levels followed the dissolution patterns responsible for the release of Zn^{2+} as also earlier suggested by Tong et al. (2015) Therefore, the observed variant nZnO effects between water matrixes from different sources were linked to differences in dissolution as influenced by water chemistry characteristics.

Results summarized in Figure 4.7 also illustrate the influence of ENPs type on ATP production. The results in Figure 4.7b show ATP levels following exposure to γ-nFe_2O_3 (compared to nZnO in Figure 4.7a) were insignificant irrespective of nominal exposure concentration and water chemistry in both water samples. In certain cases, however, like in BR γ-nFe_2O_3 was observed to induce increased ATP production levels above the control after 30 min incubation (Figure 4.7b). To the authors' knowledge, this is for the first time ATP levels on bacteria exposed to γ-nFe_2O_3 in natural water samples were observed (10–10 000 μg L^{-1}). The lack of significant effects observed by ATP measurements, even at 10 000 μg L^{-1}, suggest that γ-nFe_2O_3 may not pose any undesirable effect on microorganisms in aquatic systems, particularly at current predicted environmental concentrations of 28 ng L^{-1} (Wang, Deng, et al., 2016).

4.5 ROS production

To determine whether oxidative stress contributed to the observed effects of ENPs, ROS production was evaluated. Results showed that nZnO and nFe_2O_3 induced no significant change in intracellular ROS levels on *B. subtilis*, compared to the control, in both water samples under visible light conditions (Figure 4.8). Hence, these findings indicate that ROS production and oxidative stress were not linked to the observed nZnO toxicity.

To date, numerous studies have reported cell damage due to oxidative stress to be among the key toxicity causing mechanisms for metal-based ENPs (Dasari, Pathakoti & Hwang, 2013; von Moos & Slaveykova, 2014; Leung et al., 2016; Vale et al., 2016; Peng, Zhang, et al., 2017). For example, nZnO has been observed to induce significant ROS generation from *E. coli* relative to the control even in absence of UV illumination (Kumar et al., 2011) – although at higher concentration of 8 mg L^{-1} (80 000 μg L^{-1}) but unlikely to be found in actual freshwater systems. Dasari and Hwang (2013) observed cytotoxic effects in natural river water following exposure of nZnO to bacterial assemblages at 100 and 1 000 μg L^{-1} under both dark and light (sunlight) conditions, however; ROS generation was similar to the controls. Similarly, findings of Rago *et al* (2014) revealed no induction of oxidative stress

(ROS production) to *B. subtilis* following exposure to nZnO (10 – 250 000 µg L^{-1}); yet cytotoxic effects were observed.

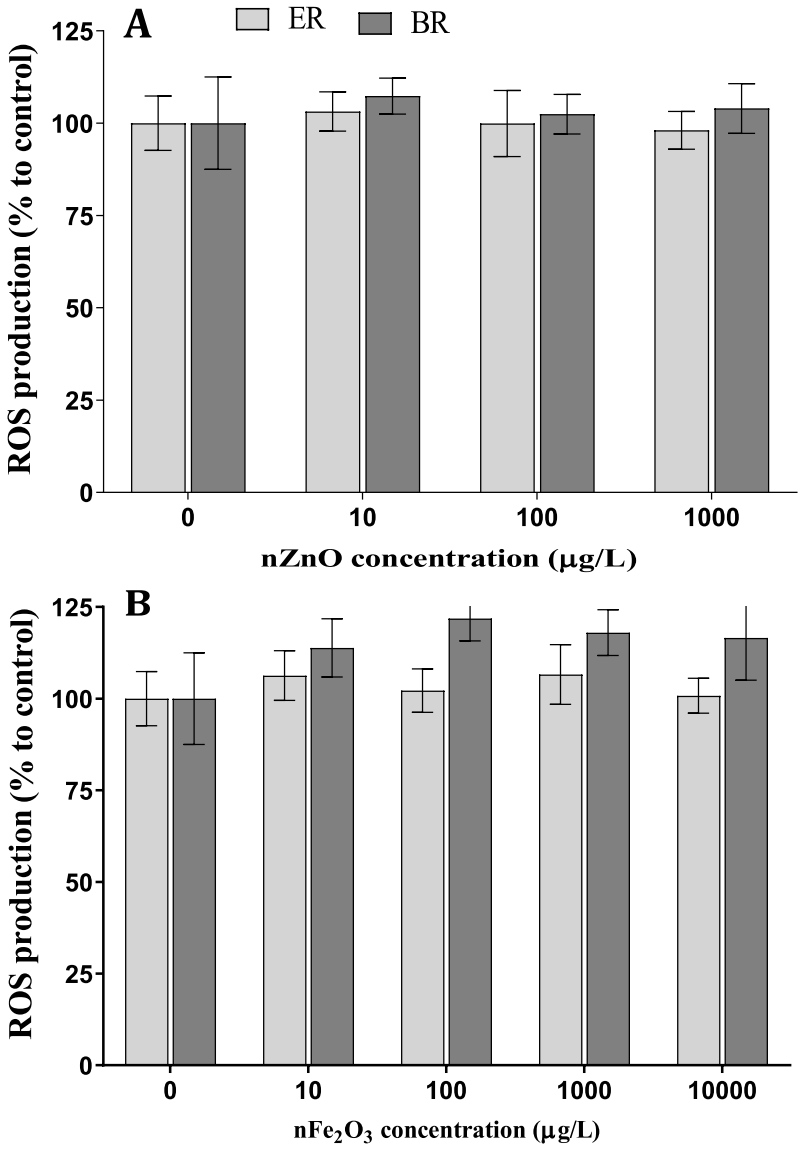

Figure 4.8: Effects of (a) nZnO and (b) nFe_2O_3 on ROS levels in BR and ER water samples. Data represents the average ± SD (n=3). Asterisks (*) represent significance levels from Tukey's post hoc tests in two-way ANOVA (*$p < 0.05$, **$p \leq 0.01$, ***≤ 0.001).

Herein, results show that nZnO induced cytotoxicity and cell membrane damage to *B. subtilis* in both river water samples; but the observed effects could not be accounted for by ROS production (as it was absent). In addition, our results are consistent with observations of Dasari et al. (2013) where cytotoxicity was evident but could not be linked to oxidative stress. As argued by Kadiyala et al. (2018), and the evidence of results from this study, on cytotoxicity and cell membrane damage to *B. subtilis* indicate that ROS generation cannot be the predominant mechanism to account for the nZnO antimicrobial activity (Matuła et al., 2016). Therefore, more analysis is essential to elucidate the likely oxidative stress implications on the toxicity of ENPs, and particularly generate knowledge that can offer valuable insights that can account for the current contradictory data.

4.6 Conclusions

In this study, the toxicity of nZnO and γ-nFe_2O_3 in natural water samples with varying physicochemical parameters were assed. Results indicated that cell viability, cell membrane integrity, and ATP production were more diminished in ER (lower NOM, low IS, etc.) compared to BR (high NOM, high IS, etc.) water samples for nZnO exposures. However, γ-nFe_2O_3 induced very low or no cytotoxicity to microorganisms at exposure concentrations investigated in this work. In addition, we demonstrated that the toxicity of ENPs to *B. subtilis* were dependent chiefly on the differences in IS and NOM in the studied water samples. ROS production was observed to be negligible for both ENPs. Moreover, with no observed interactions of nZnO and bacteria indicated that the effects of nZnO were likely driven by release of Zn^{2+}, and water chemistry played a key role as evidenced by the differences in their dissolution between the two water samples.

The study also illustrates the benefit of using multiple endpoints to assess the toxicity of ENPs as valuable insights on discrete effects were gained as certain endpoints showed no apparent responses but other revealed likely deleterious effects. For instance, in certain cases cell viability could not reveal cytotoxic effects of nZnO whereas cell membrane damage and ATP production demonstrated the effects of ENPs on bacteria. These findings suggest a plausible correlation between Zn^{2+} and observed effects at different concentrations in the

two water sources. This implies, the induced adverse interference on the metabolic pathways and cell membrane structures, which in turn, lead to the observed outcomes on bacteria, however, the nanoparticulate effects cannot be ruled out. Overall, the study highlighted the complexity and variations in natural water sample physicochemical properties that should be considered when establishing the toxicity of ENPs to bacteria.

Chapter 5: *Bacillus subtilis* responses to binary mixtures of zinc oxide and iron oxide nanoparticles in river water systems

The work herein seeks to determine the chemical and toxicological interactions of nZnO and nFe_2O_3 as binary mixtures in natural water matrices. The effect of the ENPs interactions, including the influence of solar irradiation were investigated by assessing the resultant toxicity on *B. subtilis*. The role of ROS and dissolution from ENPs interactions under varying natural water chemistry and irradiation were probed to assess *B. subtilis* stresses using bacterial cell membrane integrity as the endpoint.

5.1 Natural water characteristics

Composition of the river water samples is presented in Table 5.1. Both river water samples had pH around 8. BR water had higher concentration of major elements, and in turn, higher ionic strength compared to ER water. Dissolved organic matter (DOC) content was significantly higher in BR water than in ER water (Table 5.1).

Table 5.1: Physicochemical parameters of freshwater samples from BR and ER river

Parameter	Unit	Bloubank River (BR) water	Elands River (ER) water
pH		8.10	8.22
DOC[a]	mg C L^{-1}	9.31	6.50
Electrical conductivity	ms/m 25°C	54.7	23.1
COD[b]	mg L^{-1}	34.3	45.7
Alkalinity	mg L^{-1}	232	101
NO_3	mg L^{-1}	0.203	0.209
Cl^-	mgL^{-1}	30.7	19.1
SO_4	mg L^{-1}	33.6	4.33
PO_4	mg L^{-1}	0.009	0.005

Fe^{3+}	mg L^{-1}	<0.004	<0.004
Zn^{2+}	mg L^{-1}	<0.002	<0.002
Ca^{2+}	mg L^{-1}	48.1	16.4
Mg^{2+}	mg L^{-1}	30.3	11.1
Na^{+}	mg L^{-1}	27.7	18.0
K^{+}	mg L^{-1}	2.85	3.47
IS[c]	mM	6.36	2.50

[a]DOC: Dissolved organic carbon; [b] IS: Ionic strength, [c]AlK: Alkalinity, [#]Ionic strength, calculated by Visual MINTEQ, ver. 3.1.

5.2 ENPs characterization

The physicochemical properties of nZnO and γ-nFe_2O_3 are reported elsewhere (section 4.3), and herein only salient aspects are summarized. The γ-nFe_2O_3 were hexagonal shaped with average particle size of 41 ± 25 nm, whereas nZnO consisted of hepta-, penta-, hexa-gonal, and rod shapes with diameter ranging from 15 to 57 nm due to asymmetry of the morphology. The BET surface area (SA_{BET}) of γ-nFe_2O_3 and nZnO were 36.672 and 36.707 m^2/g, respectively. Both ENPs, as individual and binary systems, had negative ζ-potential in all river water samples (Figure 5.1 b and d), with an average of *ca* -12 mV.

Immediate aggregation of nZnO and γ-nFe_2O_3 in both river water samples post-sonication was observed (Figure 5.1a and c). nZnO formed aggregates of 385 ± 36 to 836 ± 112 nm in ER (Figure 5.1), whereas larger aggregation at 800 ± 89 to 1469 ± 41 nm in BR were measured (Figure 5.1 a and c). Similarly, γ-nFe_2O_3 aggregation was higher in BR water than ER river water, with sizes of 485 ± 59 to 796 ± 57 nm in ER and 519 ± 32 to 852 ± 39 nm in BR, respectively (Figure 5.1 a and c). Overall, aggregation of both nZnO and γ-nFe_2O_3 were lower in ER compared to BR as previously reported by Leareng et al. (2020). Moreover, aggregation was notably lower in the current water samples (collected in the summer, in November) associated to temporal-linked differences in water chemistry (see Table 4.1 and Table 5.1).

Water chemistry, including NOM composition and ionic strength contribute significantly to the transformation of ENPs in aquatic systems. Electrolytes, depending on their valence and concentrations may lead to enhanced aggregation either due to charge screening or cation binding in NOM mediated aggregation of ENPs (Liu et al., 2012; Baalousha et al., 2013; Majedi, Kelly & Lee, 2014; Wang, Zhang, et al., 2016). Therefore, the differences in cations such as Ca^{2+} and mg^{2+} could have been the contributing factor in the aggregation differences between the two river water samples, as previously discussed for both ENPs aggregation behaviour in BR and ER water (Leareng, Ubomba-Jaswa & Musee, 2020). In addition, the differences between the water chemistry components for water in table 4.1 and table 5.1 could have contributed the differences in the aggregation of ENPs, showing the influence of temporal variations in the transformation of ENPs in aquatic systems.

Binary mixtures of nZnO and γ-nFe_2O_3 exhibited larger aggregate sizes compared to those of individual ENPs (Figure 5.1 a and c). Although both ENPs were negatively charged (but relatively below -30 mV), inter particle interactions were evident between the nZnO and γ-nFe_2O_3 due to the observed larger aggregate sizes of the mixture. High measured HDD values indicated that the electrostatic repulsions between the negatively charged were outweighed by increased particle collision.

To fully understand the aggregation of the ENPs mixtures, size trends for both singles and mixtures were monitored for 2 h (Figure A 5 and 6). In both river water samples, nZnO formed aggregates, however, the aggregate sizes remained stable over 2 h. BR had higher aggregate sizes for nZnO and γ-nFe_2O_3 and were concentration dependent for nZnO (figure A5 b, c). The presence of γ-nFe_2O_3 in the binary mixture had an increase effect on aggregate sizes over time, even when lower concentrations of γ-nFe_2O_3 were tested – with a similar trend observed on the aggregation of γ-nFe_2O_3 alone (Figure A 5 and 6).

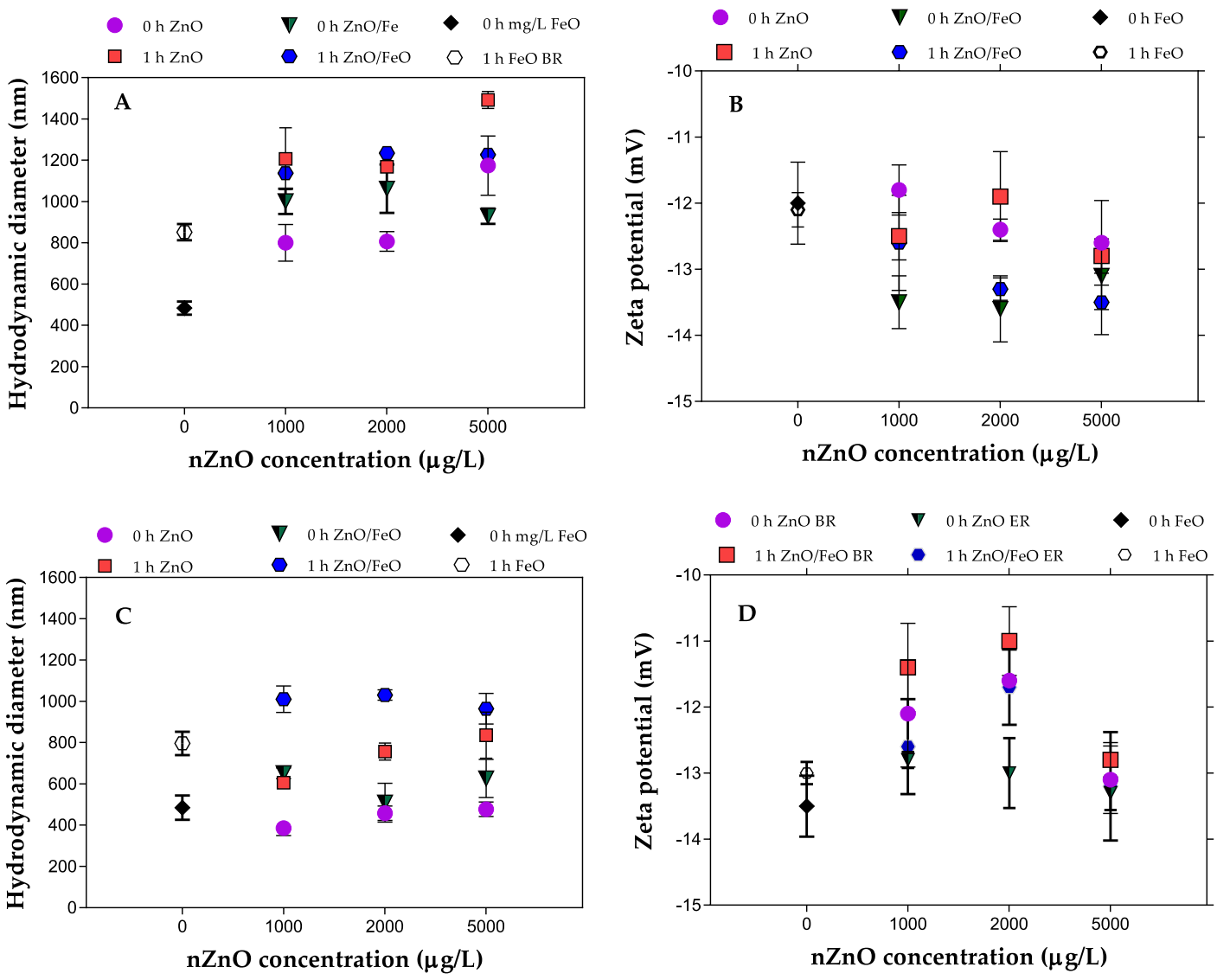

Figure 5.1: HDD and ζ-potential for nZnO and nZnO/nFe_2O_3 mixtures in (a, b) BR water and, (c, d) ER water samples.

Results on the dissolution of nZnO under solar irradiation and in the presence of γ-nFe_2O_3 in both river water samples are shown in Figure 5.2. Dissolution of nZnO in BR water did not vary significantly across all concentrations and was *ca* 100 µg L^{-1}. In ER, the Zn^{2+} was higher at about 200 µg L^{-1}, and concentration dependent on nZnO exposure dosages (Figure 5.2 a and b). These results are similar to Li et al. (2013), who reported no variation in nZnO dissolution ranging from 5 to 100 mg L^{-1} in natural water samples. Following introduction of

γ-nFe_2O_3, in both river water samples, no dissolution changes were observed except at the highest concentration of 5000 µg L^{-1} (Figure 5.2 a and b). Other previous studies have reported on the mitigating effects of nFe_2O_3 on ENPs that undergo dissolution and release ions e.g. nAg (Huynh, McCaffery & Chen, 2014; Huang et al., 2019). However, under the solar irradiation conditions used in this study, adsorption capacity of ENPs in the ENPs mixtures was not demonstrated, an aspect to be taken into account in future studies.

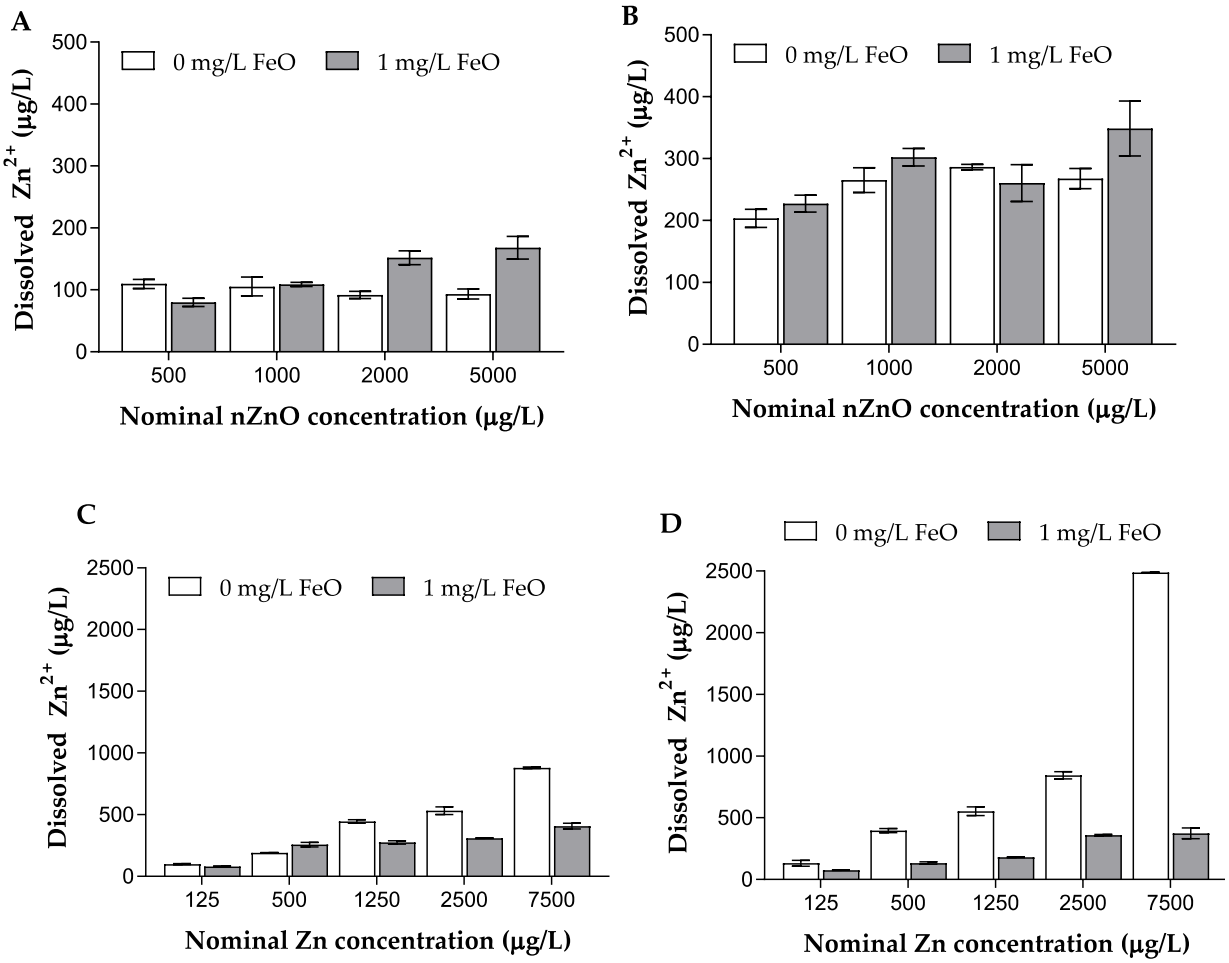

Figure 5.2: Dissolution of nZnO and γ-nFe_2O_3 mixtures in (a)BR river water, (b) ER river water under solar irradiation for 30 min, and(c, d) bioavailability of Zn^{2+} in BR and ER river water samples, respectively.

To understand the influence of γ-nFe_2O_3 on measured concentration of Zn^{2+} in the binary studies with nZnO, interactions of Zn derived from different concentrations of $ZnSO_4.7H_2O$

and γ-nFe_2O_3 was done Figure 5.2 c and d). Dissolved Zn concentration was reduced in both river water systems in both river water samples; an indication of γ-nFe_2O_3 capacity to adsorb Zn^{2+}. Hence, absence of change in dissolved concentrations of Zn^{2+} in the nZnO and γ-nFe_2O_3 mixture was linked to the heteroaggregation between the two ENPs, as demonstrated by the mixture heteroaggregation (Figure 5.1 a and c). The role of UV irradiation has been reported to alter the dissolution of nZnO and adsorption of released Zn^{2+} by other ENPs such as $nTiO_2$. Tong et al. (2014) reported unchanged concentrations of dissolved zinc in mixtures of nZnO and $nTiO_2$, which was linked to photocorrosion of nZnO that altered the adsorption of dissolved Zn^{2+} on $nTiO_2$.

5.3 Cell membrane integrity

Concentration dependent reduction in *B. subtilis* were observed following nZnO exposure (Figure 5.3a) in both river water samples. The findings were consistent with trends observed in our previous work (Leareng, Ubomba-Jaswa & Musee, 2020). The highest toxicity was observed at 5 000 μg L^{-1} for nZnO in both river water samples, and higher effects in ER water. These concentrations were significantly higher than concentration dependent-effects of nZnO by Dasari et al., (2013), who reported significant nZnO effects on E. *coli*, even at concentrations as low as 10 μg L^{-1} under solar irradiation following 30 min exposure period. Differences between the results herein and their findings can be attributed to differences in exposure media chemistry. For instance, Dasari et al. (2013) used physiological saline whereas here natural water was utilized. In this work, the presence of NOM and cations may have contributed to the decreased toxicity. Our findings, however, are in good agreement with findings of Tong et al. (2015) where nZnO on *E.coli* and *Aeromonas hydrophila* induced *ca* 10 to 20 % reduction in viability (membrane integrity) under solar irradiation at 1 000 μg L^{-1}.

No significant toxicity of γ-nFe_2O_3 under the same conditions for both river water systems compared to control were observed (Figure 5.3b). The nZnO toxicity observed herein was linked to both nZnO particulates and the released Zn^{2+} from the ENPs, and as a result, exerted effects at varying degrees. Song et al. (2020) reported that the toxicity of nZnO occurs as a mixture of dissolved Zn^{2+} and the particulates. In this study, the dissolution of

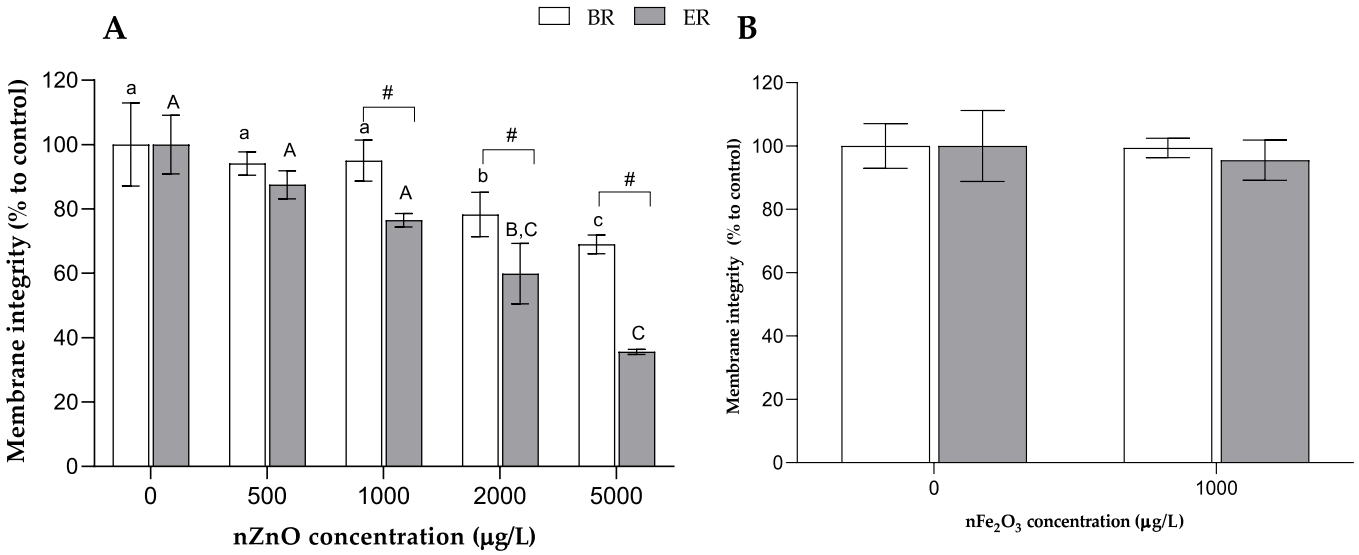

Figure 5.3: Cell membrane integrity of *B. subtilis* following exposure to (a) nZnO and (b) γ-nFe_2O_3 in BR and ER water under solar irradiation. Different letter designations between different groups indicate significant difference to the control (0 µg/L nZnO), whilst similar alphabets indicate no significant difference. (#) indicates statistical differences between river water types (Tukey's test, $\alpha = 0.05$).

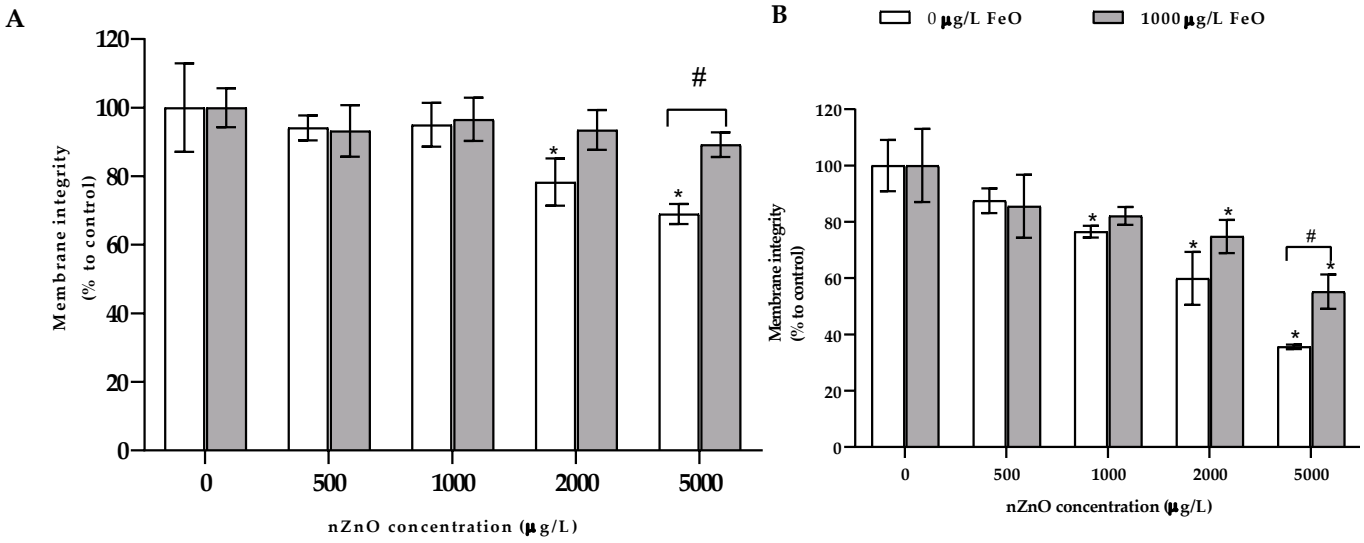

Figure 5.4: Cell membrane integrity of *B. subtilis* following exposure to mixtures of nZnO and γ-nFe_2O_3 in BR (A) and ER (B) water samples under solar irradiation. Asterisk (*) indicate significant difference to the control (o ug/L nZnO), whilst (#) indicates statistically

significant differences between same conditions and different river water types (Tukey's test, $\alpha = 0.05$).

nZnO was similar at all concentrations in both river water samples, with higher dissolution in ER water. These differences in dissolution were linked to the lower aggregate sizes in ER compared to BR. The differences in the aggregation also could imply more dispersity of nZnO in ER, with resultant higher interactions of ENPs particulates and released ions. For mixtures of ENPs at variant nZnO concentrations, and fixed γ-nFe_2O_3 similar reduced viability of *B. subtilis* was observed, and significantly at the highest concentrations of nZnO especially in ER water (Figure 5.4b).

The observed differences in the toxicity of nZnO and the nZnO/ γ-nFe_2O_3 mixtures were associated with variant aggregation sizes of individual ENPs and mixtures. Although the toxicity of nZnO was linked to its ions previously (Leareng, Ubomba-Jaswa & Musee, 2020), the possibility of nZnO-bacteria interactions was highlighted, and could not be ruled out. Herein on mixture studies, co-existence of γ-nFe_2O_3 was observed to mitigate the toxicity of nZnO, linked to the heteroaggregation of the ENPs. This was qualitatively evident from energy-dispersive x-ray analysis using SEM, where nZnO and γ-nFe_2O_3 were co-localized as binary mixtures (Figure A11), indicating plausible heteroaggregation. However, dissolution and ROS generation could not fully account for the observed toxicity for individual and binary mixtures (Figure 5.4 a). Although both individual ENPs and their mixtures were negatively charged, the possibility of interactions between ENPs and bacteria could not be ruled out; especially due to surface charge and repulsion, in agreement with observations of Tong et al. (2015). Therefore, toxicity may be a product of all mechanisms at play, including ENPs-bacteria contact. The particulate effects should be reduced where higher aggregation occurs, both for individual and mixture ENPs, as shown by observed differences in BR and ER water (Figure 5.4 a). Our conclusions are in agreement to recent findings of Song and colleagues (Song et al., 2020) where nZnO toxicity to *E. coli* was dependent on the ratios of particulates to Zn^{2+} at a given exposure time. For instance, at the initial stages of exposure,

higher fraction of particulates (negligible dissolution), toxicity was due to particulates. Moreover, the released ions were observed to exert their toxicity with increasing concentration in a time-dependent manner. Although the role of particulates on the observed toxicity is proposed, to date techniques to examine the ENP-bacteria contact are needed without distorting sample integrity. This is because current tools such as TEM distorts the sample profile through various preparation stages. To address this limitation, techniques such as Cryo-SEM should be considered for future work.

5.4 ROS assays

ROS is among the postulated mechanisms to account for the observed toxicity of nZnO and γ-nFe_2O_3 (Li et al., 2012; Dasari, Pathakoti & Hwang, 2013; Kaweeteerawat et al., 2015). This occurs when ROS are produced in excess beyond the threshold where cells cannot incorporate them into different pathways (von Moos & Slaveykova, 2014; Kadiyala et al., 2018). To elucidate whether oxidative stress contributed to the observed effects of ENPs, three ROS types, hydroxyl radical (•OH), superoxide radical anion (O_2•−), and hydrogen peroxide (H_2O_2) which forms from reaction of O_2•−,were evaluated through colorimetric and fluorescent means/probes. Figure 5.5 show results of •OH (Figure 5.5 a, b) O_2•− (Figure 5.5c ,d) and H_2O_2 (Figure 5.5 e , f) in BR and ER water, respectively. Results showed that nZnO and nFe_2O_3 induced insignificant change in all three ROS types compared to the control, in both river water samples under solar irradiation for 30 min (Figure 5.5). However, there were increased levels of H_2O_2 at 5 000 µg L^{-1} nZnO and their nZnO/nFe_2O_3 mixtures (5 000 µg L^{-1} nZnO and 1 000 µg L^{-1} nFe_2O_3), compared to their respective controls, however, these were not statistically significant from each other to account for the observed toxicity. This is consistent with other studies, for instance, Ma et al (2014) reported significant increases in ROS production at concentrations of 2 and 5 000 µg L^{-1} of nZnO. Therefore, the contribution of photogenerated ROS to the observed effects of ENPs may not be solely concentration dependent but influenced by other factors.

Both nZnO and nFe_2O_3 have been shown to generate higher $O_2\bullet-$ in water following irradiation compared to other ENPs (Li et al., 2012). However, these could be dependent on ENP concentration, exposure duration, and water chemistry (Peng, Zhang, et al., 2017). Higher ENP concentrations could lead to increased ROS due to higher surface area that enhances reaction with oxygen, while organic components could reduce the capacity for generation due to enhanced aggregation and reduced surface area (Li et al., 2014; Peng, Zhang, et al., 2017). NOM can also act as a quencher for ROS (Carlos et al., 2012), or act as a filter for UV by adsorbing photons in the range of 300 to 500 nm of the spectrum (Bae et al., 2011), leading to a reduction in generated ROS.

Overall, ROS in both water samples were insignificant to account for the observed differences in the toxicity of nZnO and nZnO/nFe_2O_3 mixtures (Figure 5.5). These findings are consistent with other studies where nZnO bacterial toxicity linked to ROS was considered negligible (Kadiyala et al., 2018). Similarly, under solar and UV irradiation, generated ROS from nZnO was not linked the observed bacterial toxicity (Barnes et al., 2013; Dasari, Pathakoti & Hwang, 2013; Orou et al., 2018). nZnO is known to undergo photocorrosion under solar and UV irradiation; which in turn, decreases their photocatalytic activity (Hariharan, 2006; Barnes et al., 2013). Therefore, in this study, the absence of differences in the ROS type levels across variant concentrations of nZnO and nZnO/Fe_2O_3 mixtures may be associated to solar irradiation. However, the 30 min solar irradiation exposure time may have been inadequate to measure the accumulated ROS produced either by individual ENPs or their binary mixtures. In addition, ROS scavenging may have occurred due to media components such as NOM, however, influence of water chemistry on ROS production (irrespective of type) was not apparent, in both water samples.

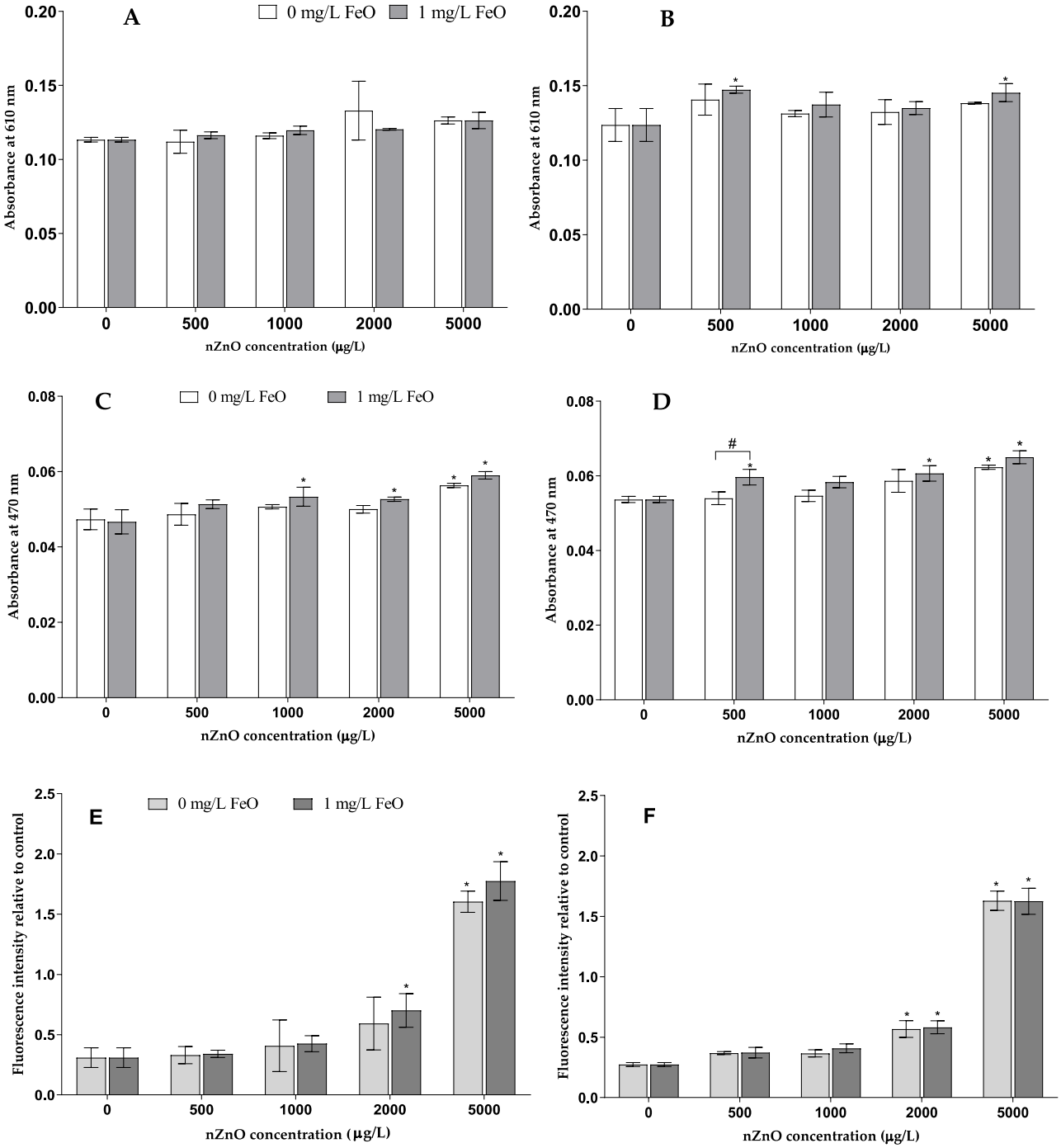

Figure 5.5: Production of ROS radicals for nZnO and γ-nFe_2O_3 mixtures under solar irradiation for 30 min. (a, b) hydroxyl radical, (c,d) superoxide anion, and (e, f) hydrogen peroxide. Asterisk (*) indicate significant difference to the control (0 ug/L nZnO), whilst (#) indicates statistically significant differences between same conditions with same nZnO concentration. (Tukey's test, α = 0.05).

5.5 Conclusions

This study shows that co-existence of nZnO and γ-nFe_2O_3 can mitigate bacterial membrane damage observed for nZnO under solar irradiation. The toxicity, however, could not be accounted for by ROS and dissolution, but nZnO particulate-bacterial interactions may played a role. Further, the higher toxicity in ER water was due to the lower aggregation of nZnO compared to BR water dependent on water physicochemical parameters. The mitigating effect in the binary mixture was likely due to the heteroaggregation of nZnO and γ-nFe_2O_3, that in turn, reduced the nZnO particulates interactions with bacteria. Findings on binary mixtures of ENPs revealed different toxicological outcomes due to their interactions, and in turn, their toxicity relative to the individual ENPs.

Our study demonstrates the outcomes of co-existing ENPs in the aquatic environment, and the essence of studies conducted for ENPs and their mixtures, particularly at environmentally relevant concentrations. This is because the precise mechanisms of toxicity for ENPs, to date, been predicated on elevated concentrations in synthetic systems, whereas outcomes at lower concentrations reveal the need for causative outcomes. Furthermore, molecular approaches are needed for ENPs toxicity to fully elucidate aquatic species responses both for individual and mixtures of ENPs under environmentally relevant conditions. Such data can offer valuable insights on the correlation of ENPs properties, exposure media characteristics, ENPs mixtures transformations, and consequent aquatic organisms' toxicological responses; thus, contributing to likely regulation of ENPs mixtures in the aquatic systems.

Chapter 6: Interactions and toxicity of zinc oxide, iron oxide and triclosan: Ternary exposures in river water systems

This chapter is focuses on the effect of TCS on the transformation of nZnO and nFe_2O_3 as both binary and ternary mixtures in natural water matrices. The influence of TCS on the zeta potential, size (hydrodynamic diameter and size trends) and dissolution of with nZnO, following their interactions as binary mixtures or ternary mixtures with nFe_2O_3 were evaluated. Lastly, these interactions and transformation insights were assessed by analysis of cell membrane integrity as a measure of toxicity to *B. subtilis.*

6.1 Water characteristics

Composition of the river water samples is presented in Table 4.1. Both river water samples had pH around 8. BR water had higher concentration of major elements and thus a higher ionic strength compared to ER water. Dissolved organic matter (DOC) content was significantly higher in in BR water than in ER water Table 5.1.

6.2 Interactions between ENPs and Triclosan in river water samples

6.2.1 Influence of TCS on ENPs

Both ENPs, as individual and binary systems with TCS, had negative ζ-potential in all river water samples (Figure 6.1). The ζ-potential for both all three mixture combinations were negative in both river water samples, between -11 and 15 mV. Therefore, the ζ-potential of nZnO or nFe_2O_3 was not significantly influenced by increasing concentrations of TCS in the binary mixtures, and these did not vary largely in BR and ER water. Similar effects were observed for the ternary mixtures, where TCS did not have any influence on the decrease or increase of ζ-potential of nZnO/ nFe_2O_3.

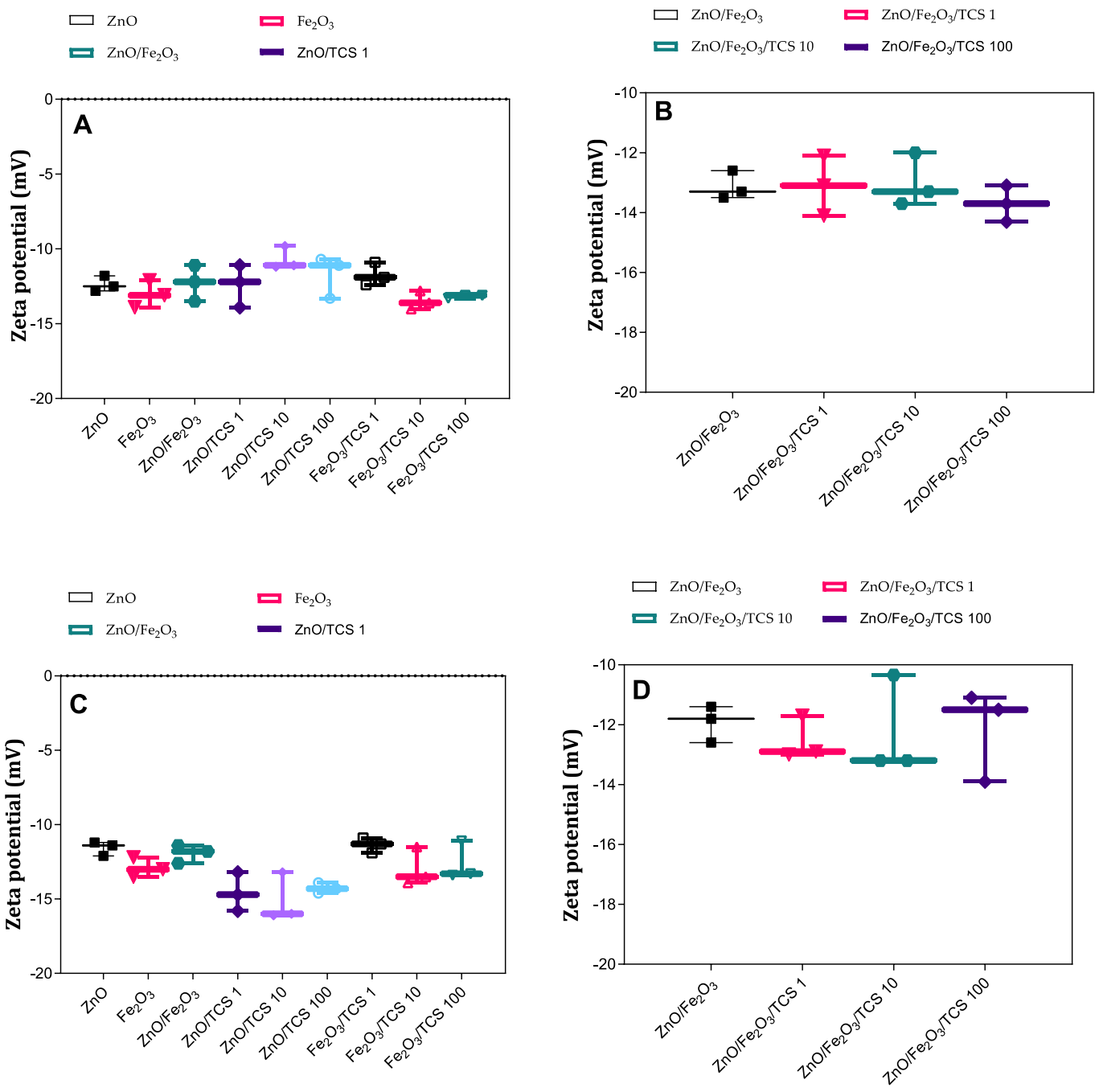

Figure 6.1: Summary analysis of zeta potential for the individual ENPs and their variant mixtures with TCS in (a, b) BR water and, (c, d) ER water samples, respectively. The summary analysis was from calculated from average results (n=3) of zeta potential measured over 2 h. No significant differences were observed between the combinations of mixtures over the 2 h interval in both river water systems.

The influence of organic pollutants on the ζ-potential of ENPs differ across studies, either due to type of organic pollutant, organic pollutant concentration effects or water chemistry influence (Li et al., 2017; Liu, Wang, et al., 2018; Khan et al., 2019). For example, Khan et al. (2019) showed that co-existence of polybrominated diphenyl ethers (PBDPEs) and nZnO had a pronounced effect on ζ-potential in freshwater compared to wastewater, whereas the effects observed in freshwater were only significant at higher concentrations at the highest concentrations (>1 000 μg L^{-1}). In another study by Li et al. (2017), nZnO ζ-potential was found to be unchanged by the presence of non-ionic nonylphenol ethoxylates (NP-9), even with increasing concentrations in milli-Q water, whereas the presence of (SDS) was found to significantly increase the ζ-potential of nZnO with increasing concentrations. In contrast, these effects were deemed to be minimal in natural water samples (Li et al. 2017). These findings are similar to those herein, where the presence of TCS in both binary mixtures with ENPs or ternary mixtures did not exert any pronounced influence on the observed ζ-potential.

6.2.2 Influence of TCS on the aggregation of ENPs

There was observed immediate aggregation for the ENPs in both river water samples (Figure 6.2) with increased aggregation, although in BR compared to ER water (Figure 6.2). In this study, exposure concentrations of nZnO and nFe_2O_3 were fixed at 1 000 ug L^{-1}, and concentrations of TCS were varied from 1 to 1 000 ug L^{-1}. The ENPs mixtures formed aggregate sizes larger than individual ENPs, likely due to heteroaggregation in both river water samples (Figure 6.2 a and b).

The aggregation of ENPs was more pronounced in BR compared to ER water. This could be linked to the influence of water physicochemical composition of BR and ER water, as reported in (Leareng, Ubomba-Jaswa & Musee, 2020). Similar aggregation behaviour was observed for binary mixtures of nZnO and nFe_2O_3, which formed the largest aggregates in both river water samples (Figure 6.2 a and b). For binary mixtures of ENPs and TCS, the organic pollutant did not have any influence on the aggregation of nFe_2O_3. However, TCS was found to reduce the extent of nZnO aggregation with increasing concentrations in both BR and ER water (Figure 6.2 a and b). Ternary mixtures aggregate sizes were reduced by the

increasing concentrations of TCS (Figure 6.2 c and d), with more stability in ER water compared to BR water. The behaviour of ENPs was linked to the influence of water physicochemical composition of BR and ER water. Specifically, the adsorption of natural organic matter (NOM)is known to either stabilize or destabilize ENPs in aqueous media (Wang et al 2016). Secondly, in aqueous media with high ionic strength, particularly due to divalent ions (e.g. Ca^{2+}, Mg^{2+}), aggregation can occur as result of two key processes. These entails either the reduction of electrical double layer (EDL) leading to reduced repulsive forces between ENP particles, or cation bridging between chains of NOM enhancing formation of aggregates (Aitken et al 2011; Wang et al 2016; Yu et al 2018), which would explain the difference in the aggregate sizes of nZnO and nFe_2O_3 in BR and ER water.

The introduction of organic contaminants can also affect the stability of ENPs suspensions through improved dispersity by altering electrostatic repulsion between ENPs (Deng et al., 2017; Zhang et al., 2019). A number of studies have investigated the influence of contaminants such as organics on behaviour and toxicity of ENPs and these are critically reviewed elsewhere (Deng et al., 2017; Liu, Nie, et al., 2018; Naasz, Altenburger & Kühnel, 2018). From these studies, physicochemical interactions of ENPs and organic pollutants have been shown to be mostly by adsorption of organics onto ENPs, including triclo-based organics (triclosan and triclocarban). In this study, increasing concentrations of triclosan were observed to stabilise the aggregation of nZnO, with minor fluctuations in HDD sizes in both river water systems. In addition, aggregation of nZnO/nFe_2O_3 mixtures was reduced by TCS presence at the highest concentrations (Figure 6.2 c and d). These effects were associated with adsorption of TCS onto ENPs which, to a lesser extent, reduced the favourable heteroaggregation between the two ENPs. To fully assess the influence of TCS on the behaviour of ENPs over the short exposure period, time resolved measurement of aggregate sizes were measured as shown in Figure 6.3 and Figure 6.4.

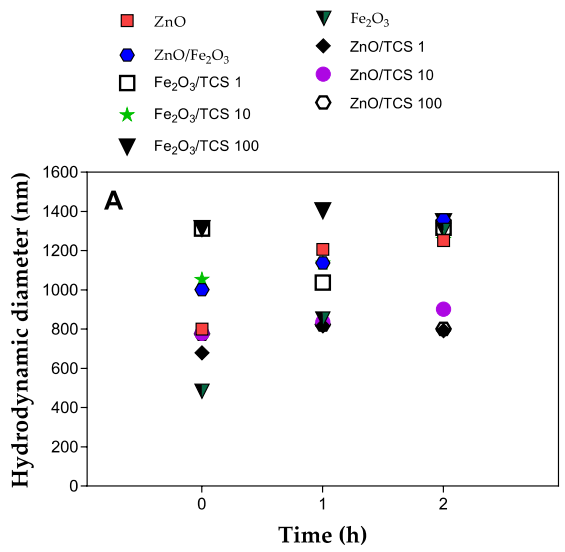
ZnO
ZnO/Fe2O3
Fe2O3/TCS 1
Fe2O3/TCS 10
Fe2O3/TCS 100
Fe2O3
ZnO/TCS 1
ZnO/TCS 10
ZnO/TCS 100
A
Hydrodynamic diameter (nm)
Time (h)

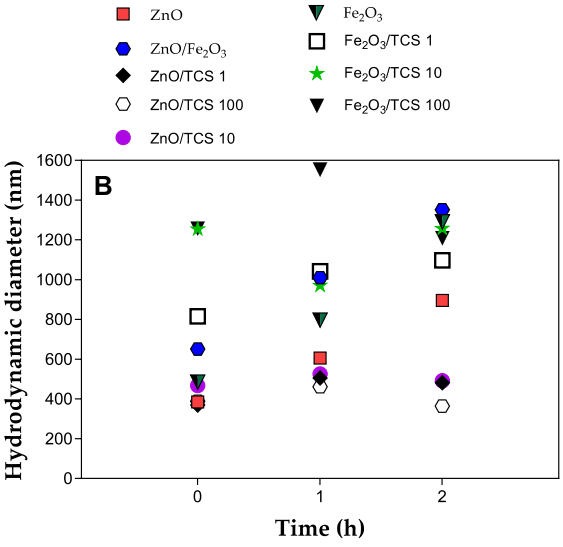
ZnO
ZnO/Fe2O3
ZnO/TCS 1
ZnO/TCS 100
ZnO/TCS 10
Fe2O3
Fe2O3/TCS 1
Fe2O3/TCS 10
Fe2O3/TCS 100
B
Hydrodynamic diameter (nm)
Time (h)

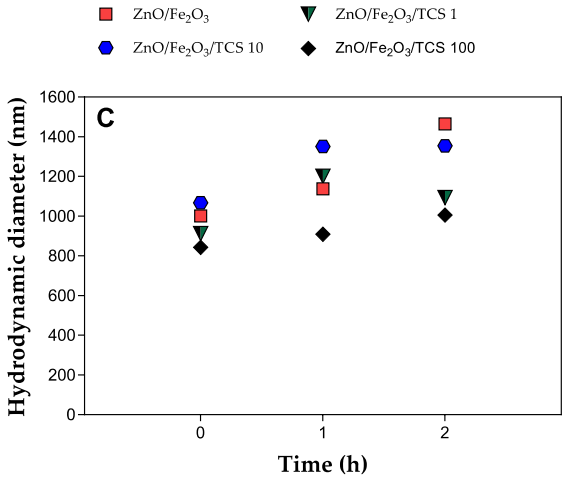
ZnO/Fe2O3
ZnO/Fe2O3/TCS 10
ZnO/Fe2O3/TCS 1
ZnO/Fe2O3/TCS 100
C
Hydrodynamic diameter (nm)
Time (h)

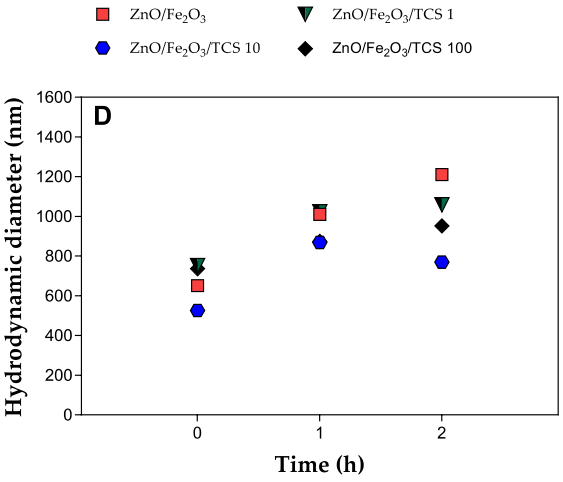
ZnO/Fe2O3
ZnO/Fe2O3/TCS 10
ZnO/Fe2O3/TCS 1
ZnO/Fe2O3/TCS 100
D
Hydrodynamic diameter (nm)
Time (h)

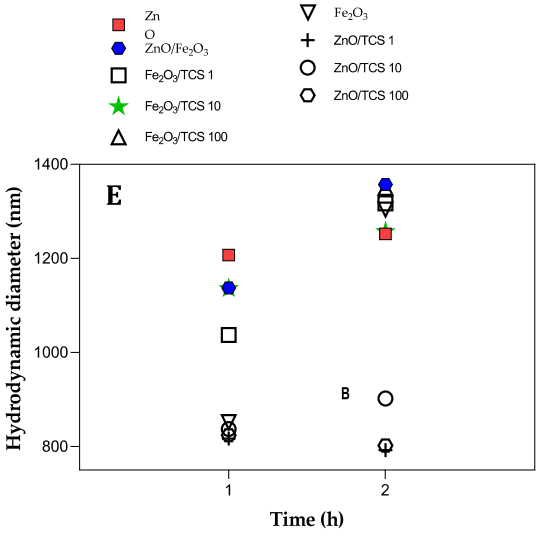
Zn
O
ZnO/Fe2O3
Fe2O3/TCS 1
Fe2O3/TCS 10
Fe2O3/TCS 100
Fe2O3
ZnO/TCS 1
ZnO/TCS 10
ZnO/TCS 100
E
B
Hydrodynamic diameter (nm)
Time (h)

Figure 6.2: HDD for nZnO and nZnO, nFe_2O_3 and triclosan mixtures. (A)Binary mixtures of BR water, (B)Binary mixtures of ER, (c)ternary mixtures in BR, (D)Ternary mixtures of ER water. the figure in E represents the expanded HDD in (A) for 1 h and 2h, in BR water for clarity.

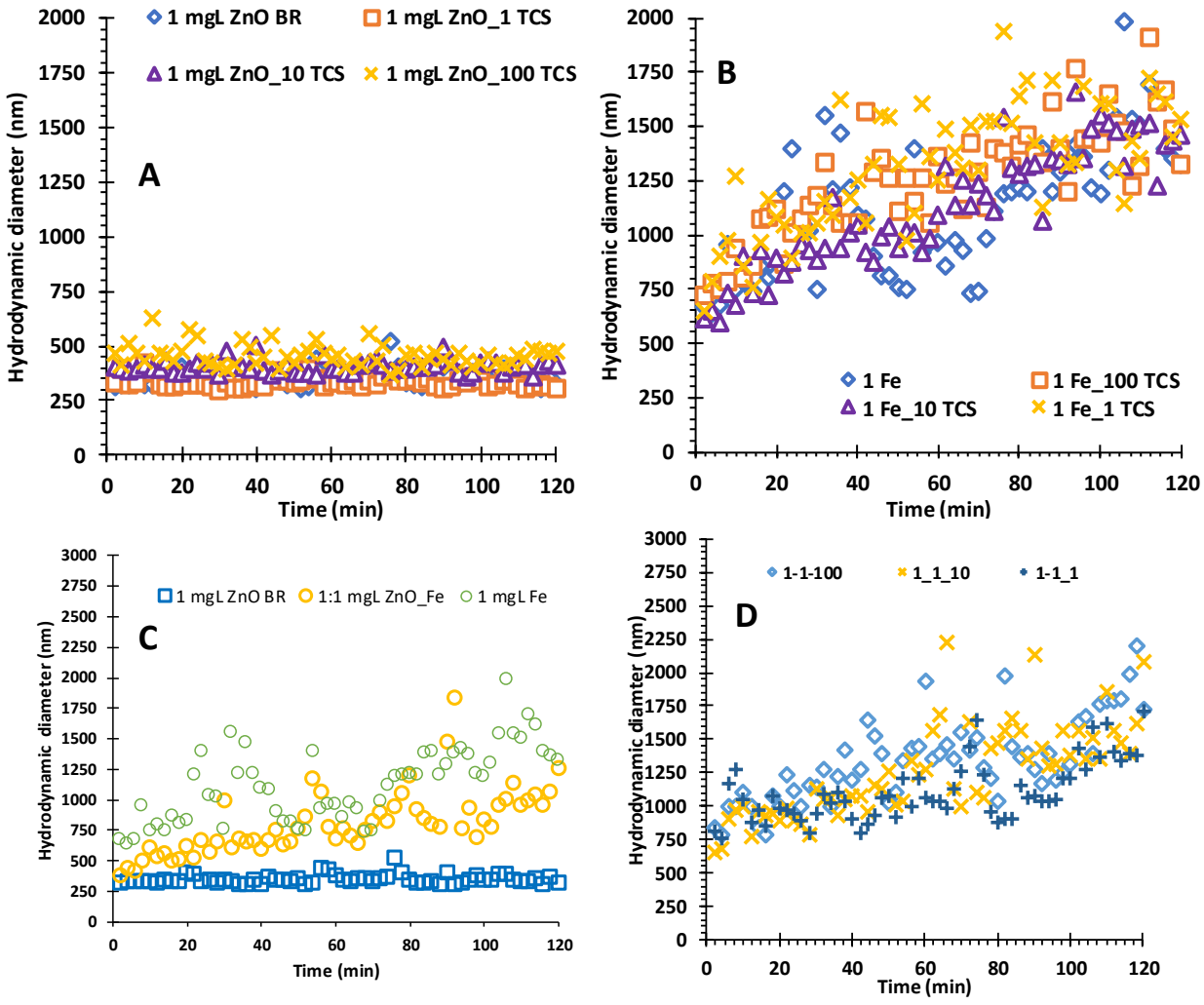

Figure 6.3: HDD measurements for (a)nZnO and TCS; (b) nFe_2O_3 -TCS; (c) nZnO- nFe_2O_3; and (d) nZnO/ nFe_2O_3 - TCS in BR water.

These size trends measurements focused on the influence of triclosan on the aggregation behaviour of ENPs. The aggregate sizes of nZnO-TCS mixtures were observed to be either similar or lower than aggregate sizes of nZnO in both river water samples, with larger

aggregates in BR water (Figure 6.3 a) compared to ER water (Figure 6.4 a), where the presence of TCS was slightly reduced the aggregate sizes of nZnO. These effects were also observed with increased nZnO concentration for both BR and ER water (Figure A7).

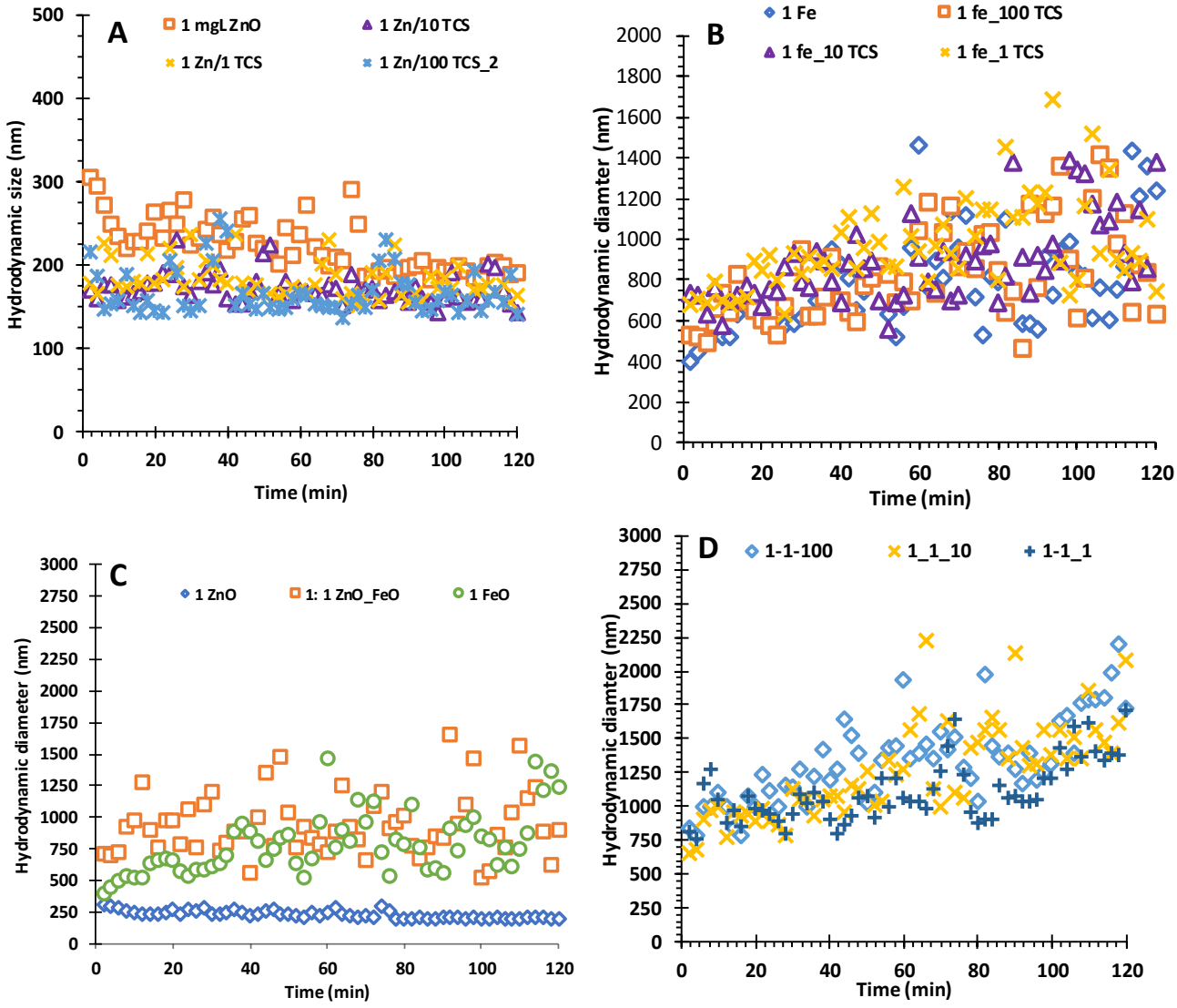

Figure 6.4: HDD measurements for (a)nZnO and TCS; (b) nFe_2O_3 -TCS; (c) nZnO- nFe_2O_3; and (d) nZnO/ nFe_2O_3 - TCS in ER water.

TCS co-existence with nFe_2O_3 only showed fluctuations in HDD measurements, however, there was no significant reduction in aggregate sizes (Figure 6.3 and Figure 6.4). There was no pronounced pattern for nFe_2O_3 aggregation with increasing TCS concentrations observed, even when different nFe_2O_3 were tested (Figure A8 and A9). Ternary mixtures also found to

aggregate, following nFe_2O_3 aggregation trends (Figure 6.3 d and 6.4 D), however, highest TCS concentrations lowered the ternary mixtures size trends.

Overall, both HDD and size trends measurements exhibited the influence of TCS, especially when co-existing with nZnO, which could be likely be linked to competitive sorption of TCS. Sorption of pollutants such as TCS on ENPs in aqueous phase through traditional separation methods such as centrifugation and filtration is still difficult (Koh et al., 2011; Engel & Chefetz, 2019; Zhang et al., 2019), especially at environmentally relevant concentrations used in this study. Therefore, to determine the likely surface complexation of TCS on nZnO and the mixtures, we measured dissolved Zn^{2+}. Dissolution of nZnO was observed to be similar to those of the ENPs binary and ternary mixtures for both river water systems (Figure 6.5). However, the binary mixtures of nZnO and TCS had the lowest concentrations of measured Zn^{2+} (Figure 6.5).

The reduction in dissolution of nZnO in the presence of TCS was linked to high adsorption of TCS, which showed that the organic pollutant could influence the dissolution of nZnO in natural water samples, even in the presence of NOM and cations. These effects have been associate with the low solubility high hydrophobicity of organic pollutants, which could lead to their adsorption on ENPs via hydrophobic ligands (Khan et al., 2019). However, further work is required to understand these mechanisms. Findings in this study were opposite to reported results from Chen et al. (2018). Although their study reported high adsorption of TCS (between 80 and 90% of TCS in wastewater and distilled water) on nCu, they observed increased aggregation of nCu from the mixtures than nCu alone. Other studies have shown the efficient adsorption (>70%) of TCS on quantum dots (Fard et al., 2017; Lin et al., 2019). Other studies have investigated the influence of organic compounds on the aggregation and dissolution of nZnO (Li et al., 2017; Liu, Wang, et al., 2018; Khan et al., 2019). For example, Zhu et al. (2020) reported reduced Zn^{2+} release upon SDS co-existence with nZnO, linked to the adsorption of the organic pollutant on the ENPs. Similarly, in these studies, the aggregate size of nZnO was reduced, due to adsorption of the organics reducing the zeta potential and inversely, increasing the repulsive energy between particulates. In this study, we did not observe significant shifts in the zeta potential of ENPs, even with increasing concentrations

of TCS (Figure 6.1). However, the same reduction in dissolution of nZnO was apparent as shown in Figure 6.5.

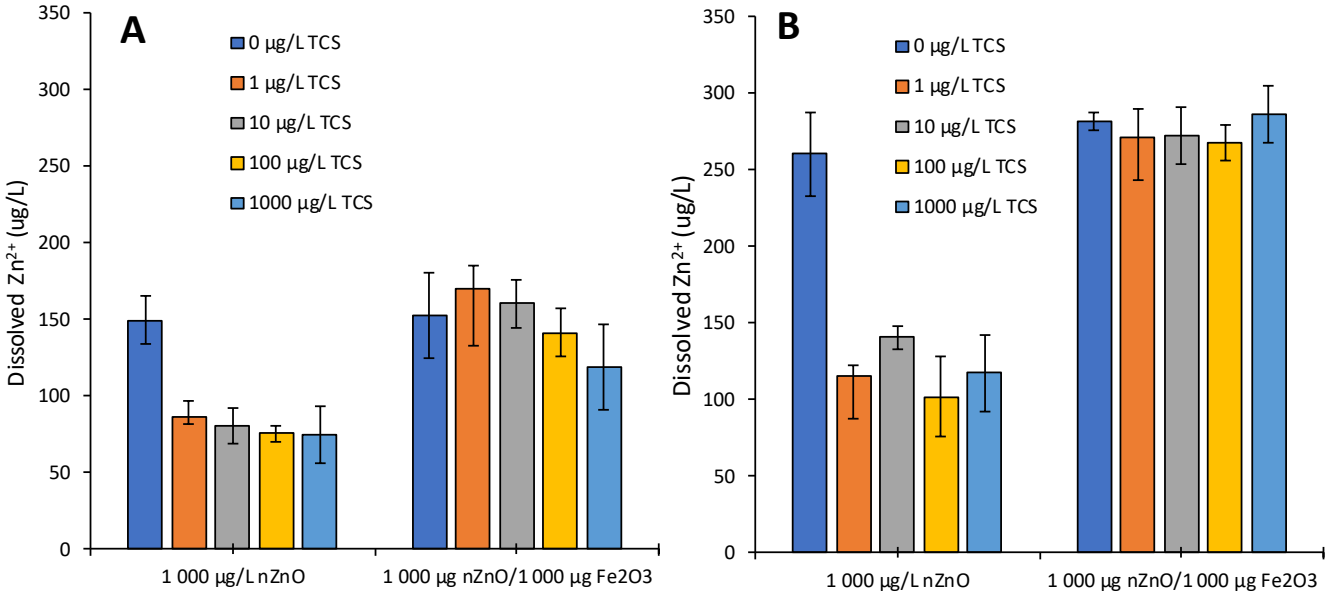

Figure 6.5: The dissolution of nZnO in binary and ternary mixtures in (a)BR river water, (b) ER river water, under visible light for 1 h.

6.3 Cytotoxicity of mixtures of nZnO, γ-nFe$_2$O$_3$ and TCS mixtures

The effects of the mixtures on cell membrane integrity are shown in Figure 6.6. There was no observed effect on the cell membrane integrity of *B. subtilis* from nFe$_2$O$_3$ exposure in both BR water and ER water, similar to (Leareng, Ubomba-Jaswa & Musee, 2020). 1 000 µg L^{-1} ZnO significantly reduced cell viability in ER water (75%), whereas minimal effect was observed in BR water. Similarly, significantly reduced membrane integrity was observed at both higher concentrations of TCS in BR water compared to ER water (Figure 6.6). At 1, 10 and 100 µg L^{-1}, there was minimal effect on membrane integrity from TCS in BR water. To further assess the toxicity of TCS we increased the 100 µg L^{-1} by tenfold to 1 000 µg L^{-1} TCS (included in the toxicity), where a significant reduction in the membrane integrity from both binaries and ternaries of ENPs and TCS was observed (Figure 6.5 and Figure 6.6).

In ternary mixtures, however, dissolution was similar to nZnO alone, and the role of γ-nFe_2O_3 in the ternaries could not be established. The presence of both ENPs could have an influence on the adsorption of TCS; thus altering the transformations from the co-existence of TCS-nZnO mixtures alone. However, we observed no significant toxicity for γ-nFe_2O_3 under the same conditions for both river water systems (Figure 6.6 a and Figure 6.6 b). The observed nZnO toxicity herein was linked to the increase in TCS concentration which exerted effects at varying degrees. The levels of toxicity induced by TCS at 1 000 μg L^{-1}, either alone or in mixtures with ENPs was significant, especially in ER water (Figure 6.6 b), even in both river water samples, highlighting the toxicity of TCS at elevated concentrations. A study on the effects of TCS and nCu (copper nanoparticles) nitrogen and phosphorus removal in an activated sludge system reported reduced removal by the presence of 1 000 TCS at 1 mg L^{-1} (Chen et al., 2018). When nCu (1 and 5 000 μg L^{-1}) was introduced as mixtures with the 1 000 μg L^{-1} triclosan, the effect of TCS was not reduced by the presence of 1 000 μg L^{-1} nCu, moreover, at the higher copper exposure concentration the effects observed for TCS increased. In this study, the effects of TCS at 1 000 μg L^{-1} were not be mitigated by the presence of nZnO, nFe_2O_3 or the ENPs binary mixtures. However, TCS effects on membrane integrity at lower concentrations were reversed in the presence of the ENPs. Therefore, the extent of adsorption for TCS on ENPs could be higher at lower concentrations.

Although nZnO was observed to significantly cause membrane damage in ER water (Figure 6.6), the effects were reduced in mixtures of TCS. The reduction in effects was associated with adsorption of TCS on nZnO, which in turn, reduced the nano-cell interactions, and effectively, the toxicity of the ENP. These findings are different from the observations by Cheng et al. (2018) where increased adsorption of TCs on nCu did not mitigate toxicity, but either did not change or elevated toxic effects due to increased Cu^{2+} release. The differences in the dissolution could likely be due to the treatments and possibly the role of water chemistry components. In their study, nCu and TCS were reacted for 24 h before they were introduced into the activated sludge reactor. The adsorption of TCS on the ENPs were shown to increase significantly after 24 h, especially in wastewater, increasing the stability of the ENPs. The differences in the dissolution in both distilled water and wastewater showed that water chemistry had significant influence on the ENP-TCS interactions and dissolution.

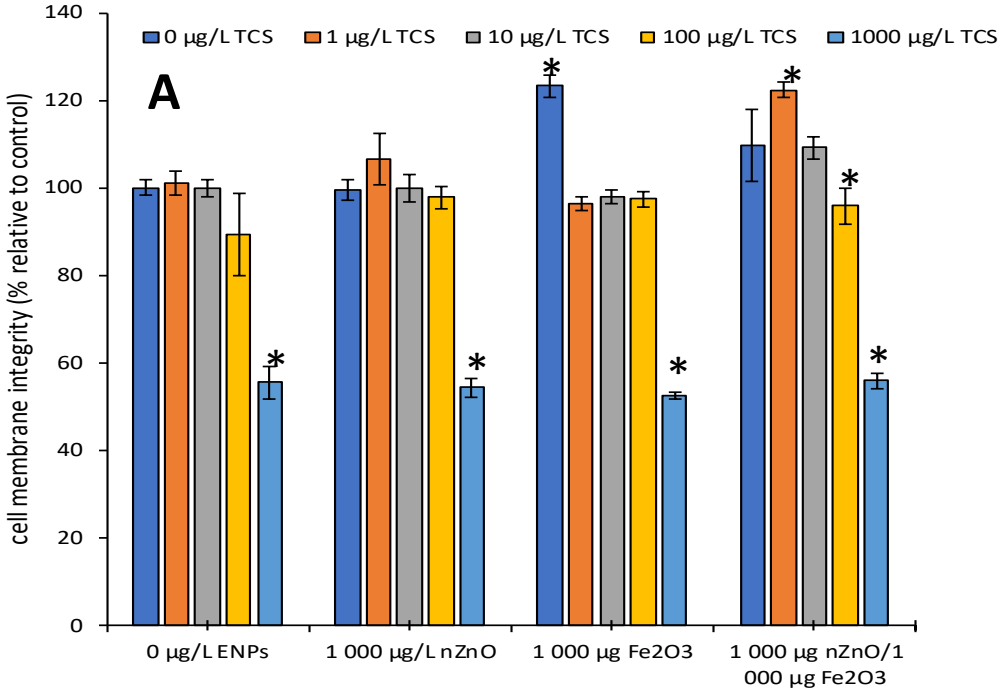
A
0 µg/L TCS
1 µg/L TCS
10 µg/L TCS
100 µg/L TCS
1000 µg/L TCS
cell membrane integrity (% relative to control)
0
20
40
60
80
100
120
140
0 µg/L ENPs
1 000 µg/L nZnO
1 000 µg Fe2O3
1 000 µg nZnO/1 000 µg Fe2O3

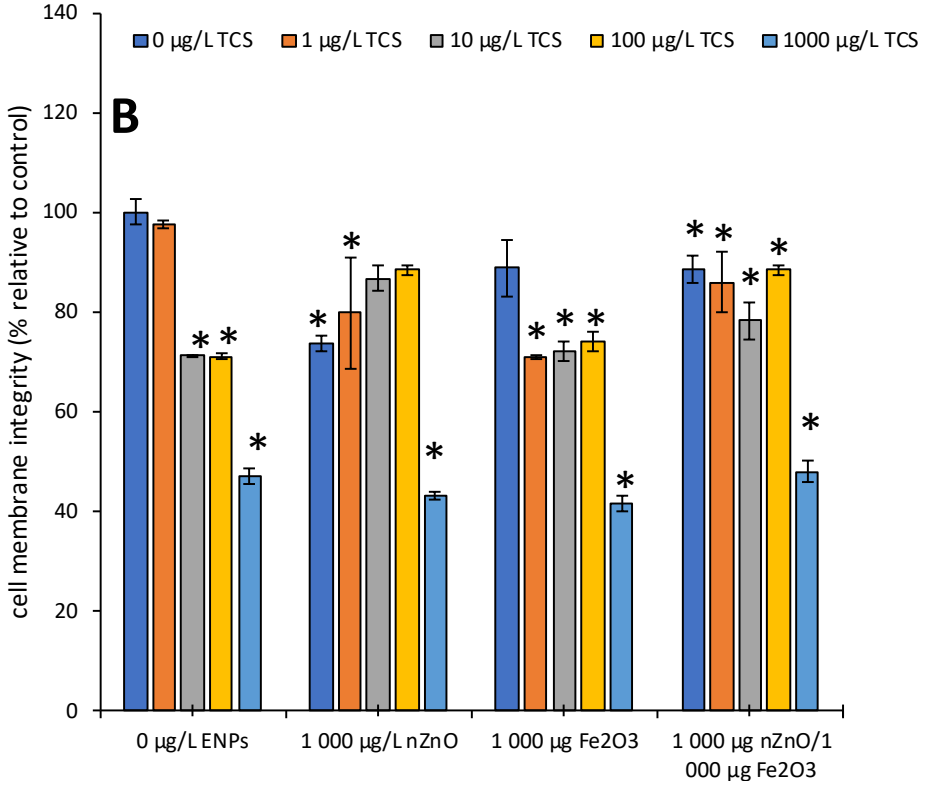
B
0 µg/L TCS
1 µg/L TCS
10 µg/L TCS
100 µg/L TCS
1000 µg/L TCS
cell membrane integrity (% relative to control)
0
20
40
60
80
100
120
140
0 µg/L ENPs
1 000 µg/L nZnO
1 000 µg Fe2O3
1 000 µg nZnO/1 000 µg Fe2O3

Figure 6.6: Cell membrane integrity of *B. subtilis* following exposure to mixtures of nZnO, γ-nFe_2O_3 TCS in (a) BR river water and (b) ER water. Asterisk (*) indicate significant difference between treatment and control (α = 0.05).

This highlights the unique interactions of chemical mixtures and warrants more investigations to enable generic inferences, given the unique features of nanoscale-based chemicals. There was no varied toxicity between TCS alone and its mixture with nFe_2O_3. However,nFe_2O_3 has also been reported to mitigate the toxicity of antibacterial agents such as ciprofloxacin to bacteria, likely through adsorption of the antibacterial agent, reducing their bioavailability (Masadeh et al., 2015).

Considerable differences in the hydrodynamic diameter between nZnO, nZnO-TCS and nZnO- γ-nFe_2O_3 -TCS ternary mixtures were also observed. Therefore, the differences in the toxicity observed between the individual binary and ternary mixtures could be linked to the dispersion state of the ENPs for nZnO with TCS compared to the increased hydrodynamic diameter for the ternary systems (Figure 6.3 and Figure 6.4). Therefore the nZnO particulate could have a higher contribution to the observed effect compared to the released ions, however these could change with increased exposure time, a finding in agreement with Song et al. (Song et al., 2020). These findings add to limited but growing studies on the interactions of ENPs and organic mixtures, however, more research is required to fully elucidate the interactions between the mixtures and the toxicological outcomes.

6.4 Conclusions

The toxicity of binary and ternary mixtures nZnO, γ-nFe_2O_3 and TCS investigated in natural water samples. The interactions of the mixtures were assessed based on the aggregation, dissolution and their effects on the cell membrane integrity of *B. subtilis*. nZnO was found to be dependent on water chemistry attributes (more in ER than BR water) with decrease in aggregate size as TCS concentration increased in both water samples. γ-nFe_2O_3 aggregate size was not changed by presence of TCS in both river water systems. TCS effects on bacteria were significant at highest concentration, while the toxicity of other mixtures were reversed or remained similar for binary and ternary mixtures. The differences in toxicity in both river

water systems were associated with the aggregation of ENPs and their mixtures due to water chemistry variations between BR and ER water. Results herein illustrate the complexity on the interactions of ENPs and other contaminants in the environment. Hence, this raises the need for further work on the mechanisms influencing the aggregation differences. ENPs will exist and interact with contaminants such as triclosan in the environment, and change the physicochemical properties and biological effects of all the contaminants. This study provides the first direct evidence on the ternary mixtures of ENPs and TCS in environmentally relevant media and concentrations of all contaminants. However, more work is needed to elucidate the mechanisms and nature of interactions at toxicity of the mixtures. Thus, further consideration of the environmental risks of mixtures will be critical for risk assessment of ENPs and mixture pollutants.

Chapter 7: Conclusions and recommendations

7.1 Concluding remarks

This study explored the cytotoxic effects of ENPs as mixtures as well as their mixtures with organic pollutants on bacteria as influenced by their transformations and natural water chemistry characteristics. The study investigated the influence of water chemistry components on the toxicity and likely mechanisms of toxicity for ENPs mixtures (ENP-ENP), while the influence of the organic contaminant on the transformations, interactions and toxicity on ENPs as binary and ternary mixtures, at concentrations of contaminants close to those likely to be in the environment. To achieve this, three objectives were set up; (i) the first objective investigated the toxicity of nZnO and γ-nFe_2O_3 on the environmentally ubiquitous bacteria, *Bacillus subtilis*, as influenced by natural water physicochemical parameters, (ii) the toxicity of binary mixtures of nZnO and γ-nFe_2O_3 on *B. subtilis* in natural water samples under solar irradiation were investigated, (iii) The influence of TCS on ENPs as binary and ternary mixtures on *B. subtilis* in natural water samples was assessed.

Objective 1: Zinc oxide and iron oxide ENPs toxicity on *Bacillus subtilis* in river water systems

The behaviour of ENPs in the natural water samples was found to be dependent on the water chemistry characteristics as shown by the larger hydrodynamic diameters of both ENPs in BR water compared to ER water. These effects also had in influence on dissolution with higher reported dissolution in ER water. The results obtained also showed that the effects of nZnO on cell viability and ATP production were diminished by the presence of high natural organic matter and ionic strength in BR water compared to ER water. The toxicity of nZnO was associated with dissolved Zn^{2+}, however the role of the particulate was not dismissed. Therefore, aggregation was found to be a major factor in the dissolution of nZnO, and toxicity of both ENPs.

The study highlighted the use of multiple endpoints to access the toxicity of ENPs, particularly at lower concentrations where effects such as cell viability are not affected or are not obvious.

Objective 2: *Bacillus subtilis* responses to binary mixtures of zinc oxide and iron oxide ENPs in river water systems

The binary ENP mixture of ENPs formed aggregates that were larger than the aggregate sizes of each ENP, pointing to heteroaggregation. The influence of water chemistry parameters was evident as larger aggregates were formed in BR water compared to ER water while higher dissolution was observed in ER compared to BR water. Under solar irradiation, nZnO dissolution was not diminished by the presence of γ-nFe_2O_3. These effects were associated with maintenance of equilibrium for Zn^{2+} in aqueous media, likely also assisted by photocorrosion of nZnO. However reduced toxicity was observed in the binary mixtures, associated with the heteroaggregation of the ENPs. ROS species were ruled out as the mechanism of toxicity under the exposure condition due to the non-significant differences between nZnO and the binary systems. The water chemistry parameters had an influence on the toxicity of ENPs, with nZnO more toxic in ER water and mitigated effects more pronounced in BR water due to the larger aggregate sizes compared to ER water.

Objective 3: Interactions and toxicity of ENPs and triclosan: Ternary exposure in river water systems

The toxicity of binary and ternary mixtures nZnO, γ-nFe_2O_3 and TCS investigated in natural water samples. The interactions of the mixtures were assessed based on the aggregation, dissolution and their effects on the cell membrane integrity of *B. subtilis,* under visible light to minimize the transformation and photodegradation of TCS. nZnO aggregate sizes were not larger than those BR water with decrease in aggregate size as TCS concentration increased in ER water sample. γ-nFe_2O_3 aggregate size was not changed by presence of TCS in both river water systems. TCS effects on bacteria were significant at highest concentration in both water samples, showing that TCS behaviour was not dependent on water physicochemical

parameters. However, the toxicity of both TCS and nZnO were reduced or remained similar for binary and ternary mixtures. river water physicochemical characteristics effects on mitigating toxic effects were more pronounced in BR compared to ER water, associated with the aggregation of ENPs and their mixtures due to water compositions (NOM and IS).

There is need for further exploration on the interactions of TCS and ENPs to fully understand the transformations processes that occur. Although this study was conducted under visible light to minimise photodegradation, and only examine processes such as aggregation and dissolution due to the presence of TCS, these should also be critically looked at to fully understand the complexation that occur in natural water under environmentally relevant conditions.

7.2 Recommendations

- Current findings on toxicity of ENPs and TCS were based on the responses of a single bacterial species, that has been reported to be more sensitive to ENPs (Baek & An, 2011; Barnes et al., 2013). However, to fully elucidate the correlation between ENPs presence at environmentally relevant conditions and aquatic organisms, studies examining the responses of bacterial communities are needed.

- There is also a need to examine the toxicity of ENPs, TCs and their mixtures following longer interaction times to fully understand the complexations that take place between the mixtures. In this work, we examine the interactions of binary mixtures of ENPs as well as the ternary under 30 min and 120 min, which may not be enough time to fully measure the extent of interactions that take place. For instance, the unchanged levels of released Zn^{2+} in nZnO and ENP mixtures may change in the longer period if given enough time for complexation to fully occur.

The use of cytotoxicity assays for ENPs and mixtures under the given exposure conditions revealed different bacterial responses to assess the effects inferred. However, there is need

for molecular studies to be incorporated in these cytotoxicity studies under environmentally relevant ENPs concentrations and exposure conditions to fully assess the environmental risks of NPs. These could be at the bacterial species level or whole community level, to allow for changes in the bacterial structure and the mechanisms through which the species and community are affected by ENPs exposures. Furthermore, the difference in the reported nZnO reported mechanisms of toxicity warrants further investigation, particularly at lower ENP concentrations. Integration of molecular approaches and atypical endpoints may help with understanding nZnO bacterial toxicity in freshwater systems.

References

Aal, N.A., Al-Hazmi, F., Al-Ghamdi, A.A., Al-Ghamdi, A.A., El-Tantawy, F. & Yakuphanoglu, F. 2015. Novel rapid synthesis of zinc oxide nanotubes via hydrothermal technique and antibacterial properties. *Spectrochimica Acta Part A: Molecular and Biomolecular Spectroscopy*. 135:871–877.

Adeleye, A.S., Pokhrel, S., Mädler, L. & Keller, A.A. 2018. Influence of nanoparticle doping on the colloidal stability and toxicity of copper oxide nanoparticles in synthetic and natural waters. *Water research*. 132:12–22.

Alhasawi, A., Auger, C., Appanna, V., Chahma, M. & Appanna, V. 2014. Zinc toxicity and ATP production in *Pseudomonas fluorescens*. *Journal of applied microbiology*. 117(1):65–73.

Ali, A., Hira Zafar, M.Z., ul Haq, I., Phull, A.R., Ali, J.S. & Hussain, A. 2016. Synthesis, characterization, applications, and challenges of iron oxide nanoparticles. *Nanotechnology, Science and Applications*. 9:49.

Altenburger, R., Brack, W., Burgess, R.M., Busch, W., Escher, B.I., Focks, A., Hewitt, L.M., Jacobsen, B.N., et al. 2019. Future water quality monitoring: improving the balance between exposure and toxicity assessments of real-world pollutant mixtures. *Environmental Sciences Europe*. 31(1):1–17.

Amde, M., Liu, J., Tan, Z.-Q. & Bekana, D. 2017. Transformation and bioavailability of metal oxide nanoparticles in aquatic and terrestrial environments. A review. *Environmental Pollution*. 230:250–267.

Amenta, V., Aschberger, K., Arena, M., Bouwmeester, H., Moniz, F.B., Brandhoff, P., Gottardo, S., Marvin, H.J., et al. 2015. Regulatory aspects of nanotechnology in the agri/feed/food sector in EU and non-EU countries. *Regulatory Toxicology and Pharmacology*. 73(1):463–476.

Anders, C.B., Eixenberger, J.E., Franco, N.A., Hermann, R.J., Rainey, K.D., Chess, J.J., Punnoose, A. & Wingett, D.G. 2018. ZnO nanoparticle preparation route influences surface reactivity, dissolution and cytotoxicity. *Environmental Science Nano*. 5:572–588.

Arnot, J.A. & Mackay, D. 2008. Policies for chemical hazard and risk priority setting: can persistence, bioaccumulation, toxicity, and quantity information be combined?

Aruoja, V., Dubourguier, H.C., Kasemets, K. & Kahru, A. 2009. Toxicity of nanoparticles of CuO, ZnO and TiO_2 to microalgae Pseudokirchneriella subcapitata. *Science of the total environment*. 407(4):1461–1468.

Aruoja, V., Pokhrel, S., Sihtmäe, M., Mortimer, M., Mädler, L. & Kahru, A. 2015. Toxicity of 12 metal-based nanoparticles to algae, bacteria and protozoa. *Environmental Science: Nano*. 2(6):630–644.

Auffan, M., Achouak, W., Rose, J., Roncato, M.-A., Chanéac, C., Waite, D.T., Mason, A., Woicik, J.C., et al. 2008. Relation between the redox state of iron-based nanoparticles and their cytotoxicity toward *Escherichia coli*. *Environmental science & technology*. 42(17):6730–6735.

Auffan, M., Rose, J., Wiesner, M.R. & Bottero, J.-Y. 2009. Chemical stability of metallic nanoparticles: a parameter controlling their potential cellular toxicity in vitro. *Environmental Pollution*. 157(4):1127–1133.

Azam, A., Ahmed, A.S., Oves, M., Khan, M.S., Habib, S.S. & Memic, A. 2012. Antimicrobial activity of metal oxide nanoparticles against Gram-positive and Gram-negative bacteria: a comparative study. *International Journal of Nanomedicine*. 7:6003–6009.

Baalousha, M. 2009. Aggregation and disaggregation of iron oxide nanoparticles: influence of particle concentration, pH and natural organic matter. *Science of the total Environment*. 407(6):2093–2101.

Baalousha, M., Manciulea, A., Cumberland, S., Kendall, K. & Lead, J.R. 2008. Aggregation and surface properties of iron oxide nanoparticles: influence of pH and natural organic matter. *Environ. Toxicol. Chem.* 27(9):1875–1882.

Baalousha, M., Nur, Y., Römer, I., Tejamaya, M. & Lead, J.R. 2013. Effect of monovalent and divalent cations, anions and fulvic acid on aggregation of citrate-coated silver nanoparticles. *Science of the Total Environment*. 454–455:119–131.

Backhaus, T. & Faust, M. 2012. Predictive environmental risk assessment of chemical mixtures: a conceptual framework. *Environmental science & technology*. 46(5):2564–2573.

Bae, E., Park, H.-J., Yoon, J., Kim, Y., Choi, K. & Yi, J. 2011. Bacterial uptake of silver nanoparticles in the presence of humic acid and AgNO3. *Korean Journal of Chemical Engineering*. 28(1):267–271. DOI: 10.1007/s11814-010-0351-z.

Baek, Y.-W. & An, Y.-J. 2011. Microbial toxicity of metal oxide nanoparticles (CuO, NiO, ZnO, and Sb_2O_3) to *Escherichia coli*, *Bacillus subtilis*, and *Streptococcus aureus*. *Science of the Total Environment*. 409:1603–1608.

Baek, S., Joo, S.H., Kumar, N. & Toborek, M. 2017. Antibacterial effect and toxicity pathways of industrial and sunscreen ZnO nanoparticles on *Escherichia coli*. *Journal of environmental chemical engineering*. 5(3):3024–3032.

Bandyopadhyay, S., Plascencia-Villa, G., Mukherjee, A., Rico, C.M., José-Yacamán, M., Peralta-Videa, J.R. & Gardea-Torresdey, J.L. 2015. Comparative phytotoxicity of ZnO NPs, bulk ZnO, and ionic zinc onto the alfalfa plants symbiotically associated with *Sinorhizobium* meliloti in soil. *Science of the Total Environment*. 515:60–69.

Barnes, R.J., Molina, R., Xu, J., Dobson, P.J. & Thompson, I.P. 2013. Comparison of TiO_2 and ZnO nanoparticles for photocatalytic degradation of methylene blue and the correlated inactivation of gram-positive and gram-negative bacteria. *Journal of nanoparticle research*. 15(2):1432.

Bäuerlein, P.S., Emke, E., Tromp, P., Hofman, J.A.M.H., Carboni, A., Schooneman, F., de Voogt, P. & van Wezel, A.P. 2017. Is there evidence for man-made nanoparticles in the Dutch environment? *Science of The Total Environment*. 576:273–283. DOI: 10.1016/j.scitotenv.2016.09.206.

Baun, A., Sayre, P., Steinhäuser, K.G. & Rose, J. 2017. Regulatory relevant and reliable methods and data for determining the environmental fate of manufactured nanomaterials. *NanoImpact*. 8:1–10.

Behra, R. & Krug, H. 2008. Nanoecotoxicology: Nanoparticles at large. *Nature Nanotechnology*. 3(5):253.

Besha, A.T., Liu, Y., Fang, C., Bekele, D.N. & Naidu, R. 2019. Assessing the interactions between micropollutants and nanoparticles in engineered and natural aquatic environments. *Critical Reviews in Environmental Science and Technology*. 1–81.

Bhatt, I. & Tripathi, B.N. 2011. Interaction of engineered nanoparticles with various components of the environment and possible strategies for their risk assessment. *Chemosphere*. 82(3):308–317. DOI: 10.1016/j.chemosphere.2010.10.011.

Bian, S.W., Mudunkotuwa, I.A., Rupasinghe, T. & Grassian, V.H. 2011. Aggregation and dissolution of 4 nm ZnO nanoparticles in aqueous environments: Influence of pH, ionic strength, size, and ddsorption of humic acid. *Langmuir*. 27:6059–6068.

Bitragunta, S.P., Palani, S.G., Gopala, A., Sarkar, S.K. & Kandukuri, V.R. 2017. Detection of TiO_2 Nanoparticles in Municipal Sewage Treatment Plant and Their Characterization Using Single Particle ICP-MS. *Bulletin of environmental contamination and toxicology*. 98(5):595–600.

Blair, B.D., Crago, J.P., Hedman, C.J. & Klaper, R.D. 2013. Pharmaceuticals and personal care products found in the Great Lakes above concentrations of environmental concern. *Chemosphere*. 93(9):2116–2123. DOI: 10.1016/j.chemosphere.2013.07.057.

Boholm, M. & Arvidsson, R. 2016. A definition framework for the terms nanomaterial and nanoparticle. *NanoEthics*. 10(1):25–40.

Bopp, S.K., Kienzler, A., Richarz, A.-N., van der Linden, S.C., Paini, A., Parissis, N. & Worth, A.P. 2019. Regulatory assessment and risk management of chemical mixtures: challenges and ways forward. *Critical Reviews in Toxicology*. 49(2):174–189. DOI: 10.1080/10408444.2019.1579169.

Bour, A., Mouchet, F., Silvestre, J., Gauthier, L. & Pinelli, E. 2015. Environmentally relevant approaches to assess nanoparticles ecotoxicity: A review. *Journal of hazardous materials*. 283:764–777.

Boverhof, D.R., Bramante, C.M., Butala, J.H., Clancy, S.F., Lafranconi, M., West, J. & Gordon, S.C. 2015. Comparative assessment of nanomaterial definitions and safety evaluation considerations. *Regulatory toxicology and pharmacology*. 73(1):137–150.

Boxall, A.B.A. 2012. New and emerging water pollutants arising from agriculture.

Brack, W., Dulio, V., Ågerstrand, M., Allan, I., Altenburger, R., Brinkmann, M., Bunke, D., Burgess, R.M., et al. 2017. Towards the review of the European Union Water Framework Directive: Recommendations for more efficient assessment and management of chemical contamination in European surface water resources. *Science of The Total Environment*. 576:720–737. DOI: 10.1016/j.scitotenv.2016.10.104.

Brausch, J.M. & Rand, G.M. 2011. A review of personal care products in the aquatic environment: environmental concentrations and toxicity. *Chemosphere*. 82(11):1518–1532.

Buchman, J.T., Rahnamoun, A., Landy, K.M., Zhang, X., Vartanian, A.M., Jacob, L.M., Murphy, C.J., Hernandez, R., et al. 2018. Using an environmentally-relevant panel of Gram-negative bacteria to assess the toxicity of polyallylamine hydrochloride-wrapped gold nanoparticles. *Environmental Science: Nano*. 5(2):279–288.

Buchman, J.T., Hudson-Smith, N.V., Landy, K.M. & Haynes, C.L. 2019. Understanding Nanoparticle Toxicity Mechanisms To Inform Redesign Strategies To Reduce Environmental Impact. *Accounts of chemical research*.

Bundschuh, M., Seitz, F., Rosenfeldt, R.R. & Schulz, R. 2016. Effects of nanoparticles in fresh waters: risks, mechanisms and interactions. *Freshwater Biology*. 61(12):2185–2196.

Bundschuh, M., Filser, J., Lüderwald, S., McKee, M.S., Metreveli, G., Schaumann, G.E., Schulz, R. & Wagner, S. 2018. Nanoparticles in the environment: where do we come from, where do we go to? *Environmental Sciences Europe*. 30(1):6.

Burns, E.E., Carter, L.J., Snape, J., Thomas-Oates, J. & Boxall, A.B. 2018. Application of prioritization approaches to optimize environmental monitoring and testing of pharmaceuticals. *Journal of Toxicology and Environmental Health, Part B*. 21(3):115–141.

Bystrzejewska-Piotrowska, G., Golimowski, J. & Urban, P.L. 2009. Nanoparticles: their potential toxicity, waste and environmental management. *Waste Management*. 29(9):2587–2595.

Caballero-Diaz, E. & Cases, M.V. 2016. Analytical methodologies for nanotoxicity assessment. *TrAC Trends in Analytical Chemistry*. 84:160–171.

Caldwell, D.J., Mastrocco, F., Margiotta-Casaluci, L. & Brooks, B.W. 2014. An integrated approach for prioritizing pharmaceuticals found in the environment for risk assessment, monitoring and advanced research. *Chemosphere*. 115:4–12.

Cao, Y.C. 2008. Nanomaterials for biomedical applications.

Carey, D.E. & McNamara, P.J. 2015. The impact of triclosan on the spread of antibiotic resistance in the environment. *Frontiers in microbiology*. 5:780.

Carlos, L., Cipollone, M., Soria, D.B., Sergio Moreno, M., Ogilby, P.R., García Einschlag, F.S. & Mártire, D.O. 2012. The effect of humic acid binding to magnetite nanoparticles on the photogeneration of reactive oxygen species. *Separation and Purification Technology*. 91:23–29. DOI: 10.1016/j.seppur.2011.08.028.

Cervantes-Avilés, P., Huang, Y. & Keller, A.A. 2019. Incidence and persistence of silver nanoparticles throughout the wastewater treatment process. *Water Research*. 156:188–198. DOI: 10.1016/j.watres.2019.03.031.

Chen, H., Cheng, Y., Meng, D., Xue, G., Jiang, M. & Li, X. 2018. Joint effect of triclosan and copper nanoparticles on wastewater biological nutrient removal. *Environmental technology*. 39(19):2447–2456.

Cheng, X., Zhao, H., Huo, L., Gao, S. & Zhao, J. 2004. ZnO nanoparticulate thin film: preparation, characterization and gas-sensing property. *Sensors and Actuators B: chemical*. 102(2):248–252.

Choi, S., Johnston, M., Wang, G.-S. & Huang, C.P. 2018. A seasonal observation on the distribution of engineered nanoparticles in municipal wastewater treatment systems exemplified by TiO_2 and ZnO. *Science of The Total Environment*. 625:1321–1329. DOI: 10.1016/j.scitotenv.2017.12.326.

Clarke, B.O. & Smith, S.R. 2011. Review of 'emerging'organic contaminants in biosolids and assessment of international research priorities for the agricultural use of biosolids. *Environment international*. 37(1):226–247.

Collin, B., Auffan, M., Johnson, A.C., Kaur, I., Keller, A.A., Lazareva, A., Lead, J.R., Ma, X., et al. 2014. Environmental release, fate and ecotoxicological effects of manufactured ceria nanomaterials. *Environmental Science: Nano*. 1(6):533–548.

Colman, B.P., Espinasse, B., Richardson, C.J., Matson, C.W., Lowry, G.V., Hunt, D.E., Wiesner, M.R. & Bernhardt, E.S. 2014. Emerging contaminant or an old toxin in disguise? Silver nanoparticle impacts on ecosystems. *Environmental Science & Technology*. 48(9):5229–5236.

Conway, J.R., Adeleye, A.S., Gardea-Torresdey, J. & Keller, A.A. 2015. Aggregation, dissolution, and transformation of copper nanoparticles in natural waters. *Environmental science & technology*. 49(5):2749–2756.

Dann, A.B. & Hontela, A. 2011. Triclosan: environmental exposure, toxicity and mechanisms of action. *Journal of applied toxicology*. 31(4):285–311.

Dasari, T.P. & Hwang, H.-M. 2013. Effect of humic acids and sunlight on the cytotoxicity of engineered zinc oxide and titanium dioxide nanoparticles to a river bacterial assemblage. *Journal of Environmental Sciences*. 25(9):1925–1935.

Dasari, T.P., Pathakoti, K. & Hwang, H.-M. 2013. Determination of the mechanism of photoinduced toxicity of selected metal oxide nanoparticles (ZnO, CuO, Co_3O_4 and TiO_2) to *E. coli* bacteria. *Journal of Environmental Sciences*. 25(5):882–888.

Daughton, C.G. 2004. Non-regulated water contaminants: emerging research. *Environmental Impact Assessment Review*. 24(7–8):711–732. DOI: 10.1016/j.eiar.2004.06.003.

De Leersnyder, I., De Gelder, L., Van Driessche, I. & Vermeir, P. 2018. Influence of growth media components on the antibacterial effect of silver ions on Bacillus subtilis in a liquid growth medium. *Scientific Reports*. 8(1). DOI: 10.1038/s41598-018-27540-9.

Deng, R., Lin, D., Zhu, L., Majumdar, S., White, J.C., Gardea-Torresdey, J.L. & Xing, B. 2017. Nanoparticle interactions with co-existing contaminants: joint toxicity, bioaccumulation and risk. *Nanotoxicology*. 11(5):591–612. DOI: 10.1080/17435390.2017.1343404.

Dhillon, G., Kaur, S., Pulicharla, R., Brar, S., Cledón, M., Verma, M. & Surampalli, R. 2015. Triclosan: Current Status, Occurrence, Environmental Risks and Bioaccumulation Potential.

International Journal of Environmental Research and Public Health. 12(5):5657–5684. DOI: 10.3390/ijerph120505657.

Diamond, J.M., Latimer, H.A., Munkittrick, K.R., Thornton, K.W., Bartell, S.M. & Kidd, K.A. 2011. Prioritizing contaminants of emerging concern for ecological screening assessments. *Environmental toxicology and chemistry*. 30(11):2385–2394.

Dickinson, E. 2012. Use of nanoparticles and microparticles in the formation and stabilization of food emulsions. *Trends in Food Science & Technology*. 24(1):4–12.

Dinali, R., Ebrahiminezhad, A., Manley-Harris, M., Ghasemi, Y. & Berenjian, A. 2017. Iron oxide nanoparticles in modern microbiology and biotechnology. *Critical reviews in microbiology*. 43(4):493–507.

Domingos, R.F., Gélabert, A., Carreira, S., Cordeiro, A., Sivry, Y. & Benedetti, M.F. 2015. Metals in the aquatic environment—interactions and implications for the speciation and bioavailability: a critical overview. *Aquatic geochemistry*. 21(2–4):231–257.

Dowhan, W. & Bogdanov, M. 2002. Functional roles of lipids in membranes. In *New comprehensive biochemistry*. V. 36. Elsevier. 1–35.

Drury, B., Scott, J., Rosi-Marshall, E.J. & Kelly, J.J. 2013. Triclosan exposure increases triclosan resistance and influences taxonomic composition of benthic bacterial communities. *Environmental science & technology*. 47(15):8923–8930.

Du, J., Tang, J., Xu, S., Ge, J., Dong, Y., Li, H. & Jin, M. 2018. ZnO nanoparticles: recent advances in ecotoxicity and risk assessment. *Drug and Chemical Toxicology*. (September, 28):1–12. DOI: 10.1080/01480545.2018.1508218.

Dumont, E., Johnson, A.C., Keller, V.D. & Williams, R.J. 2015. Nano silver and nano zinc-oxide in surface waters–Exposure estimation for Europe at high spatial and temporal resolution. *Environmental pollution*. 196:341–349.

Dupont, C.L., Grass, G. & Rensing, C. 2011. Copper toxicity and the origin of bacterial resistance—new insights and applications. *Metallomics*. 3(11):1109–1118.

Earl, A.M., Losick, R. & Kolter, R. 2008. Ecology and genomics of *Bacillus subtilis*. *Trends in microbiology*. 16(6):269–275.

Ebele, A.J., Abou-Elwafa Abdallah, M. & Harrad, S. 2017. Pharmaceuticals and personal care products (PPCPs) in the freshwater aquatic environment. *Emerging Contaminants*. 3(1):1–16. DOI: 10.1016/j.emcon.2016.12.004.

El-Sayed, M.A. 2001. Some interesting properties of metals confined in time and nanometer space of different shapes. *Accounts of chemical research*. 34(4):257–264.

Emami-Karvani, Z. & Chehrazi, P. 2011. Antibacterial activity of ZnO nanoparticle on gram-positive and gram-negative bacteria. *Afr J Microbiol Res*. 5(12):1368–1373.

Engel, M. & Chefetz, B. 2019. The missing link between carbon nanotubes, dissolved organic matter and organic pollutants. *Advances in Colloid and Interface Science*. 271:101993. DOI: 10.1016/j.cis.2019.101993.

European Commission. 2011. *Commission recommendation of 18 October 2011 on the definition of nanomaterial*. Official Journal of the European Union.

European Commission. 2012. Communication from the Commission to the Councilthe combination effects of chemicals. *Chemical Mixtures, COM*. 10.

European Commission. 2016. *Commission implementing decision (EU) 2016/110: Not approving triclosan as an existing active substance for use in biocidal products for product type1.* Available: http:// eur-lex.europa.eu/legal-content/EN/TXT/?Uri=uriserv%3AOJ.L_.2016.021.01. 0086.01.ENG [2019, December 04].

Fabrega, J., Luoma, S.N., Tyler, C.R., Galloway, T.S. & Lead, J.R. 2011. Silver nanoparticles: Behaviour and effects in the aquatic environment. *Environment International*. 37(2):517–531. DOI: 10.1016/j.envint.2010.10.012.

Fan, A.M. & Alexeeff, G. 2010. Nanotechnology and nanomaterials: toxicology, risk assessment, and regulations. *Journal of nanoscience and nanotechnology*. 10(12):8646–8657.

Fang, X., Yu, R., Li, B., Somasundaran, P. & Chandran, K. 2010. Stresses exerted by ZnO, CeO_2 and anatase TiO_2 nanoparticles on the *Nitrosomonas europaea*. *Journal of colloid and interface science*. 348(2):329–334.

Fard, M.A., Vosoogh, A., Barkdoll, B. & Aminzadeh, B. 2017. Using polymer coated nanoparticles for adsorption of micropollutants from water. *Colloids and Surfaces A: Physicochemical and Engineering Aspects*. 531:189–197.

Farnoud, A.M. & Nazemidashtarjandi, S. 2019. Emerging investigator series: interactions of engineered nanomaterials with the cell plasma membrane; what have we learned from membrane models? *Environmental Science: Nano*. 6(1):13–40.

Farré, M., Gajda-Schrantz, K., Kantiani, L. & Barceló, D. 2009. Ecotoxicity and analysis of nanomaterials in the aquatic environment. *Analytical and Bioanalytical Chemistry*. 393(1):81–95. DOI: 10.1007/s00216-008-2458-1.

Fatehah, M.O., Aziz, H.A. & Stoll, S. 2014a. Stability of ZnO Nanoparticles in Solution. Influence of pH, Dissolution, Aggregation and Disaggregation Effects. *Journal of Colloid Science and Biotechnology*. 3(1):75–84. DOI: 10.1166/jcsb.2014.1072.

Fatehah, M.O., Aziz, H.A. & Stoll, S. 2014b. Nanoparticle properties, behavior, fate in aquatic systems and characterization methods. *Journal of Colloid Science and Biotechnology*. 3(2):111–140.

Florencio, L., Field, J.A. & Lettinga, G. 1994. Importance of cobalt for individual trophic groups in an anaerobic methanol-degrading consortium. *Appl. Environ. Microbiol.* 60(1):227–234.

Food and Drug Administration. 2016. *FDA issues final rule on safety and effectiveness of antibacterial soaps.* Available: https://www.fda.gov/NewsEvents/Newsroom/PressAnnouncements/ucm517478. htm [2019, December 04].

Fréchette-Viens, L., Hadioui, M. & Wilkinson, K.J. 2019. Quantification of ZnO nanoparticles and other Zn containing colloids in natural waters using a high sensitivity single particle ICP-MS. *Talanta*. 200:156–162. DOI: 10.1016/j.talanta.2019.03.041.

Gambino, M., Marzano, V., Villa, F., Vitali, A., Vannini, C., Landini, P. & Cappitelli, F. 2015. Effects of sublethal doses of silver nanoparticles on *Bacillus subtilis* planktonic and sessile cells. *Journal of applied microbiology*. 118(5):1103–1115.

Garner, K.L. & Keller, A.A. 2014. Emerging patterns for engineered nanomaterials in the environment: a review of fate and toxicity studies. *Journal of Nanoparticle Research*. 16(8):2503.

Gogoi, A., Mazumder, P., Tyagi, V.K., Tushara Chaminda, G.G., An, A.K. & Kumar, M. 2018. Occurrence and fate of emerging contaminants in water environment: A review. *Groundwater for Sustainable Development*. 6:169–180. DOI: 10.1016/j.gsd.2017.12.009.

Goswami, L., Kim, K.-H., Deep, A., Das, P., Bhattacharya, S.S., Kumar, S. & Adelodun, A.A. 2017. Engineered nano particles: nature, behavior, and effect on the environment. *Journal of environmental management*. 196:297–315.

Gottschalk, F., Sonderer, T., Scholz, R.W. & Nowack, B. 2009. Modeled Environmental Concentrations of Engineered Nanomaterials (TiO_2, ZnO, Ag, CNT, Fullerenes) for Different Regions. *Environmental Science & Technology*. 43(24):9216–9222. DOI: 10.1021/es9015553.

Grandgirard, D., Furi, L., Ciusa, M.L., Baldassarri, L., Knight, D.R., Morrissey, I., Largiadèr, C.R., Leib, S.L., et al. 2015. Mutations upstream of fabI in triclosan resistant Staphylococcus aureus strains are associated with elevated fabI gene expression. *BMC genomics*. 16(1):345.

Grillo, R., Rosa, A.H. & Fraceto, L.F. 2015. Engineered nanoparticles and organic matter: a review of the state-of-the-art. *Chemosphere*. 119:608–619.

Gunsolus, I.L. & Haynes, C.L. 2015. Analytical aspects of nanotoxicology. *Analytical chemistry*. 88(1):451–479.

Guo, J. & Iwata, H. 2017. Risk assessment of triclosan in the global environment using a probabilistic approach. *Ecotoxicology and Environmental Safety*. 143:111–119. DOI: 10.1016/j.ecoenv.2017.05.020.

Halden, R.U., Lindeman, A.E., Aiello, A.E., Andrews, D., Arnold, W.A., Fair, P., Fuoco, R.E., Geer, L.A., et al. 2017. The florence statement on triclosan and triclocarban. *Environmental health perspectives*. 125(6):064501.

Hansen, S.F., Heggelund, L.R., Besora, P.R., Mackevica, A., Boldrin, A. & Baun, A. 2016. Nanoproducts–what is actually available to European consumers? *Environmental Science: Nano*. 3(1):169–180.

Haq, A.N.U., Nadhman, A., Ullah, I., Mustafa, G., Yasinzai, M. & Khan, I. 2017. Synthesis Approaches of Zinc Oxide Nanoparticles: The Dilemma of Ecotoxicity. *Journal of Nanomaterials*. DOI: 10.1155/2017/8510342.

Hariharan, C. 2006. Photocatalytic degradation of organic contaminants in water by ZnO nanoparticles: Revisited. *Applied Catalysis A: General*. 304:55–61.

Hartmann, J., van der Aa, M., Wuijts, S., de Roda Husman, A.M. & van der Hoek, J.P. 2018. Risk governance of potential emerging risks to drinking water quality: Analysing current practices. *Environmental Science & Policy*. 84:97–104.

Hartmann, N.I.B., Skjolding, L.M., Hansen, S.F., Baun, A., Kjølholt, J. & Gottschalk, F. 2014. Environmental fate and behaviour of nanomaterials: new knowledge on important transfomation processes.

He, X., Aker, W.G., Fu, P.P. & Hwang, H.-M. 2015. Toxicity of engineered metal oxide nanomaterials mediated by nano–bio–eco–interactions: a review and perspective. *Environmental Science: Nano*. 2(6):564–582.

Hegde, K., Brar, S.K., Verma, M. & Surampalli, R.Y. 2016. Current understandings of toxicity, risks and regulations of engineered nanoparticles with respect to environmental microorganisms. *Nanotechnology for Environmental Engineering*. 1(1):5.

Heinlaan, M., Ivask, A., Blinova, I., Dubourguier, H.-C. & Kahru, A. 2008. Toxicity of nanosized and bulk ZnO, CuO and TiO_2 to bacteria *Vibrio fischeri* and crustaceans *Daphnia magna* and *Thamnocephalus platyurus*. *Chemosphere*. 71(7):1308–1316.

Heys, K.A., Shore, R.F., Pereira, M.G., Jones, K.C. & Martin, F.L. 2016. Risk assessment of environmental mixture effects. *RSC Advances*. 6(53):47844–47857.

Hitchman, A., Smith, G.H.S., Ju-Nam, Y., Sterling, M. & Lead, J.R. 2013. The effect of environmentally relevant conditions on PVP stabilised gold nanoparticles. *Chemosphere*. 90(2):410–416.

Holden, P.A., Schimel, J.P. & Godwin, H.A. 2014. Five reasons to use bacteria when assessing manufactured nanomaterial environmental hazards and fates. *Current Opinion in Biotechnology*. 27:73–78.

Holden, P.A., Gardea-Torresdey, J.L., Klaessig, F., Turco, R.F., Mortimer, M., Hund-Rinke, K., Cohen Hubal, E.A., Avery, D., et al. 2016. Considerations of environmentally relevant test conditions for improved evaluation of ecological hazards of engineered nanomaterials. *Environmental science & technology*. 50(12):6124–6145.

Hou, J., Wu, Y., Li, X., Wei, B., Li, S. & Wang, X. 2018. Toxic effects of different types of zinc oxide nanoparticles on algae, plants, invertebrates, vertebrates and microorganisms. *Chemosphere*. 193:852–860.

Huang, B.Q. & Yeung, E.C. 2015. Chemical and physical fixation of cells and tissues: an overview. In *Plant microtechniques and protocols*. Springer. 23–43.

Huang, B., Wei, Z.-B., Yang, L.-Y., Pan, K. & Miao, A.-J. 2019. Combined Toxicity of Silver Nanoparticles with Hematite or Plastic Nanoparticles toward Two Freshwater Algae. *Environmental science & technology*. 53(7):3871–3879.

Huang, Y., Zhang, Y., Liu, L., Fan, S., Wei, Y. & He, J. 2006. Controlled synthesis and field emission properties of ZnO nanostructures with different morphologies. *Journal of nanoscience and nanotechnology*. 6(3):787–790.

Huang, Y.C., Fan, R., Grusak, M.A., Sherrier, J.D. & Huang, C. 2014. Effects of nano-ZnO on the agronomically relevant Rhizobium–legume symbiosis. *Science of the Total Environment*. 497:78–90.

Huynh, K.A., McCaffery, J.M. & Chen, K.L. 2014. Heteroaggregation reduces antimicrobial activity of silver nanoparticles: evidence for nanoparticle–cell proximity effects. *Environmental Science & Technology Letters*. 1(9):361–366.

Imlay, J.A. 2015. Transcription factors that defend bacteria against reactive oxygen species. *Annual review of microbiology*. 69:93–108.

Iswarya, V., Bhuvaneshwari, M., Chandrasekaran, N. & Mukherjee, A. 2016. Individual and binary toxicity of anatase and rutile nanoparticles towards Ceriodaphnia dubia. *Aquatic Toxicology*. 178:209–221. DOI: 10.1016/j.aquatox.2016.08.007.

Ivask, A., Juganson, K., Bondarenko, O., Mortimer, M., Aruoja, V., Kasemets, K., Blinova, I., Heinlaan, M., et al. 2014. Mechanisms of toxic action of Ag, ZnO and CuO nanoparticles to

selected ecotoxicological test organisms and mammalian cells in vitro: a comparative review. *Nanotoxicology*. 8(sup1):57–71.

Jagini, S., Konda, S., Bhagawan, D. & Himabindu, V. 2019. Emerging contaminant (triclosan) identification and its treatment: a review. *SN Applied Sciences*. 1(6):640.

Jain, A., Bhargava, R. & Poddar, P. 2013. Probing interaction of Gram-positive and Gram-negative bacterial cells with ZnO nanorods. *Materials Science and Engineering: C*. 33(3):1247–1253.

Jarrell, K.F., Saulnier, M. & Ley, A. 1987. Inhibition of methanogenesis in pure cultures by ammonia, fatty acids, and heavy metals, and protection against heavy metal toxicity by sewage sludge. *Canadian journal of microbiology*. 33(6):551–554.

Jiang, W., Mashayekhi, H. & Xing, B. 2009. Bacterial toxicity comparison between nano-and micro-scaled oxide particles. *Environ. Pollut.* 157(5):1619–1625.

Juganson, K., Ivask, A., Blinova, I., Mortimer, M. & Kahru, A. 2015. NanoE-Tox: New and in-depth database concerning ecotoxicity of nanomaterials. *Beilstein journal of nanotechnology*. 6(1):1788–1804.

Kadiyala, U., Turali-Emre, E.S., Bahng, J.H., Kotov, N.A. & VanEpps, J.S. 2018. Unexpected insights into antibacterial activity of zinc oxide nanoparticles against methicillin resistant *Staphylococcus aureus (MRSA)*. *Nanoscale*. 10(10):4927–4939.

Kahru, A. & Ivask, A. 2012. Mapping the dawn of nanoecotoxicological research. *Accounts of Chemical Research*. 46(3):823–833.

Kang, S., Pinault, M., Pfefferle, L.D. & Elimelech, M. 2007. Single-walled carbon nanotubes exhibit strong antimicrobial activity. *Langmuir*. 23(17):8670–8673.

Kang, S., Herzberg, M., Rodrigues, D.F. & Elimelech, M. 2008. Antibacterial effects of carbon nanotubes: size does matter! *Langmuir*. 24(13):6409–6413.

Kaweeteerawat, C., Ivask, A., Liu, R., Zhang, H., Chang, C.H., Low-Kam, C., Fischer, H., Ji, Z., et al. 2015. Toxicity of Metal Oxide Nanoparticles in *Escherichia coli* Correlates with Conduction Band and Hydration Energies. *Environmental Science & Technology*. 49(2):1105–1112. DOI: 10.1021/es504259s.

Keller, A.A. & Lazareva, A. 2013. Predicted releases of engineered nanomaterials: from global to regional to local. *Environmental Science & Technology Letters*. 1(1):65–70.

Keller, A.A., Wang, H., Zhou, D., Lenihan, H.S., Cherr, G., Cardinale, B.J., Miller, R. & Ji, Z. 2010. Stability and aggregation of metal oxide nanoparticles in natural aqueous matrices. *Environmental science & technology*. 44(6):1962–1967.

Khan, R., Inam, M., Zam, S., Park, D. & Yeom, I. 2018. Assessment of Key Environmental Factors Influencing the Sedimentation and Aggregation Behavior of Zinc Oxide Nanoparticles in Aquatic Environment. *Water*. 10(5):660. DOI: 10.3390/w10050660.

Khan, R., Inam, M., Khan, S., Park, D. & Yeom, I. 2019. Interaction between Persistent Organic Pollutants and ZnO NPs in Synthetic and Natural Waters. *Nanomaterials*. 9(3):472. DOI: 10.3390/nano9030472.

Kiser, M., Westerhoff, P., Benn, T., Wang, Y., Perez-Rivera, J. & Hristovski, K. 2009. Titanium nanomaterial removal and release from wastewater treatment plants. *Environmental science & technology*. 43(17):6757–6763.

Klaessig, F.C. 2018. Dissolution as a paradigm in regulating nanomaterials. *Environmental Science: Nano*. 5(5):1070–1077.

Klaine, S.J., Alvarez, P.J.J., Batley, G.E., Fernandes, T.F., Handy, R.D., Lyon, D.Y., Mahendra, S., McLaughlin, M.J., et al. 2008. Nanomaterials in the environment: Behavior, fate, bioavailability, and effects. *Environmental Toxicology and Chemistry*. 27(9):1825–1851. DOI: 10.1897/08-090.1.

Ko, K.-S., Koh, D.-C. & Kong, I. 2017. Evaluation of the Effects of Nanoparticle Mixtures on Brassica Seed Germination and Bacterial Bioluminescence Activity Based on the Theory of Probability. *Nanomaterials*. 7(10):344. DOI: 10.3390/nano7100344.

Koh, B., Park, J.B., Hou, X. & Cheng, W. 2011. Comparative Dispersion Studies of Single-Walled Carbon Nanotubes in Aqueous Solution. *The Journal of Physical Chemistry B*. 115(11):2627–2633. DOI: 10.1021/jp110376h.

Kohli, A. & Alpar, H. 2004. Potential use of nanoparticles for transcutaneous vaccine delivery: effect of particle size and charge. *International journal of pharmaceutics*. 275(1–2):13–17.

Krishnaraj, C., Jagan, E., Rajasekar, S., Selvakumar, P., Kalaichelvan, P. & Mohan, N. 2010. Synthesis of silver nanoparticles using Acalypha indica leaf extracts and its antibacterial activity against water borne pathogens. *Colloids and Surfaces B: Biointerfaces*. 76(1):50–56.

Kumar, R. & Chawla, J. 2014. Removal of cadmium ion from water/wastewater by nano-metal oxides: a review. *Water Quality, Exposure and Health*. 5(4):215–226.

Kumar, A., Pandey, A.K., Singh, S.S., Shanker, R. & Dhawan, A. 2011. Engineered ZnO and TiO_2 nanoparticles induce oxidative stress and DNA damage leading to reduced viability of *Escherichia coli*. *Free Radical Biology and Medicine*. 51(10):1872–1881.

Kunhikrishnan, A., Shon, H.K., Bolan, N.S., El Saliby, I. & Vigneswaran, S. 2015. Sources, Distribution, Environmental Fate, and Ecological Effects of Nanomaterials in Wastewater Streams. *Critical Reviews in Environmental Science and Technology*. 45(4):277–318. DOI: 10.1080/10643389.2013.852407.

Kunst, F., Ogasawara, N., Moszer, I., Albertini, A., Alloni, G., Azevedo, V., Bertero, M., Bessieres, P., et al. 1997. The complete genome sequence of the gram-positive bacterium Bacillus subtilis. *Nature*. 390(6657):249–256.

Lai, L., Li, S.-J., Feng, J., Mei, P., Ren, Z.-H., Chang, Y.-L. & Liu, Y. 2017. Effects of surface charges on the bactericide activity of CdTe/ZnS quantum dots: a cell membrane disruption perspective. *Langmuir*. 33(9):2378–2386.

Lai, R.W.S., Yeung, K.W.Y., Yung, M.M.N., Djurišić, A.B., Giesy, J.P. & Leung, K.M.Y. 2018. Regulation of engineered nanomaterials: current challenges, insights and future directions. *Environmental Science and Pollution Research*. 25(4):3060–3077. DOI: 10.1007/s11356-017-9489-0.

Landis, W.G. & Chapman, P.M. (in press). Well past time to stop using NOELs and LOELs. *Integrated Environmental Assessment and Management*. 7(4):vi–viii. DOI: 10.1002/ieam.249.

Lapresta-Fernández, A., Fernández, A. & Blasco, J. 2012. Nanoecotoxicity effects of engineered silver and gold nanoparticles in aquatic organisms. *TrAC Trends in Analytical Chemistry*. 32:40–59.

Lead, J.R., Batley, G.E., Alvarez, P.J., Croteau, M., Handy, R.D., McLaughlin, M.J., Judy, J.D. & Schirmer, K. 2018. Nanomaterials in the environment: behavior, fate, bioavailability, and effects—an updated review. *Environmental toxicology and chemistry*. 37(8):2029–2063.

Leareng, S.K., Ubomba-Jaswa, E. & Musee, N. 2020. Toxicity of zinc oxide and iron oxide engineered nanoparticles to *Bacillus subtilis* in river water systems. *Environmental Science: Nano*. 7:172–185.

Lee, S.Y., Shim, E.S., Kang, H.S., Pang, S.S. & Kang, J.S. 2005. Fabrication of ZnO thin film diode using laser annealing. *Thin solid films*. 473(1):31–34.

Lehutso, R.F., Daso, A.P. & Okonkwo, J.O. 2017. Occurrence and environmental levels of triclosan and triclocarban in selected wastewater treatment plants in Gauteng Province, South Africa. *Emerging Contaminants*. 3(3):107–114. DOI: 10.1016/j.emcon.2017.07.001.

Lehutso, R.F., Tancu, Y., Maity, A. & Thwala, M. 2020. Aquatic toxicity of transformed and product-released engineered nanomaterials: An overview of the current state of knowledge. *Process Safety and Environmental Protection*. (March). DOI: 10.1016/j.psep.2020.03.002.

Lei, C., Zhang, L., Yang, K., Zhu, L. & Lin, D. 2016. Toxicity of iron-based nanoparticles to green algae: Effects of particle size, crystal phase, oxidation state and environmental aging. *Environmental pollution*. 218:505–512.

Lei, C., Sun, Y., Tsang, D.C. & Lin, D. 2018. Environmental transformations and ecological effects of iron-based nanoparticles. *Environmental Pollution*.

Lekamge, S., Ball, A.S., Shukla, R. & Nugegoda, D. 2020. The toxicity of nanoparticles to organisms in freshwater. *Reviews of Environmental Contamination and Toxicology Volume 248*. 1–80.

Lemire, J.A., Harrison, J.J. & Turner, R.J. 2013. Antimicrobial activity of metals: mechanisms, molecular targets and applications. *Nature Reviews Microbiology*. 11(6):371.

Leopold, K., Philippe, A., Wörle, K. & Schaumann, G.E. 2016. Analytical strategies to the determination of metal-containing nanoparticles in environmental waters. *TrAC Trends in Analytical Chemistry*. 84:107–120.

Leung, C.Y., Tu, Y., Tang, B.Z. & Wang, W.-X. 2019. Dissolution kinetics of zinc oxide nanoparticles: real-time monitoring using a Zn^{2+}-specific fluorescent probe. *Environ. Sci. Nano.* 6(7):2259–2268.

Leung, Y.H., Xu, X., Ma, A.P., Liu, F., Ng, A.M., Shen, Z., Gethings, L.A., Guo, M.Y., et al. 2016. Toxicity of ZnO and TiO_2 to *Escherichia coli* cells. *Scientific reports*. 6:35243.

Li, M., Pokhrel, S., Jin, X., Mädler, L., Damoiseaux, R. & Hoek, E.M. 2010. Stability, bioavailability, and bacterial toxicity of ZnO and iron-doped ZnO nanoparticles in aquatic media. *Environmental science & technology*. 45(2):755–761.

Li, M., Zhu, L. & Lin, D. 2011. Toxicity of ZnO nanoparticles to <i>Escherichia coli</sub>: mechanism and the influence of medium components. *Environ. Sci. Technol.* 45(5):1977–1983.

Li, M., Lin, D. & Zhu, L. 2013. Effects of water chemistry on the dissolution of ZnO nanoparticles and their toxicity to *Escherichia coli*. *Environmental Pollution*. 173:97–102.

Li, X., Yoneda, M., Shimada, Y. & Matsui, Y. 2017. Effect of surfactants on the aggregation and sedimentation of zinc oxide nanomaterial in natural water matrices. *Science of The Total Environment*. 581–582:649–656. DOI: 10.1016/j.scitotenv.2016.12.175.

Li, Y., Zhang, W., Niu, J. & Chen, Y. 2012. Mechanism of Photogenerated Reactive Oxygen Species and Correlation with the Antibacterial Properties of Engineered Metal-Oxide Nanoparticles. *ACS Nano*. 6(6):5164–5173. DOI: 10.1021/nn300934k.

Li, Y., Niu, J., Zhang, W., Zhang, L. & Shang, E. 2014. Influence of Aqueous Media on the ROS-Mediated Toxicity of ZnO Nanoparticles toward Green Fluorescent Protein-Expressing *Escherichia coli* under UV-365 Irradiation. *Langmuir*. 30(10):2852–2862. DOI: 10.1021/la5000028.

Lin, D., Story, S.D., Walker, S.L., Huang, Q., Liang, W. & Cai, P. 2017. Role of pH and ionic strength in the aggregation of TiO_2 nanoparticles in the presence of extracellular polymeric substances from Bacillus subtilis. *Environmental Pollution*. 228:35–42. DOI: 10.1016/j.envpol.2017.05.025.

Lin, Y., Jin, X., Owens, G. & Chen, Z. 2019. Simultaneous removal of mixed contaminants triclosan and copper by green synthesized bimetallic iron/nickel nanoparticles. *Science of The Total Environment*. 695:133878. DOI: 10.1016/j.scitotenv.2019.133878.

Lindström, A., Buerge, I.J., Poiger, T., Bergqvist, P.-A., Müller, M.D. & Buser, H.-R. 2002. Occurrence and environmental behavior of the bactericide triclosan and its methyl derivative in surface waters and in wastewater. *Environmental science & technology*. 36(11):2322–2329.

Liu, N., Wang, Y., Ge, F., Liu, S. & Xiao, H. 2018. Antagonistic effect of nano-ZnO and cetyltrimethyl ammonium chloride on the growth of Chlorella vulgaris: Dissolution and accumulation of nano-ZnO. *Chemosphere*. 196:566–574. DOI: 10.1016/j.chemosphere.2017.12.184.

Liu, W.-S., Peng, Y.-H., Shiung, C.-E. & Shih, Y. 2012. The effect of cations on the aggregation of commercial ZnO nanoparticle suspension. *Journal of Nanoparticle Research*. 14(12). DOI: 10.1007/s11051-012-1259-9.

Liu, Y., Yan, Z., Xia, J., Wang, K., Ling, X. & Yan, B. 2017. Potential Toxicity in Crucian Carp Following Exposure to Metallic Nanoparticles of Copper, Chromium, and Their Mixtures: A Comparative Study. *Polish Journal of Environmental Studies*. 26(5):2085–2094. DOI: 10.15244/pjoes/69251.

Liu, Y., Nie, Y., Wang, J., Wang, J., Wang, X., Chen, S., Zhao, G., Wu, L., et al. 2018. Mechanisms involved in the impact of engineered nanomaterials on the joint toxicity with environmental pollutants. *Ecotoxicology and Environmental Safety*. 162:92–102. DOI: 10.1016/j.ecoenv.2018.06.079.

Louie, S.M., Tilton, R.D. & Lowry, G.V. 2016. Critical review: impacts of macromolecular coatings on critical physicochemical processes controlling environmental fate of nanomaterials. *Environ. Sci. Nano*. 3(2):283–310.

Lowry, G.V., Gregory, K.B., Apte, S.C. & Lead, J.R. 2012. Transformations of nanomaterials in the environment.

Lowry, G.V., Hill, R.J., Harper, S., Rawle, A.F., Hendren, C.O., Klaessig, F., Nobbmann, U., Sayre, P., et al. 2016. Guidance to improve the scientific value of zeta-potential measurements in nanoEHS. *Environmental Science: Nano*. 3(5):953–965.

Luche, S., Eymard-Vernain, E., Diemer, H., Van Dorsselaer, A., Rabilloud, T. & Lelong, C. 2016. Zinc oxide induces the stringent response and major reorientations in the central metabolism of *Bacillus subtilis*. *Journal of proteomics*. 135:170–180.

Lv, J., Zhang, S., Luo, L., Han, W., Zhang, J., Yang, K. & Christie, P. 2012. Dissolution and microstructural transformation of ZnO nanoparticles under the influence of phosphate. *Environ. Sci. Technol.* 46(13):7215–7221.

Lyndall, J., Barber, T., Mahaney, W., Bock, M. & Capdevielle, M. 2017. Evaluation of triclosan in Minnesota lakes and rivers: Part I – ecological risk assessment. *Ecotoxicology and Environmental Safety*. 142:578–587. DOI: 10.1016/j.ecoenv.2017.04.049.

Ma, H., Williams, P.L. & Diamond, S.A. 2013. Ecotoxicity of manufactured ZnO nanoparticles–a review. *Environmental Pollution*. 172:76–85.

Ma, H., Wallis, L.K., Diamond, S., Li, S., Canas-Carrell, J. & Parra, A. 2014. Impact of solar UV radiation on toxicity of ZnO nanoparticles through photocatalytic reactive oxygen species (ROS) generation and photo-induced dissolution. *Environmental pollution*. 193:165–172.

Majedi, S.M., Kelly, B.C. & Lee, H.K. 2014. Combined effects of water temperature and chemistry on the environmental fate and behavior of nanosized zinc oxide. *Science of The Total Environment*. 496:585–593.

Maness, P.-C., Smolinski, S., Blake, D.M., Huang, Z., Wolfrum, E.J. & Jacoby, W.A. 1999. Bactericidal activity of photocatalytic TiO_2 reaction: toward an understanding of its killing mechanism. *Appl. Environ. Microbiol.* 65(9):4094–4098.

Manke, A., Wang, L. & Rojanasakul, Y. 2013. Mechanisms of nanoparticle-induced oxidative stress and toxicity. *BioMed research international*. 2013.

Mansour, F., Al-Hindi, M., Saad, W. & Salam, D. 2016. Environmental risk analysis and prioritization of pharmaceuticals in a developing world context. *Science of The Total Environment*. 557:31–43.

Masadeh, M.M., Karasneh, G.A., Al-Akhras, M.A., Albiss, B.A., Aljarah, K.M., Al-azzam, S.I. & Alzoubi, K.H. 2015. Cerium oxide and iron oxide nanoparticles abolish the antibacterial activity of ciprofloxacin against gram positive and gram negative biofilm bacteria. *Cytotechnology*. 67(3):427–435. DOI: 10.1007/s10616-014-9701-8.

Matuła, K., Richter, Ł., Adamkiewicz, W., Åkerström, B., Paczesny, J. & Hołyst, R. 2016. Influence of nanomechanical stress induced by ZnO nanoparticles of different shapes on the viability of cells. *Soft matter*. 12(18):4162–4169.

Maurer-Jones, M.A., Gunsolus, I.L., Murphy, C.J. & Haynes, C.L. 2013. Toxicity of engineered nanoparticles in the environment. *Analytical chemistry*. 85(6):3036–3049.

Mensch, A.C., Hernandez, R.T., Kuether, J.E., Torelli, M.D., Feng, Z.V., Hamers, R.J. & Pedersen, J.A. 2017. Natural organic matter concentration impacts the interaction of functionalized diamond nanoparticles with model and actual bacterial membranes. *Environmental science & technology*. 51(19):11075–11084.

Miao, A., Zhang, X., Luo, Z., Chen, C., Chin, W., Santschi, P.H. & Quigg, A. 2010. Zinc oxide–engineered nanoparticles: dissolution and toxicity to marine phytoplankton. *Environmental Toxicology and Chemistry*. 29(12):2814–2822.

Miranda, R.R., Damaso da Silveira, A.L.R., de Jesus, I.P., Grötzner, S.R., Voigt, C.L., Campos, S.X., Garcia, J.R.E., Randi, M.A.F., et al. 2016. Effects of realistic concentrations of TiO2 and ZnO nanoparticles in Prochilodus lineatus juvenile fish. *Environmental Science and Pollution Research*. 23(6):5179–5188. DOI: 10.1007/s11356-015-5732-8.

Misra, S.K., Dybowska, A., Berhanu, D., Luoma, S.N. & Valsami-Jones, E. 2012. The complexity of nanoparticle dissolution and its importance in nanotoxicological studies. *Science of the total environment*. 438:225–232.

Mitrano, D., Ranville, J., Bednar, A., Kazor, K., Hering, A. & Higgins, C. 2014. Tracking dissolution of silver nanoparticles at environmentally relevant concentrations in laboratory, natural, and processed waters using single particle ICP-MS (spICP-MS). *Environmental Science: Nano*. 1(3):248–259.

Moeta, P.J., Wesley-Smith, J., Maity, A. & Thwala, M. 2019. Nano-enabled products in South Africa and the assessment of environmental exposure potential for engineered nanomaterials. *SN Applied Sciences*. 1(6). DOI: 10.1007/s42452-019-0584-3.

Montaseri, H. & Forbes, P.B.C. 2016. A review of monitoring methods for triclosan and its occurrence in aquatic environments. *TrAC Trends in Analytical Chemistry*. 85:221–231. DOI: 10.1016/j.trac.2016.09.010.

Moore, M. 2006. Do nanoparticles present ecotoxicological risks for the health of the aquatic environment? *Environment international*. 32(8):967–976.

von Moos, N. & Slaveykova, V.I. 2014. Oxidative stress induced by inorganic nanoparticles in bacteria and aquatic microalgae–state of the art and knowledge gaps. *Nanotoxicology*. 8(6):605–630.

Murínová, S. & Dercová, K. 2014. Response mechanisms of bacterial degraders to environmental contaminants on the level of cell walls and cytoplasmic membrane. *International journal of microbiology*. 2014.

Murray, K.E., Thomas, S.M. & Bodour, A.A. 2010. Prioritizing research for trace pollutants and emerging contaminants in the freshwater environment. *Environmental pollution*. 158(12):3462–3471.

Musee, N. 2010. Nanotechnology risk assessment from a waste management perspective: Are the current tools adequate? *Human and Experimental Toxicology*. 1–16.

Musee, N. 2017. A model for screening and prioritizing consumer nanoproduct risks: A case study from South Africa. *Environment international*. 100:121–131.

Musee, N. 2018a. Environmental risk assessment of triclosan and triclocarban from personal care products in South Africa. *Environmental Pollution*. 242:827–838.

Musee, N. 2018b. Comment on “risk assessments show engineered nanomaterials to be of low environmental concern”. *Environmental science & technology*. 52(12):6723–6724.

Musee, N., Zvimba, J.N., Schaefer, L.M., Nota, N., Sikhwivhilu, L.M. & Thwala, M. 2014. Fate and behavior of ZnO-and Ag-engineered nanoparticles and a bacterial viability assessment in a

simulated wastewater treatment plant. *Journal of Environmental Science and Health, Part A*. 49(1):59–66.

Naasz, S., Altenburger, R. & Kühnel, D. 2018. Environmental mixtures of nanomaterials and chemicals: The Trojan-horse phenomenon and its relevance for ecotoxicity. *Science of The Total Environment*. 635:1170–1181. DOI: 10.1016/j.scitotenv.2018.04.180.

Nagarajan, R. 2008. Nanoparticles: building blocks for nanotechnology. ACS Publications.

Naidu, R. & Wong, M.H. 2013. Contaminants of emerging concern. *Science of The Total Environment*. 463–464:1077–1078. DOI: 10.1016/j.scitotenv.2013.05.085.

Naidu, R., Jit, J., Kennedy, B. & Arias, V. 2016. Emerging contaminant uncertainties and policy: The chicken or the egg conundrum. *Chemosphere*. 154:385–390.

Navarro, E., Baun, A., Behra, R., Hartmann, N.B., Filser, J., Miao, A.-J., Quigg, A., Santschi, P.H., et al. 2008. Environmental behavior and ecotoxicity of engineered nanoparticles to algae, plants, and fungi. *Ecotoxicology*. 17(5):372–386.

Nebbioso, A. & Piccolo, A. 2013. Molecular characterization of dissolved organic matter (DOM): a critical review. *Anal. Bioanal. Chem.* 405(1):109–124.

Nel, A., Xia, T., Mädler, L. & Li, N. 2006. Toxic potential of materials at the nanolevel. *science*. 311(5761):622–627.

Niazi, J.H. & Gu, M.B. 2009. Toxicity of metallic nanoparticles in microorganisms-a review. In *Atmospheric and biological environmental monitoring*. Springer. 193–206.

Nishi, I., Kawakami, T. & Onodera, S. 2008. Monitoring of Triclosan in the Surface Water of the Tone Canal, Japan. *Bulletin of Environmental Contamination and Toxicology*. 80(2):163–166. DOI: 10.1007/s00128-007-9338-9.

Noguera-Oviedo, K. & Aga, D.S. 2016. Lessons learned from more than two decades of research on emerging contaminants in the environment. *Journal of hazardous materials*. 316:242–251.

O'Brien, R.W. & White, L.R. 1978. Electrophoretic mobility of a spherical colloidal particle. *Journal of the Chemical Society, Faraday Transactions 2: Molecular and Chemical Physics*. 74:1607–1626.

Odzak, N., Kistler, D., Behra, R. & Sigg, L. 2014. Dissolution of metal and metal oxide nanoparticles in aqueous media. *Environmental Pollution*. 191:132–138. DOI: 10.1016/j.envpol.2014.04.010.

Odzak, N., Kistler, D. & Sigg, L. 2017. Influence of daylight on the fate of silver and zinc oxide nanoparticles in natural aquatic environments. *Environmental Pollution*. 226:1–11.

Oggioni, M.R., Furi, L., Coelho, J.R., Maillard, J.-Y. & Martinez, J.L. 2013. Recent advances in the potential interconnection between antimicrobial resistance to biocides and antibiotics. *Expert review of anti-infective therapy*. 11(4):363–366.

Oleszkiewicz, J. & Sharma, V. 1990. Stimulation and inhibition of anaerobic processes by heavy metals—a review. *Biological Wastes*. 31(1):45–67.

Onyekonwu, M.O. & Ogolo, N.A. 2010. Investigating the use of nanoparticles in enhancing oil recovery. Society of Petroleum Engineers.

Orou, S.F.C., Hang, K.J., Thien, M.T., Ying, Y.L., Diem, N.D.N., Goh, B.H., Pung, S.Y. & Pung, Y.F. 2018. Antibacterial activity by ZnO nanorods and ZnO nanodisks: A model used to illustrate "Nanotoxicity Threshold". *Journal of industrial and engineering chemistry*. 62:333–340.

Pagano, L., Pasquali, F., Majumdar, S., De la Torre-Roche, R., Zuverza-Mena, N., Villani, M., Zappettini, A., Marra, R.E., et al. 2017. Exposure of Cucurbita pepo to binary combinations of engineered nanomaterials: physiological and molecular response. *Environmental Science: Nano*. 4(7):1579–1590. DOI: 10.1039/C7EN00219J.

Park, S., Woodhall, J., Ma, G., Veinot, J.G., Cresser, M.S. & Boxall, A.B. 2014. Regulatory ecotoxicity testing of engineered nanoparticles: are the results relevant to the natural environment? *Nanotoxicology*. 8(5):583–592.

Parveen, S., Wani, A.H., Shah, M.A., Devi, H.S., Bhat, M.Y. & Koka, J.A. 2018. Preparation, characterization and antifungal activity of iron oxide nanoparticles. *Microbial Pathogenesis*. 115:287–292. DOI: 10.1016/j.micpath.2017.12.068.

Patil, U., Adireddy, S., Jaiswal, A., Mandava, S., Lee, B. & Chrisey, D. 2015. In vitro/in vivo toxicity evaluation and quantification of iron oxide nanoparticles. *International journal of molecular sciences*. 16(10):24417–24450.

Peijnenburg, W.J., Baalousha, M., Chen, J., Chaudry, Q., Von der kammer, F., Kuhlbusch, T.A., Lead, J., Nickel, C., et al. 2015. A review of the properties and processes determining the fate of engineered nanomaterials in the aquatic environment. *Critical Reviews in Environmental Science and Technology*. 45(19):2084–2134.

Peng, C., Zhang, W., Gao, H., Li, Y., Tong, X., Li, K., Zhu, X., Wang, Y., et al. 2017. Behavior and potential impacts of metal-based engineered nanoparticles in aquatic environments. *Nanomaterials*. 7(1):21.

Peng, Y.-H., Tsai, Y.-C., Hsiung, C.-E., Lin, Y.-H. & Shih, Y. 2017. Influence of water chemistry on the environmental behaviors of commercial ZnO nanoparticles in various water and wastewater samples. *Journal of hazardous materials*. 322:348–356.

Penn, S.G., He, L. & Natan, M.J. 2003. Nanoparticles for bioanalysis. *Current opinion in chemical biology*. 7(5):609–615.

Peters, R.J.B., van Bemmel, G., Milani, N.B.L., den Hertog, G.C.T., Undas, A.K., van der Lee, M. & Bouwmeester, H. 2018. Detection of nanoparticles in Dutch surface waters. *Science of The Total Environment*. 621:210–218. DOI: 10.1016/j.scitotenv.2017.11.238.

Petersen, E.J., Diamond, S.A., Kennedy, A.J., Goss, G.G., Ho, K., Lead, J., Hanna, S.K., Hartmann, N.B., et al. 2015. Adapting OECD aquatic toxicity tests for use with manufactured nanomaterials: key issues and consensus recommendations. *Environmental science & technology*. 49(16):9532–9547.

Petrovic, M. 2003. Analysis and removal of emerging contaminants in wastewater and drinking water. *TrAC Trends in Analytical Chemistry*. 22(10):685–696. DOI: 10.1016/S0165-9936(03)01105-1.

Philippe, A. & Schaumann, G.E. 2014. Interactions of dissolved organic matter with natural and engineered inorganic colloids: a review. *Environmental Science & Technology*. 48(16):8946–8962.

Piccinno, F., Gottschalk, F., Seeger, S. & Nowack, B. 2012. Industrial production quantities and uses of ten engineered nanomaterials in Europe and the world. *Journal of Nanoparticle Research*. 14(9):1109.

Pramanik, S., Hill, S.K.E., Zhi, B., Hudson-Smith, N.V., Wu, J.J., White, J.N., McIntire, E.A., Kondeti, V.S.S.K., et al. 2018. Comparative toxicity assessment of novel Si quantum dots and their traditional Cd-based counterparts using bacteria models *Shewanella oneidensis* and *Bacillus subtilis*. *Environmental Science: Nano*. 5(8):1890–1901. DOI: 10.1039/C8EN00332G.

Project on Emerging Nanotechnologies (PEN). n.d.

Qiu, T.A., Clement, P.L. & Haynes, C.L. 2018. Linking nanomaterial properties to biological outcomes: analytical chemistry challenges in nanotoxicology for the next decade. *Chemical communications*. 54(91):12787–12803.

Quik, J.T., Stuart, M.C., Wouterse, M., Peijnenburg, W., Hendriks, A.J. & van de Meent, D. 2012. Natural colloids are the dominant factor in the sedimentation of nanoparticles. *Environmental Toxicology and Chemistry*. 31(5):1019–1022.

Quik, J.T.K., Vonk, J.A., Hansen, S.F., Baun, A. & Meent, D.V.D. 2011. How to assess exposure of aquatic organisms to manufactured nanoparticles? *Environment international*. 37:1068–1077.

Rago, I., Chandraiahgari, C.R., Bracciale, M.P., De Bellis, G., Zanni, E., Guidi, M.C., Sali, D., Broggi, A., et al. 2014. Zinc oxide microrods and nanorods: different antibacterial activity and their mode of action against Gram-positive bacteria. *RSC Advances*. 4(99):56031–56040.

Ramaswamy, B.R., Shanmugam, G., Velu, G., Rengarajan, B. & Larsson, D.G.J. 2011. GC–MS analysis and ecotoxicological risk assessment of triclosan, carbamazepine and parabens in Indian rivers. *Journal of Hazardous Materials*. 186(2):1586–1593. DOI: 10.1016/j.jhazmat.2010.12.037.

Ranmadugala, D., Ebrahiminezhad, A., Manley-Harris, M., Ghasemi, Y. & Berenjian, A. 2017. The effect of iron oxide nanoparticles on *Bacillus subtilis* biofilm, growth and viability. *Process Biochemistry*.

Rauscher, H., Roebben, G., Amenta, V., Sanfeliu, A.B., Calzolai, L., Emons, H., Gaillard, C., Gibson, N., et al. 2014. Towards a review of the EC Recommendation for a definition of the term" nanomaterial" Part 1: Compilation of information concerning the experience with the definition. *Rauscher and G. Roebben, JRC Scientific and Policy Report EUR*. 26567.

Reed, R., Martin, D., Bednar, A., Montaño, M., Westerhoff, P. & Ranville, J. 2017. Multi-day diurnal measurements of Ti-containing nanoparticle and organic sunscreen chemical release during recreational use of a natural surface water. *Environmental Science: Nano*. 4(1):69–77.

Reiss, R., Lewis, G. & Griffin, J. 2009. An ecological risk assessment for triclosan in the terrestrial environment. *Environmental Toxicology and Chemistry: An International Journal*. 28(7):1546–1556.

Ren, C., Hu, X. & Zhou, Q. 2016. Influence of environmental factors on nanotoxicity and knowledge gaps thereof. *NanoImpact*. 2:82–92.

Ricardo Energy and Environment. 2016. *Support for 3rd regulatory review on nanomaterials-environmental legislation: Interim/Background Report.*

Ricart, M., Guasch, H., Alberch, M., Barceló, D., Bonnineau, C., Geiszinger, A., Ferrer, J., Ricciardi, F., et al. 2010. Triclosan persistence through wastewater treatment plants and its potential toxic effects on river biofilms. *Aquatic Toxicology*. 100(4):346–353.

Richardson, S.D. & Kimura, S.Y. 2016. Water Analysis: Emerging Contaminants and Current Issues. *Analytical Chemistry*. 88(1):546–582. DOI: 10.1021/acs.analchem.5b04493.

Richardson, S.D. & Ternes, T.A. 2005. Water analysis: emerging contaminants and current issues. *Analytical chemistry*. 77(12):3807–3838.

Riddick, T.M. 1968. Control of colloid stability through zeta potential. *Blood*. 10(1).

Rimayi, C., Odusanyaa, D., Weiss, J.M., Boer, J. de & Chimuka, L. 2018. Contaminants of emerging concern in the Hartbeespoort Dam catchment and the uMngeni River estuary 2016 pollution incident, South Africa. *Science of The Total Environment*. 627:1008–1017.

Roco, M.C., Mirkin, C.A. & Hersam, M.C. 2011. Nanotechnology research directions for societal needs in 2020: summary of international study.

Ruttkay-Nedecky, B., Krystofova, O., Nejdl, L. & Adam, V. 2017. Nanoparticles based on essential metals and their phytotoxicity. *Journal of nanobiotechnology*. 15(1):33.

Sauvé, S. & Desrosiers, M. 2014. A review of what is an emerging contaminant. *Chemistry Central Journal*. 8(1). DOI: 10.1186/1752-153X-8-15.

Scherer, P., Lippert, H. & Wolff, G. 1983. Composition of the major elements and trace elements of 10 methanogenic bacteria determined by inductively coupled plasma emission spectrometry. *Biological trace element research*. 5(3):149–163.

Scheringer, M. 2008. Nanoecotoxicology: environmental risks of nanomaterials. *Nature Nanotechnology*. 3(6):322.

Schirmer, K. & Auffan, M. 2015. Nanotoxicology in the environment. *Environmental Science: Nano*. 2(6):561–563.

Schmid, K. & Riediker, M. 2008. Use of nanoparticles in Swiss industry: a targeted survey.

Schriks, M., Heringa, M.B., van der Kooi, M.M., de Voogt, P. & van Wezel, A.P. 2010. Toxicological relevance of emerging contaminants for drinking water quality. *Water research*. 44(2):461–476.

Schwartzberg, A.M. & Zhang, J.Z. 2008. Novel optical properties and emerging applications of metal nanostructures. *The Journal of Physical Chemistry C*. 112(28):10323–10337.

Selck, H., Handy, R.D., Fernandes, T.F., Klaine, S.J. & Petersen, E.J. 2016. Nanomaterials in the aquatic environment: A European Union–United States perspective on the status of ecotoxicity testing, research priorities, and challenges ahead. *Environmental toxicology and chemistry*. 35(5):1055–1067.

Sharma, V.K., Sayes, C.M., Guo, B., Pillai, S., Parsons, J.G., Wang, C., Yan, B. & Ma, X. 2019. Interactions between silver nanoparticles and other metal nanoparticles under environmentally relevant conditions: A review. *Science of The Total Environment*. 653:1042–1051. DOI: 10.1016/j.scitotenv.2018.10.411.

Sirelkhatim, A., Mahmud, S., Seeni, A., Kaus, N.H.M., Ann, L.C., Bakhori, S.K.M., Hasan, H. & Mohamad, D. 2015. Review on zinc oxide nanoparticles: antibacterial activity and toxicity mechanism. *Nano-Micro Letters*. 7(3):219–242.

Skjolding, L.M., Sørensen, S.N., Hartmann, N.B., Hjorth, R., Hansen, S.F. & Baun, A. 2016. Aquatic ecotoxicity testing of nanoparticles—the quest to disclose nanoparticle effects. *Angewandte Chemie International Edition*. 55(49):15224–15239.

Son, J., Vavra, J. & Forbes, V.E. 2015. Effects of water quality parameters on agglomeration and dissolution of copper oxide nanoparticles (CuO-NPs) using a central composite circumscribed design. *Science of the total Environment*. 521:183–190.

Song, K., Zhang, W., Sun, C., Hu, X., Wang, J. & Yao, L. 2020. Dynamic cytotoxicity of ZnO nanoparticles and bulk particles to *Escherichia coli*: A view from unfixed ZnO particle: Zn^{2+} ratio. *Aquatic Toxicology*. 220:105407. DOI: 10.1016/j.aquatox.2020.105407.

Srivastava, V., Gusain, D. & Sharma, Y.C. 2015. Critical review on the toxicity of some widely used engineered nanoparticles. *Industrial & Engineering Chemistry Research*. 54(24):6209–6233.

Stabryla, L.M., Johnston, K.A., Millstone, J.E. & Gilbertson, L.M. 2018. Emerging investigator series: it's not all about the ion: support for particle-specific contributions to silver nanoparticle antimicrobial activity. *Environmental Science: Nano*. 5(9):2047–2068.

Stasinakis, A.S., Gatidou, G., Mamais, D., Thomaidis, N.S. & Lekkas, T.D. 2008. Occurrence and fate of endocrine disrupters in Greek sewage treatment plants. *Water research*. 42(6–7):1796–1804.

Sun, Q., Lv, M., Hu, A., Yang, X. & Yu, C.-P. 2014. Seasonal variation in the occurrence and removal of pharmaceuticals and personal care products in a wastewater treatment plant in Xiamen, China. *Journal of hazardous materials*. 277:69–75.

Sun, T.Y., Gottschalk, F., Hungerbühler, K. & Nowack, B. 2014. Comprehensive probabilistic modelling of environmental emissions of engineered nanomaterials. *Environmental pollution*. 185:69–76.

Suresh, A.K., Pelletier, D.A. & Doktycz, M.J. 2013. Relating nanomaterial properties and microbial toxicity. *Nanoscale*. 5:463–474.

Sutherland, W.J., Bailey, M.J., Bainbridge, I.P., Brereton, T., Dick, J.T., Drewitt, J., Dulvy, N.K., Dusic, N.R., et al. 2008. Future novel threats and opportunities facing UK biodiversity identified by horizon scanning. *Journal of Applied Ecology*. 45(3):821–833.

Tang, S.C.N. & Lo, I.M.C. 2013. Magnetic nanoparticles: Essential factors for sustainable environmental applications. *Water Research*. 47:2613–2632.

The Nanodatabase. 2016. *Jointly Published by: DTU Environment, the Danish Ecological Council and Danish Consumer Council.* Available: www.nanodb.dk [2016, January 01].

Thwala, M., Klaine, S.J. & Musee, N. 2016. Interactions of metal-based engineered nanoparticles with aquatic higher plants: A review of the state of current knowledge. *Environmental toxicology and chemistry*. 35(7):1677–1694.

Tiede, K., Hanssen, S.F., Westerhoff, P., Fern, G.J., Hankin, S.M., Aitken, R.J., Chaudhry, Q. & Boxall, A.B. 2016. How important is drinking water exposure for the risks of engineered nanoparticles to consumers? *Nanotoxicology*. 10(1):102–110.

Tong, T., Fang, K., Thomas, S.A., Kelly, J.J., Gray, K.A. & Gaillard, J.-F. 2014. Chemical interactions between nano-ZnO and nano-TiO_2 in a natural aqueous medium. *Environmental science & technology*. 48(14):7924–7932.

Tong, T., Wilke, C.M., Wu, J., Binh, C.T.T., Kelly, J.J., Gaillard, J.-F. & Gray, K.A. 2015. Combined toxicity of nano-ZnO and nano-TiO_2: from single-to multinanomaterial systems. *Environmental science & technology*. 49(13):8113–8123.

Tu, Y., Lv, M., Xiu, P., Huynh, T., Zhang, M., Castelli, M., Liu, Z., Huang, Q., et al. 2013. Destructive extraction of phospholipids from *Escherichia coli* membranes by graphene nanosheets. *Nature nanotechnology*. 8(8):594.

Turan, N.B., Erkan, H.S., Engin, G.O. & Bilgili, M.S. 2019. Nanoparticles in the aquatic environment: Usage, properties, transformation and toxicity—A review. *Process Safety and Environmental Protection*. 130:238–249. DOI: 10.1016/j.psep.2019.08.014.

USEPA, U. 2016. *Priority Chemicals | Waste Minimization | Wastes | US EPA*. Available: https://archive.epa.gov/epawaste/hazard/wastemin/web/html/priority.html [2020, February 22].

Valdiglesias, V., Fernandez-Bertolez, N., Kiliç, G., Costa, C., Costa, S., Fraga, S., Bessa, M.J., Pasaro, E., et al. 2016. Are iron oxide nanoparticles safe? Current knowledge and future perspectives. *Journal of Trace Elements in Medicine and Biology*. 38:53–63.

Vale, G., Mehennaoui, K., Cambier, S., Libralato, G., Jomini, S. & Domingos, R.F. 2016. Manufactured nanoparticles in the aquatic environment-biochemical responses on freshwater organisms: a critical overview. *Aquatic Toxicology*. 170:162–174.

Vance, M.E., Kuiken, T., Vejerano, E.P., McGinnis, S.P., Jr., M.F.H., Rejeski, D. & Hull, M.S. 2015. Nanotechnology in the real world: Redeveloping the nanomaterial consumer products inventory. *Beilstein Journal of Nanotechnology*. 6:1769–1780.

Wang, Y. & Nowack, B. 2018a. Environmental Risk Assessment of Engineered Nano-SiO_2, Nano Iron Oxides, Nano-CeO_2, Nano-Al_2O_3, and Quantum Dots. *Environmental Toxicology and Chemistry*. 37(5):1387–1395.

Wang, Y. & Nowack, B. 2018b. Dynamic probabilistic material flow analysis of nano-SiO_2, nano iron oxides, nano-CeO_2, nano-Al<sub>2O3, and quantum dots in seven European regions. *Environmental pollution*. 235:589–601.

Wang, D., Gao, Y., Lin, Z., Yao, Z. & Zhang, W. 2014. The joint effects on *Photobacterium phosphoreum* of metal oxide nanoparticles and their most likely coexisting chemicals in the environment. *Aquatic toxicology*. 154:200–206.

Wang, D., Lin, Z., Wang, T., Yao, Z., Qin, M., Zheng, S. & Lu, W. 2016. Where does the toxicity of metal oxide nanoparticles come from: the nanoparticles, the ions, or a combination of both? *Journal of hazardous materials*. 308:328–334.

Wang, H., Adeleye, A.S., Huang, Y., Li, F. & Keller, A.A. 2015. Heteroaggregation of nanoparticles with biocolloids and geocolloids. *Advances in Colloid and Interface Science*. 226:24–36. DOI: 10.1016/j.cis.2015.07.002.

Wang, Y., Deng, L., Caballero-Guzman, A. & Nowack, B. 2016. Are engineered nano iron oxide particles safe? An environmental risk assessment by probabilistic exposure, effects and risk modeling. *Nanotoxicology*. 10(10):1545–1554.

Wang, Z., Zhang, L., Zhao, J. & Xing, B. 2016. Environmental processes and toxicity of metallic nanoparticles in aquatic systems as affected by natural organic matter. *Environmental Science: Nano*. 3(2):240–255.

Westerhoff, P., Zhang, Y., Crittenden, J. & Chen, Y. 2008. Properties of commercial nanoparticles that affect their removal during water treatment. *Nanoscience and Nanotechnology: Environmental and Health Impacts. NJ: John Wiley and Sons*. 71–90.

Wiechers, J.W. & Musee, N. 2010. Engineered inorganic nanoparticles and cosmetics: facts, issues, knowledge gaps and challenges. *Journal of Biomedical Nanotechnology*. 6(5):408–431.

Wilke, C.M., Tong, T., Gaillard, J.-F. & Gray, K.A. 2016. Attenuation of microbial stress due to nano-Ag and nano-TiO_2 interactions under dark conditions. *Environmental science & technology*. 50(20):11302–11310.

Wilke, C.M., Gaillard, J.-F. & Gray, K.A. 2017. The critical role of light in moderating microbial stress due to mixtures of engineered nanomaterials. *Environmental Science Nano*.

Wilke, C.M., Wunderlich, B., Gaillard, J.-F. & Gray, K.A. 2018. Synergistic bacterial stress results from exposure to nano-Ag and nano-TiO_2 mixtures under light in environmental media. *Environmental science & technology*. 52(5):3185–3194.

Wilke, C.M., Petersen, C., Alsina, M.A., Gaillard, J.-F. & Gray, K.A. 2019. Photochemical interactions between n-Ag_2S and n-TiO_2 amplify their bacterial stress response. *Environmental Science: Nano*. 6(1):115–126.

Xiao, Y., Vijver, M.G. & Peijnenburg, W.J. 2018. Impact of water chemistry on the behavior and fate of copper nanoparticles. *Environmental pollution*. 234:684–691.

Xu, P., Zeng, G.M., Huang, D.L., Feng, C.L., Hu, S., Zhao, M.H., Lai, C., Wei, Z., et al. 2012. Use of iron oxide nanomaterials in wastewater treatment: a review. *Science of the Total Environment*. 424:1–10.

Yamanaka, M., Hara, K. & Kudo, J. 2005. Bactericidal actions of a silver ion solution on *Escherichia coli*, studied by energy-filtering transmission electron microscopy and proteomic analysis. *Applied and environmental microbiology*. 71(11):7589–7593.

Yezhelyev, M.V., Gao, X., Xing, Y., Al-Hajj, A., Nie, S. & O'Regan, R.M. 2006. Emerging use of nanoparticles in diagnosis and treatment of breast cancer. *The lancet oncology*. 7(8):657–667.

Yi, J. & Cheng, J. 2017. Effects of water chemistry and surface contact on the toxicity of silver nanoparticles to *Bacillus subtilis*. *Ecotoxicology*. 26(5):639–647.

Yu, R., Wu, J., Liu, M., Zhu, G., Chen, L., Chang, Y. & Lu, H. 2016. Toxicity of binary mixtures of metal oxide nanoparticles to *Nitrosomonas europaea*. *Chemosphere*. 153:187–197.

Yu, S., Liu, J., Yin, Y. & Shen, M. 2018. Interactions between engineered nanoparticles and dissolved organic matter: A review on mechanisms and environmental effects. *Journal of Environmental Sciences*. 63:198–217.

Yu-sen, E.L., Vidic, R.D., Stout, J.E., McCartney, C.A. & Victor, L.Y. 1998. Inactivation of *Mycobacterium avium* by copper and silver ions. *Water Res.* 32(7):1997–2000.

Zhang, X., Song, K., Liu, J., Zhang, Z., Wang, C. & Li, H. 2019. Sorption of triclosan by carbon nanotubes in dispersion: The importance of dispersing properties using different surfactants. *Colloids and Surfaces A: Physicochemical and Engineering Aspects*. 562:280–288.

Zhou, D. & Keller, A.A. 2010. Role of morphology in the aggregation kinetics of ZnO nanoparticles. *Water research*. 44(9):2948–2956.

Zhu, K., Zhang, L., Mu, L., Ma, J., Wang, X., Li, C., Cui, Y. & Li, A. 2020. Antagonistic effect of zinc oxide nanoparticle and surfactant on anaerobic digestion: Focusing on the microbial community changes and interactive mechanism. *Bioresource Technology*. 297:122382. DOI: 10.1016/j.biortech.2019.122382.

Zhu, M., Wang, H., Keller, A.A., Wang, T. & Li, F. 2014. The effect of humic acid on the aggregation of titanium dioxide nanoparticles under different pH and ionic strengths. *Science of the Total Environment*. 487:375–380.

Appendices

Appendix A

Potential interference of ENPs with Live/dead assay kit

In this study, 100% viable cells (standard curve) was used to determine the possible effects the ENPs used in this study could have on the fluorescent probes. We interacted the ENPs and cells at all concentrations, added the SYTO9 (green) and propidium iodide (red) dyes, and incubated for 15 min (Tong et al. 2013; Wilke et al., 2016). The fluorescence intensity was then measured using a Flouroskan Ascent FL multimode reader (Thermo Scientific). The level of cell membrane integrity of the ENP interacted cells and non-interacted cells was compared to determine the influence of ENPs on the fluorescence of the Dyes.

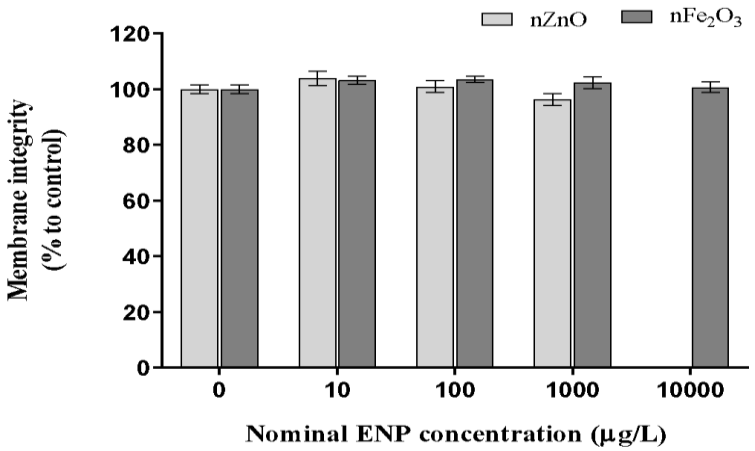

Figure A1: Effects of ENPs on the Live/Dead BacLight assay.

Appendix B

Potential interference of ENPs with ATP assay

To assess the interference of ENPs and ensure the effects observed were due to ENPs and the varying concentrations used in the study, we used a procedure described by Tong et al (2015) and Wilke et al (2016). ENPs were incubated with 100 µl Bactiter Glo assay reagent for 10 min in the dark. Cell were then added, and the mixture incubated for another 5 min in

the dark. Luminescence was recorder on the Flouroskan Ascent FL microplate reader (Thermofisher). Results below show that the assay was not affected by the concentrations of the ENPs used in the study (Figure A2).

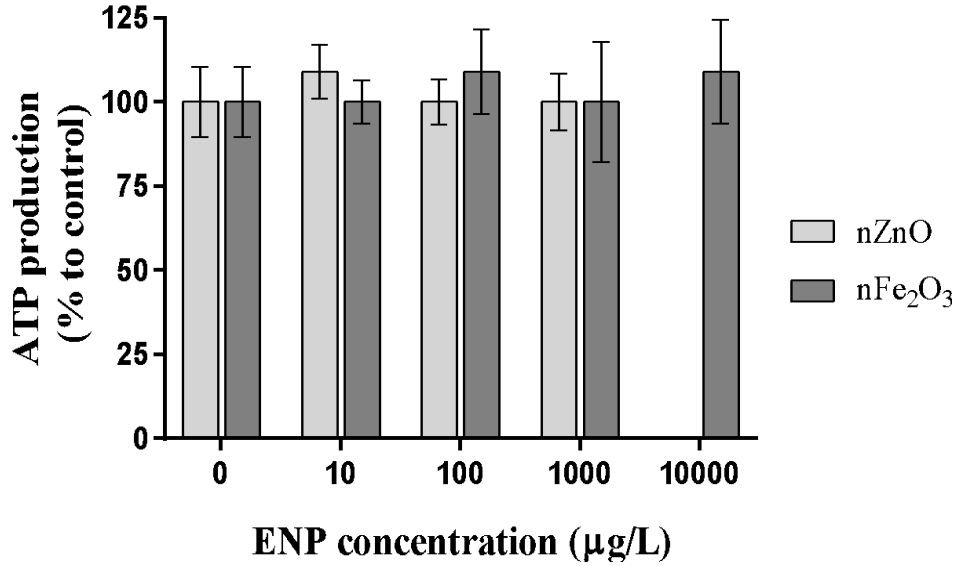

Figure A2: Assessment of ENPs potential interference with the Bactiter Glo assay for ATP production measurement. The luminescence signal produced at all concentrations were not significantly different from the control. The ENPs did not interfere with the assay measurements in this study.

Appendix C

ROS detection assay

A comparison of the intracellular ROS quantification method using DCF-DA as described in Lin et al (2014) was compared to the method used in the study. Both methods did not yield significantly different results. Herein, the fluorescence intensity of DCF-DA was measured to determine the extent of ROS generation in the water samples alone, or the nanomaterials, in the absence of bacteria. In this study, 150 µL of the tested ENPs concentrations and controls (river water) were transferred to 96-well microplates and incubated with DCF-DA (100 µM final concentration) for 30 min at 37°C under dark conditions (covered with aluminium foil). DCF fluorescence intensity was measured with a Flouroscan Ascent FL microplate reader

(ThermoFisher, USA) at an excitation and emission wavelengths of 485 and 538 nm, respectively, to quantify ROS activity both in the water sample and nanomaterial concentrations. ROS production was expressed as percentage fluorescence of the control (minus the ENPS) over the exposed samples. For each test, three replicates of each sample were added per plate, and two plates were used to ensure reproducibility.

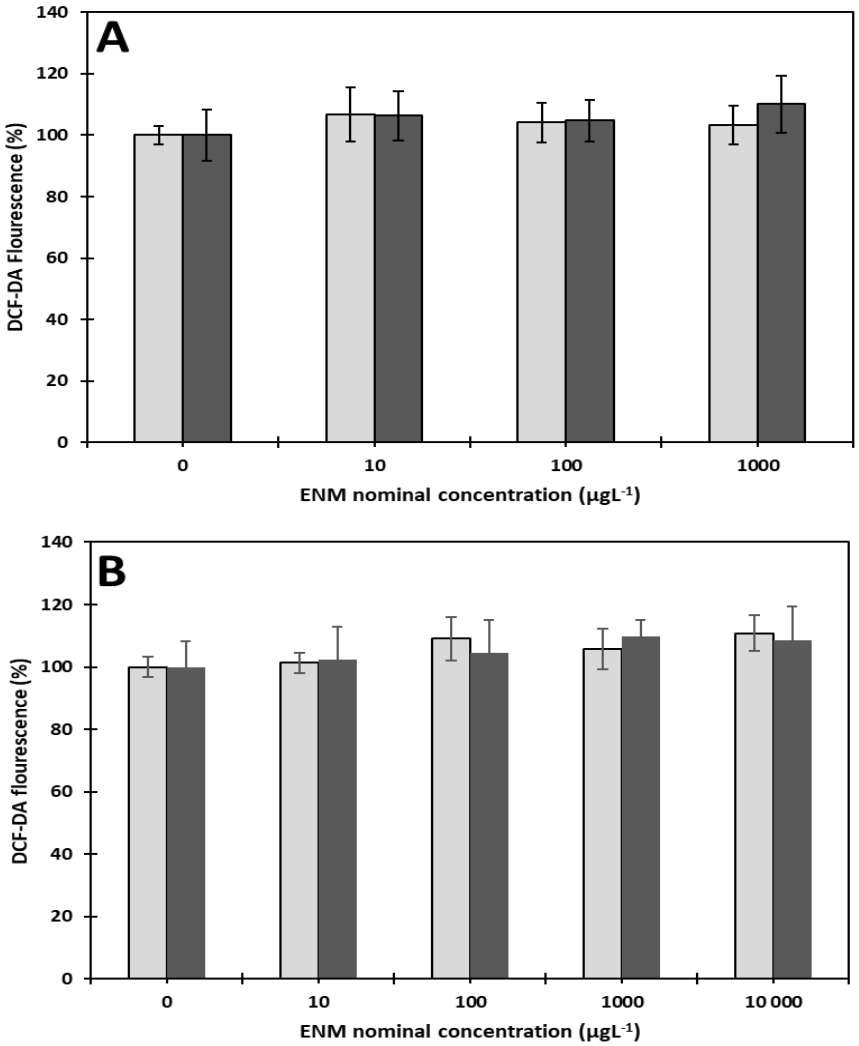

Figure A3**:** Fluorescence of DCF-DA in water and (a) ZnO nanoparticles and (b) Fe_2O_3 nanoparticles. There was no significant difference in the amount of ROS was produced by the ENPs, showing lack of interference or false positive results.

Appendix D

Effects of solar irradiation on bacterial membrane integrity

Exposure cultures were prepared by inoculating a single colony from overnight solid agar plates into LB broth and shaken for 4 h at 30 °C until mid-exponential phase (0.4 – 0.5 at OD_{600nm}). Following centrifugation at 4500 xg for 10 min, cells were subsequently washed twice and lastly resuspended in the filtered river water. The cells were finally diluted to a final concentration of 2 x 10^8 cells/mℓ in ER water, as measured by plate counting. The bacteria was exposed to solar irradiation exposure studies were done under natural sunlight at noon at the university of Pretoria, South Africa for 30 and 60 min. The cell membrane integrity was assessed as detailed in section 3.7 of the methodology.

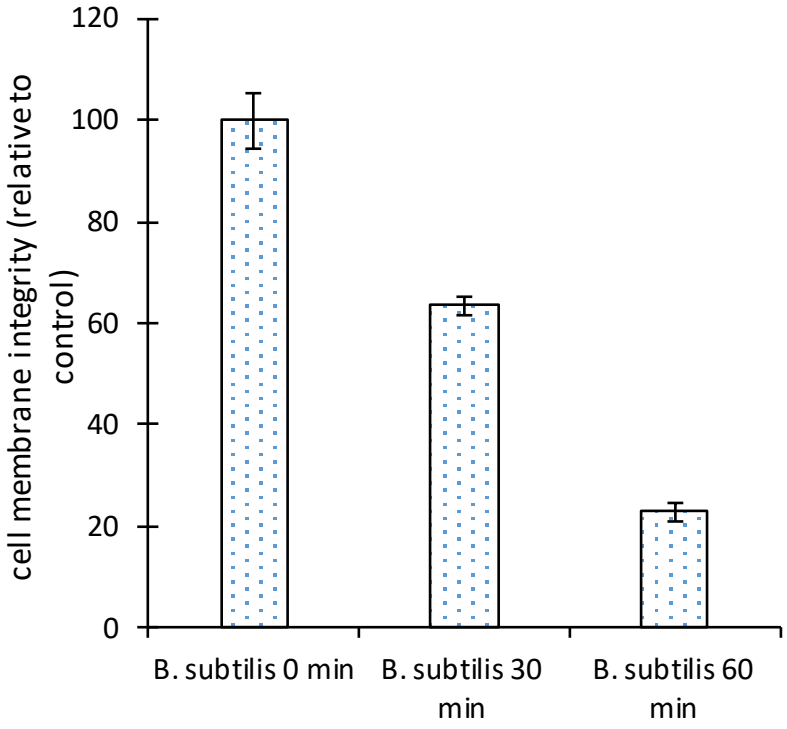

Figure A4: Effects of solar irradiation on *Bacillus subtilis* without ENPs over 1 h. the 30 min exposure time was chosen for solar irradiation experiments using binary mixtures.

Appendix E

Size trend analysis of ENPs of binary mixtures

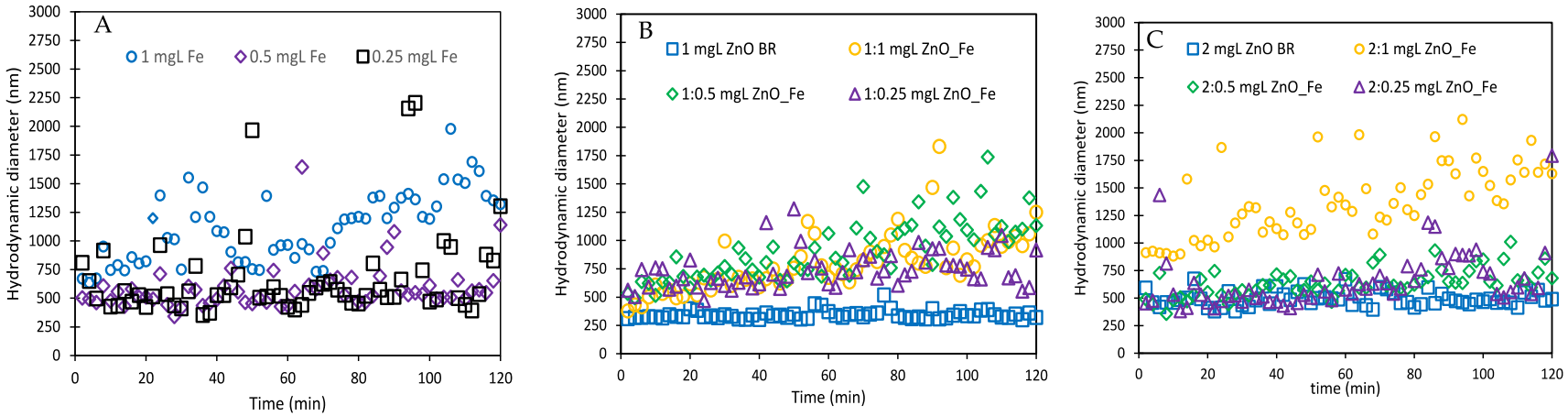

Figure A5: Aggregation kinetics for nFe_2O_3, nZnO, and nZnO/nFe_2O_3 mixtures in BR water. Aggregate sizes for (A) 0.25, 0.5 and 1 mg/L nFe_2O_3; (B) 0.25, 0.5 and 1 mg/L nFe_2O_3 with 1 mg/L nZnO; (C) 0.25, 0.5 and 1 mg/L nFe_2O_3 with 2 mg/L nZnO.

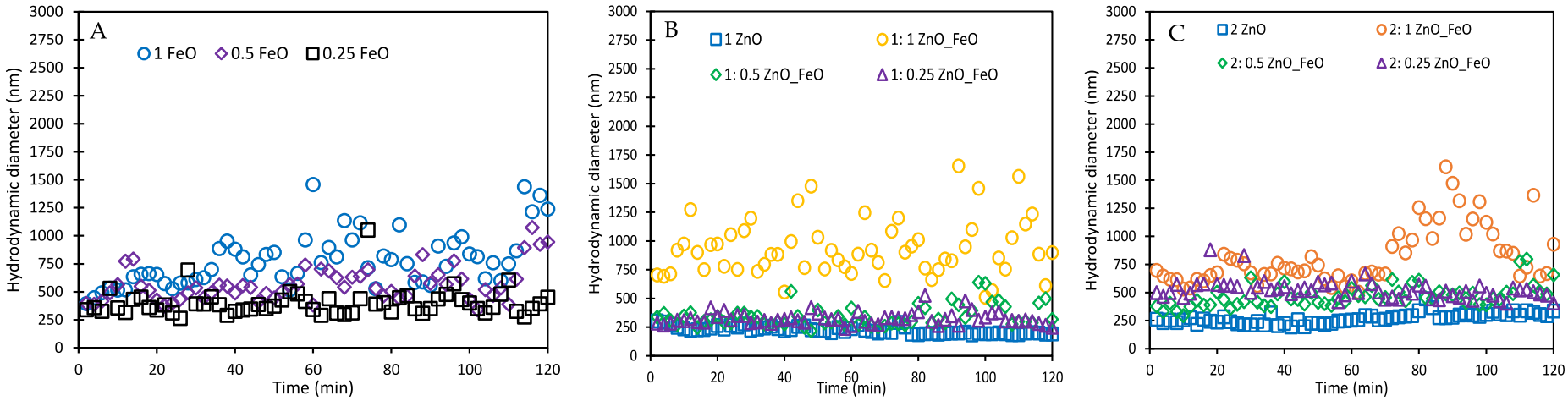

Figure A6: Aggregation kinetics for nFe_2O_3, nZnO, and $nZnO/nFe_2O_3$ mixtures in ER water. Aggregate sizes for (A) 0.25, 0.5 and 1 mg/L nFe_2O_3; (B) 0.25, 0.5 and 1 mg/L nFe_2O_3 with 1 mg/L nZnO; (C) 0.25, 0.5 and 1 mg/L nFe_2O_3 with 2 mg/L nZnO.

Appendix F

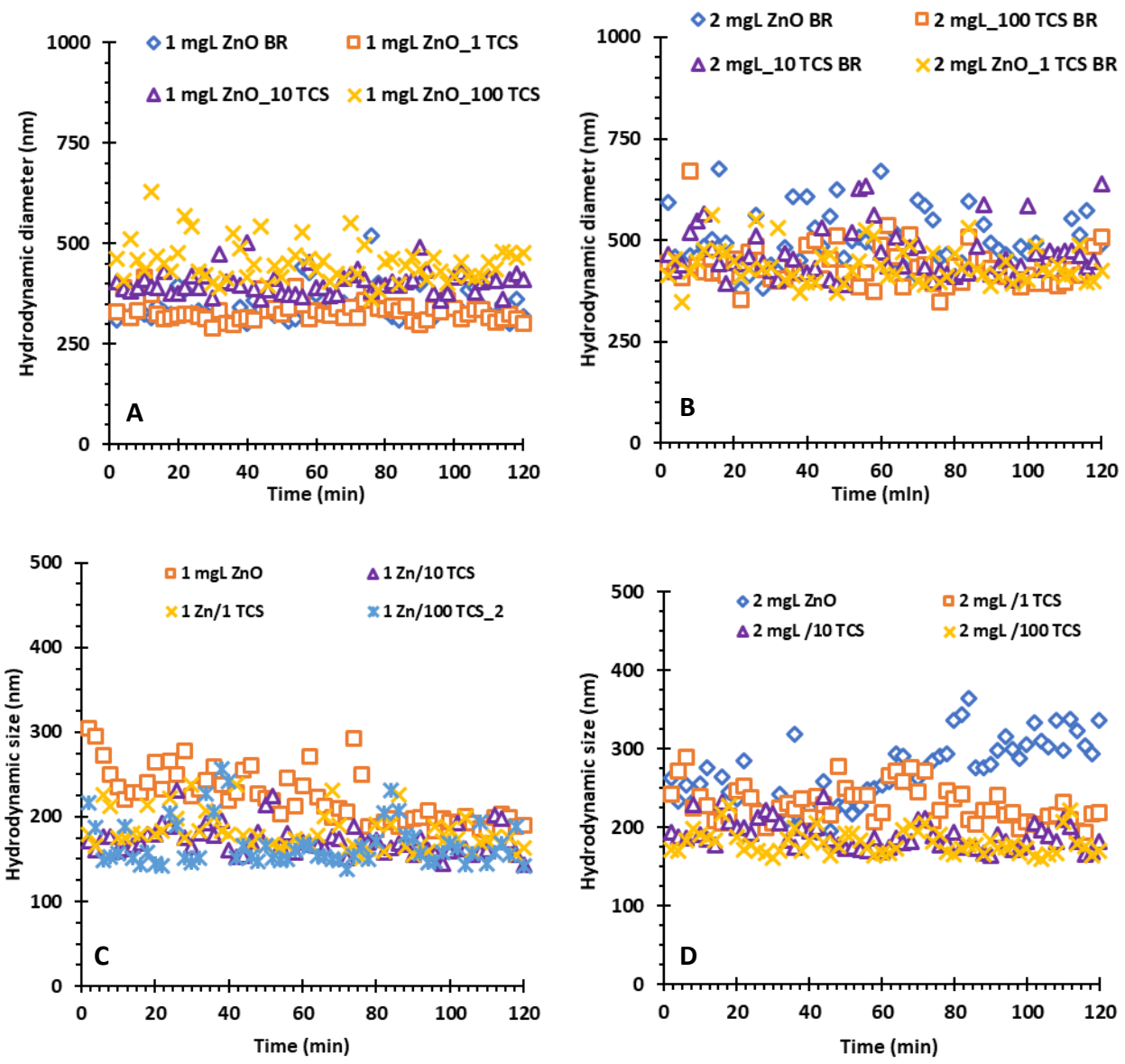

Figure A7: Aggregation kinetics of binary mixtures of nZnO and TCS in BR and ER water. (a) 1 mg/L nZnO with 1, 10 and 100 µg/L TCS in BR water; (b) 2 mg/L nZnO with 1, 10 and 100 µg/L TCS in BR water; (c) 1 mg/L nZnO with 1, 10 and 100 µg/L TCS in ER water; (d) 2 mg/L nZnO with 1, 10 and 100 µg/L TCS in ER water.

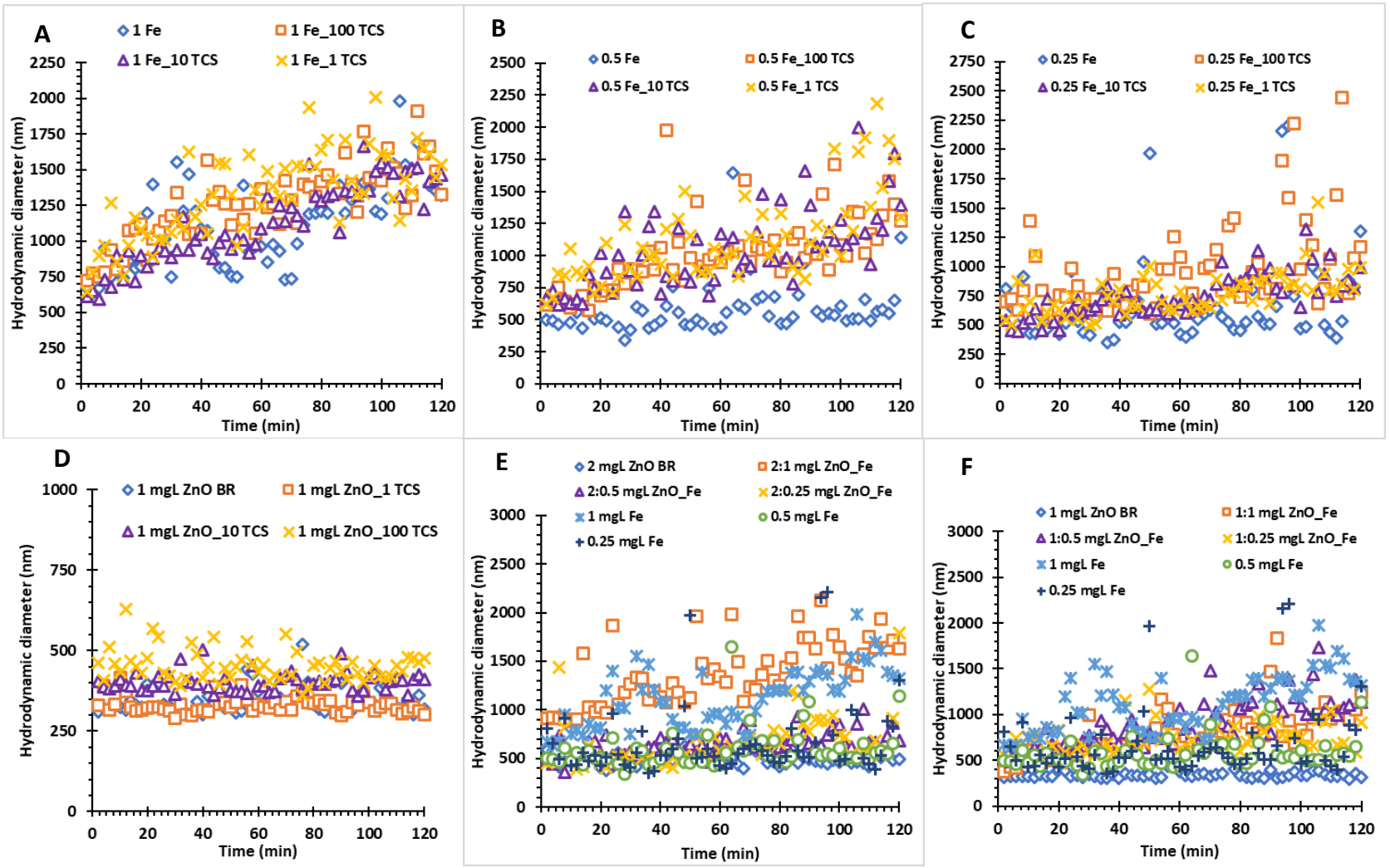

FigureA8: Aggregation kinetics of binary mixtures of γ-nFe_2O_3 and TCS in BR water. (a) 1 mg/L γ-nFe_2O_3 with 1, 10 and 100 µg/L TCS in BR water; (b) 0.5 mg/L γ-nFe_2O_3 with 1, 10 and 100 µg/L TCS in BR water; (c) 0.25 mg/L γ-nFe_2O_3 with 1, 10 and

100 µg/L TCS in BR water; (d) 1 mg/L nZnO with 1, 10 and 100 µg/L TCS in BR water; (e) 2 mg/L nZnO with 0.25, 0.5 and 1 mg/L γ-nFe_2O_3 in BR water; (f) 2 mg/L nZnO with 0.25, 0.5 and 1 mg/L γ-nFe_2O_3 in BR water.

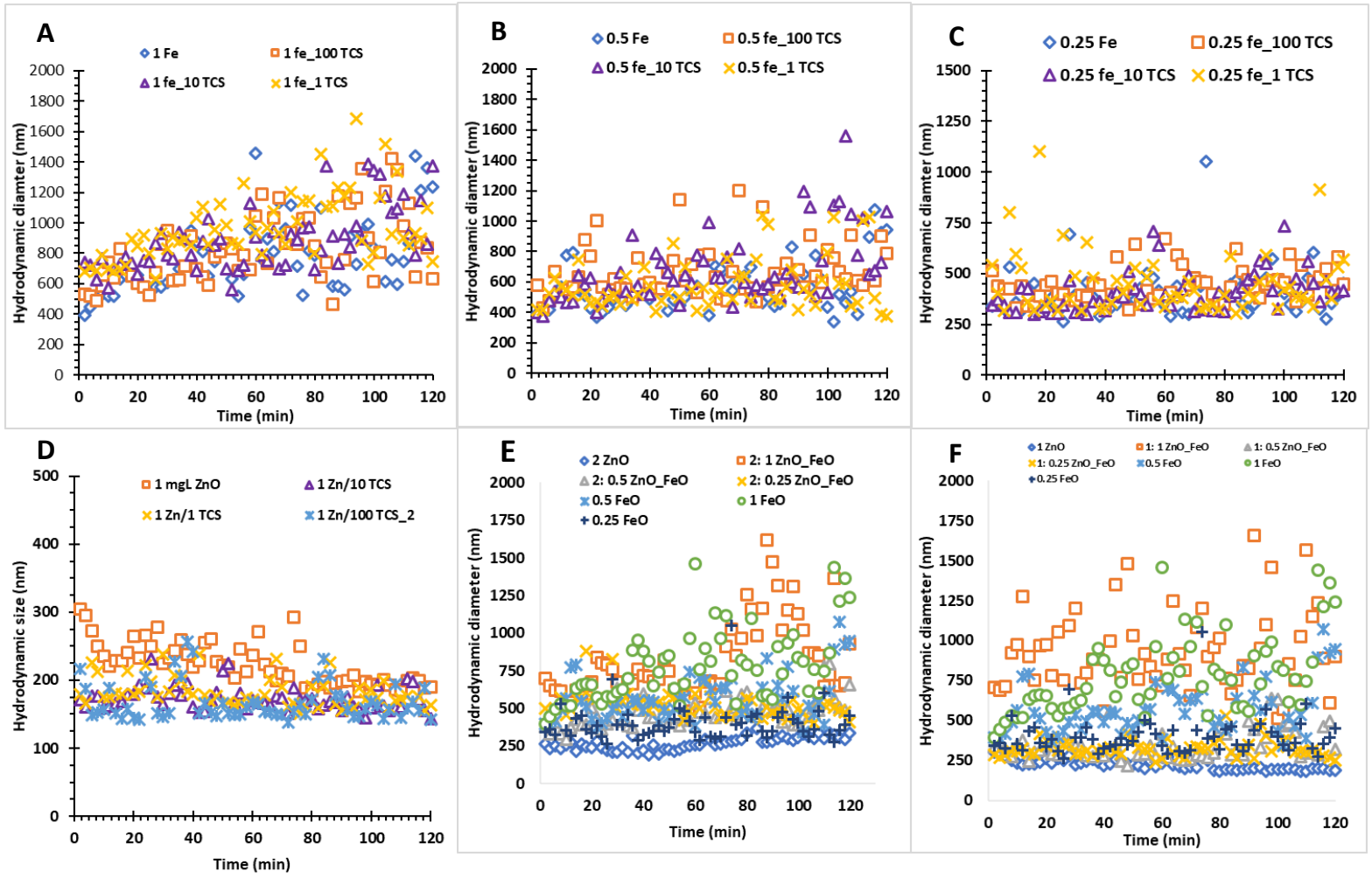

Figure A9: Aggregation kinetics of binary mixtures of γ-nFe_2O_3 and TCS in BR water. (a) 1 mg/L γ-nFe_2O_3 with 1, 10 and 100 µg/L TCS in BR water; (b) 0.5 mg/L γ-nFe_2O_3 with 1, 10 and 100 µg/L TCS in BR water; (c) 0.25 mg/L γ-nFe_2O_3 with 1, 10 and 100 µg/L TCS in BR water; (d) 1 mg/L nZnO with 1, 10 and 100 µg/L TCS in BR water; (e) 2 mg/L nZnO with 0.25, 0.5 and 1 mg/L γ-nFe_2O_3 in ER water; (f) 2 mg/L nZnO with 0.25, 0.5 and 1 mg/L γ-nFe_2O_3 in ER water.

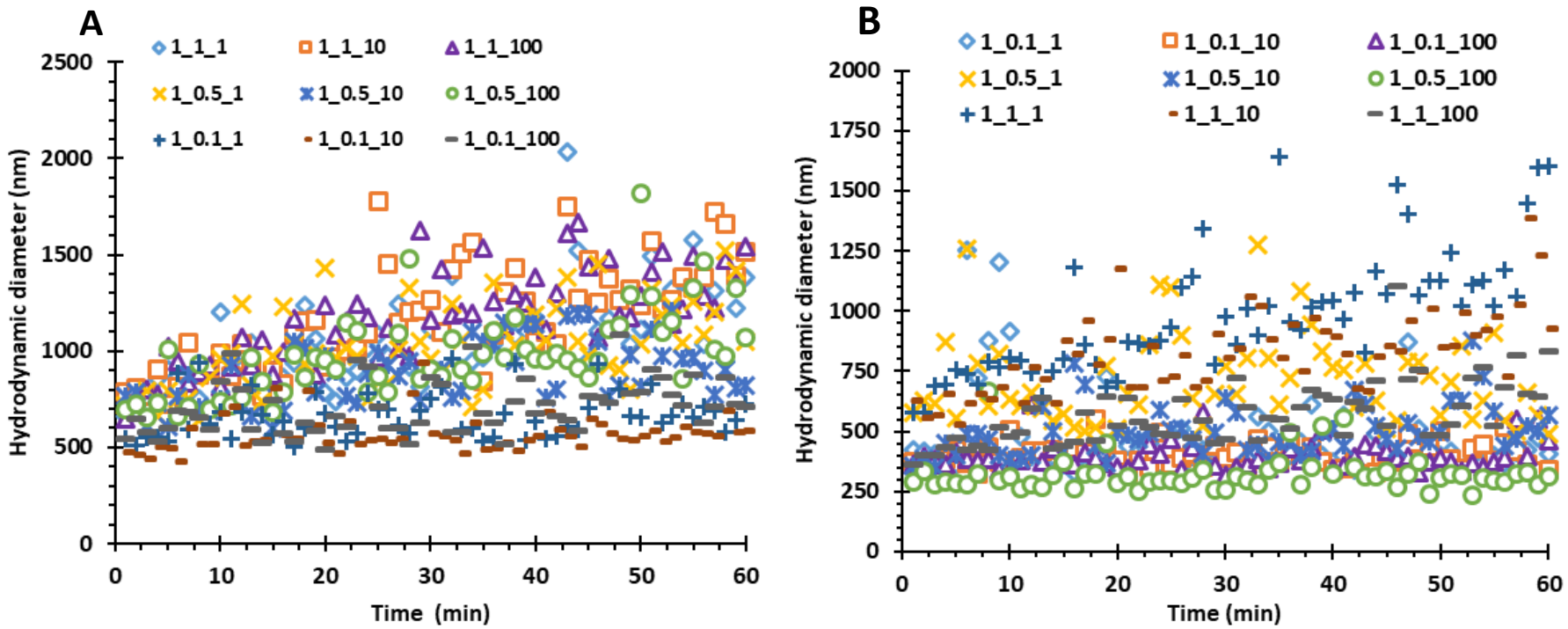

Figure A10: Aggregation kinetics of ternary mixtures of nZnO, γ-nFe_2O_3 and TCS in BR and ER water. (a) 1 mg/L nZnO with 0.1, 0.5,1 mg/L γ-nFe_2O_3; 0.1, 10 and 100 µg/L TCS in BR water; (b) 1 mg/L nZnO with 0.1, 0.5,1 mg/L γ-nFe_2O_3; 0.1, 10 and 100 µg/L TCS in ER water.

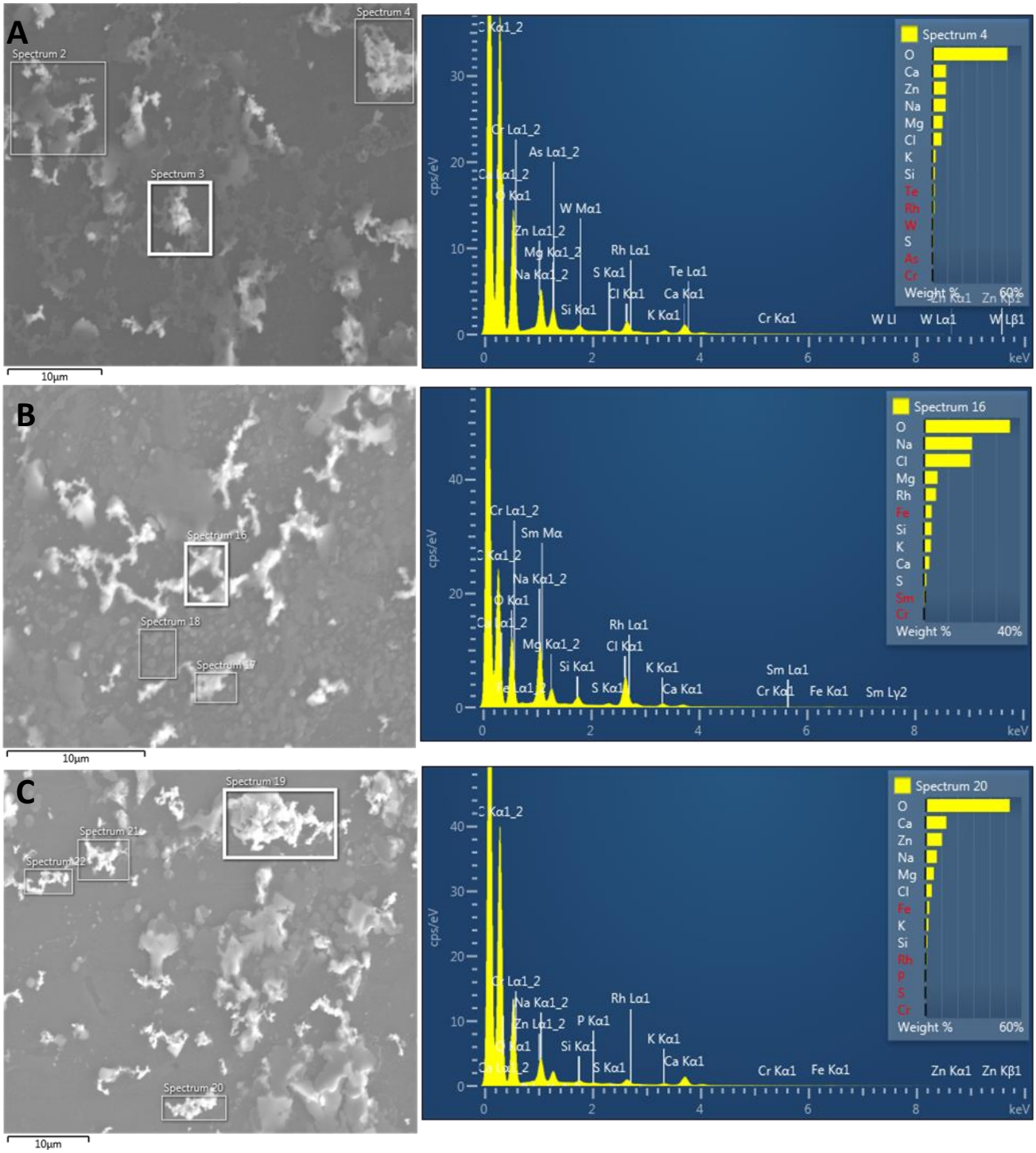

Figure A11: SEM images of aggregates of (a) nZnO; (b) nFe_2O_3 and (c) ENPS binary mixtures in BR water. The energy-dispersive x-ray spectra represents the highlighted regions.